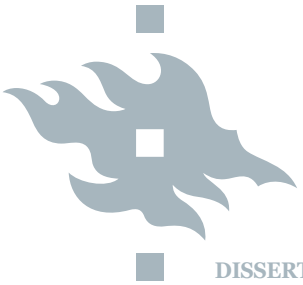

DISSERTATIONES SCHOLAE DOCTORALIS AD SANITATEM INVESTIGANDAM
UNIVERSITATIS HELSINKIENSIS

31/2018

TIINA LIPIÄINEN

Stability and Analysis of Solid-State Forms in Pharmaceutical Powders

DIVISION OF PHARMACEUTICAL CHEMISTRY AND TECHNOLOGY
FACULTY OF PHARMACY
DOCTORAL PROGRAMME IN DRUG RESEARCH
UNIVERSITY OF HELSINKI

Division of Pharmaceutical Chemistry and Technology
Faculty of Pharmacy
University of Helsinki
Finland

Stability and analysis of solid-state forms in pharmaceutical powders

by

Tiina Lipiäinen

ACADEMIC DISSERTATION

To be presented, with the permission of the Faculty of Pharmacy of the University of Helsinki, for public examination in Auditorium 2, Infocenter Korona (Viikinkaari 11, Helsinki), on the 25th May 2018, at 12 noon.

Helsinki 2018

Supervisors

Professor Anne M. Juppo
Division of Pharmaceutical Chemistry and Technology
Faculty of Pharmacy
University of Helsinki
Finland

Associate Professor Clare J. Strachan
Division of Pharmaceutical Chemistry and Technology
Faculty of Pharmacy
University of Helsinki
Finland

Doctor Marikki Peltoniemi
The Pharmaceutical Learning Centre
Helsinki
Finland

Reviewers

Senior Research Fellow Cushla McGoverin
Department of Physics
University of Auckland
New Zealand

Associate Principal Scientist Michael Quayle
Pharmaceutical Development
AstraZeneca
Gothenburg
Sweden

Opponent

Professor Anne Marie Healy
School of Pharmacy and Pharmaceutical Sciences
Trinity College Dublin
Ireland

Dissertationes Scholae Doctoralis Ad Sanitatem Investigandam Universitatis Helsinkiensis

ISBN 978-951-51-4282-5 (paperback)
ISBN 978-951-51-4283-2 (PDF)
ISSN 2342-3161 (print)
ISSN 2342-317X (online)

Hansaprint Oy
Turku 2018

Abstract

The solid-state form can directly affect the quality of a pharmaceutical product, and solid-state transformations can lead to reduced or unpredictable therapeutic effects. Formulation and manufacturing processes can impact solid-state stability. In the pharmaceutical industry there is a need to detect, quantify and control the solid-state behaviour of powders during processes and storage. Reliable and convenient analytical methods are crucial. The overall aim of this thesis was to evaluate strategies for controlling stability and analysing solid-state forms in pharmaceutical powders. New excipients for stabilisation of spray-dried protein formulations, as well as Raman spectroscopy-based methods for solid-state quantification, new in the pharmaceutical field, were investigated.

Melibiose and isomalt were evaluated as possible new stabilising excipients for spray-dried protein formulations. The process behaviour of these two carbohydrates, and the physical stability of amorphous isomalt and melibiose powders were evaluated in comparison to sucrose and trehalose. Both could be spray dried into amorphous powders, but melibiose was more applicable for spray drying processes and showed better physical stability than isomalt.

In the subsequent study, the protein-stabilising efficacy and process behaviour of melibiose in spray-dried protein formulations was investigated in comparison to the current standard protein-stabilising excipient, trehalose. Protein formulations with melibiose could be spray dried into amorphous powders that were physically stable, contained lower moisture contents and protected protein activity at least as well as formulations with trehalose.

Low-frequency Raman spectroscopy for quantitative analysis of solid-state form mixtures was investigated, in order to evaluate its potential advantage over the established mid-frequency Raman spectroscopy analysis. Standard spectral processing and multivariate data analysis methods were used. Low-frequency Raman spectroscopy was found better than conventional mid-frequency Raman spectroscopy analysis, because of higher signal intensity and solid-state sensitivity.

In the final study, time-gated Raman spectroscopy was tested for quantitative solid-state analysis of fluorescent pharmaceutical powder mixtures. Fluorescence interference occasionally limits the feasibility of conventional Raman spectroscopy analysis. Both standard multivariate analysis methods as well as kernel-based methods were used for data analysis. It was found that time-gated Raman spectroscopy, particularly when combined with kernel-based data analysis methods, provided benefits for the quantitative analysis of materials suffering from fluorescence.

In summary, melibiose was identified as a promising excipient to stabilise spray-dried protein formulations. Low-frequency and time-gated Raman spectroscopy were found advantageous for solid-state analysis, also with fluorescent materials, and they may be useful techniques for various solid-state monitoring applications.

Acknowledgements

This work was carried out at the Division of Pharmaceutical Chemistry and Technology, Faculty of Pharmacy, University of Helsinki, Finland and at the Department of Chemistry, University of Otago, New Zealand during the years of 2011-2018. I gratefully acknowledge all the funding sources that made the work possible, including the European Union (FP7 MAREX project), Academy of Finland, The Finnish Ministry of Education, The Finnish Pharmaceutical Society, Research Foundation of the University of Helsinki, TEKES, Finnish Cultural Foundation and University of Helsinki Research Funds.

I express my deep and sincere gratitute to all my supervisors for widening my outlook on science and other important topics in life. I would like to thank Prof. Anne Juppo for making all of this possible by giving me the chance to join her research group, and for her guidance and trust in me. I am thankful to Dr. Marikki Peltoniemi for her invaluable help, encouragement and friendship. I wish to thank Prof. Clare Strachan for all her support, advice and endlessly encouraging attitude. I am grateful also to my former supervisors Prof. Heikki Vuorela, Prof. Arto Urtti, Dr. Teijo Yrjönen and Dr. Sanjay Sarkhel for the support and making the start of this work possible. Thank you all for sharing your expertise and knowledge with me, and for believing in my abilities even in the moments I doubted them. There is so much I have learned from all of you.

I wish to thank all co-authors – Dr. Heikki Räikkönen, M.Sc. Anna-Maija Kolu, Dr. Sara Fraser-Miller, Prof. Keith Gordon, Dr. Jenni Pessi, M.Sc. Parisa Movahedi, Dr. Juha Koivistoinen, Dr. Lauri Kurki, Dr. Mari Tenhunen, Prof. Jouko Yliruusi, Prof. Jukka Heikkonen and Prof. Tapio Pahikkala – for sharing their expertise and experience with me, and for the great discussions and the valuable scientific contribution to this work. A special acknowledgement to Prof. Keith Gordon who kindly welcomed me to his laboratory at University of Otago and who, together with Dr. Sara Fraser-Miller, offered their sincere cooperation, assistance and expertise. I wish to thank both for their hospitality and all the help, which made my visit to New Zealand scientifically very productive and overall a wonderful experience. I also wish to specially thank Dr. Heikki Räikkönen for his enthusiasm, outstanding technical assistance, and the fruitful discussions around powders, spray drying and many other topics. My most sincere thank you to M.Sc. Anna-Maija Kolu, M.Sc. Isabell Immohr, M. Sc. Robert Lang, M. Sc. Pauline Frederiks, Karoliina Koponen and M. Sc. Irma Gomes. Your hard work resulted in fine Master's theses and research projects, and also helped me in completing this work. We also shared many funny moments in the lab; it was a pleasure working with you.

I am grateful to all my past and present colleagues at the Department of Pharmaceutical Chemistry and Technology, as well as the MAREX team, for the pleasant working atmosphere. The constant support and friendly discussions have made it all so much easier. It has been a pleasure working with all of you, and I have made such good memories during these years. My

deepest thanks to everyone for that. A special thanks goes to Sanna, Heli, Kristina, Ruzica and Päivi – with you I shared the very start and end of this journey, and along it countless laughs and wonderful moments, in and outside the lab, and many achievements in life, but also some darker moments and academic frustration. I am extremely grateful for these shared moments and your friendship. During these years, I have had the privilege to meet so many amazing people in Helsinki, Turku, Lappeenranta, Kuopio, Tartu, Gothenburg, San Antonio, La Laguna, Naples, Denver, Belgrade, Dublin, Reno, Graz, Dunedin… Thank you for all the collaborations, top quality discussions, excellent company and lifelong memories!

I would also like to thank all my friends for giving me the chance to take my mind out of the work from time to time, and reminding me of the other important things in life.

I am deeply grateful to my parents, Maarit and Juha, my brothers Harri and Valtteri, my sister, Janna, and her husband SongPing, for their patience, trust in me and never-ending support. A special acknowledgement to Valtteri for the last-moment-before-printing scientific discussion. My warmest thanks go to my beloved Jani for his love, understanding and being there for me.

Helsinki, May 2018

Tiina Lipiäinen

Contents

List of original publications

This thesis is based on the following publications, which are referred to in the text by their respective roman numerals (**I-IV**):

I **Lipiäinen T**, Peltoniemi M, Räikkönen H, Juppo A. Spray-dried amorphous isomalt and melibiose, two potential protein-stabilizing excipients. *International Journal of Pharmaceutics*. 2016; 510(1): 311-322.

II **Lipiäinen T**, Räikkönen H, Kolu A-M, Peltoniemi M, Juppo A. Comparison of melibiose and trehalose as stabilising excipients for spray-dried β-galactosidase formulations. *International Journal of Pharmaceutics*. 2018; 543(1-2): 21-28.

III **Lipiäinen T**, Fraser-Miller SJ, Gordon KC, Strachan CJ. Direct comparison of low- and mid-frequency Raman spectroscopy for quantitative solid-state pharmaceutical analysis. *Journal of Pharmaceutical and Biomedical Analysis*. 2018; 149: 343-350.

IV **Lipiäinen T***, Pessi J*, Movahedi P, Koivistoinen J, Kurki L, Tenhunen M, Yliruusi J, Juppo AM, Heikkonen J, Pahikkala T, Strachan CJ. Time-gated Raman spectroscopy for quantitative determination of solid-state forms of fluorescent pharmaceuticals. *Analytical Chemistry*. 2018; 90(7): 4832-4839.

The publications are referred to in the text by their roman numerals. In publication IV, the first two authors contributed equally to the work (*).

List of additional publications

Additional publications, which are not included in the experimental part of this thesis are listed below:

1. **Lipiäinen T**, Peltoniemi M, Sarkhel S, Yrjönen T, Vuorela H, Urtti A, Juppo A. Formulation and stability of cytokine therapeutics. *Journal of Pharmaceutical Sciences*. 2015; 104(2): 307-26

2. Semjonov K, Salm M, **Lipiäinen T**, Kogermann K, Lust A, Laidmäe I, Antikainen O, Strachan CJ, Ehlers H, Yliruusi J, Heinämäki J. Interdependence of particle properties and bulk powder behavior of indomethacin in quench-cooled molten two-phase solid dispersions. *International Journal of Pharmaceutics*. 2018; 541(1-2): 188-197.

3. Laurén P*, Paukkonen H*, **Lipiäinen T**, D Yujiao, Oksanen T, Räikkönen H, Ehlers H, Laaksonen P, Yliperttula M, Laaksonen T. Bioadhesive nanofibrillated cellulose films for drug release. Submitted manuscript, 2018.

Abbreviations

ANOVA	Analysis of variance
API	Active pharmaceutical ingredient
ATR	Attenuated total reflectance
CSD	Cambridge Structural Database
DSC	Differential scanning calorimetry
FTIR	Fourier-transform infrared
FT-Raman	Fourier-transform Raman spectroscopy
ICH	International Conference on Harmonization
IR	Infrared
PAT	Process analytical technology
PCA	Principal component analysis
PLS	Partial least squares
RH	Relative humidity
RLS	Regularised least squares
RMSECV	Root-mean square error of cross validation
RMSEP	Root-mean square error of prediction
SEM	Scanning electron microscopy
SNV	Standard normal variate
T_g	Glass transition temperature
T_{inlet}	Inlet temperature
T_{outlet}	Outlet temperature
XRPD	X-ray powder diffraction

1 Introduction

Solid-state properties are critically important in pharmaceutical product development and manufacturing, because they can directly affect the quality of a drug product [1, 2]. Common to the diverse types of pharmaceutical solids is that solid-state transformations can lead to reduced or unpredictable therapeutic effects. Such changes can affect the active pharmaceutical ingredient directly (e.g. different physicochemical properties of different forms) or indirectly (e.g. by influencing the stability of the product). There is a need to understand, control and monitor solid-state behaviour during pharmaceutical processes and storage. Formulation and manufacturing processes affect the solid-state structure, and they must be designed so that the product has the intended properties that also remain stable during storage. Reliable analytical methods for solid-state characterisation are crucial.

Therapeutic proteins have become a major drug class in the pharmaceutical industry. The biological activity of proteins is determined by their molecular conformation, which is sensitive to various instabilities. Degradation of the native structure and formation of protein aggregates can result in loss of activity or harmful immunologic responses. Some degradation pathways can be inhibited by drying, but the drying process itself, as well as storage in the dried state, can also be harmful to proteins. Stabilising excipients are generally needed to preserve the protein structure and activity. Low-molecular-weight compounds that are efficient in hydrogen bonding with the protein are often good stabilisers, provided that they form an amorphous singe-phase matrix structure [3]. Disaccharides, such as trehalose and sucrose, are often used for this purpose. With amorphous systems, stability becomes a concern, because they may spontaneously convert to a thermodynamically more stable form (i.e. crystallise). The likelihood of crystallisation can be affected by choice of formulation excipients and processing conditions.

Spray-drying is an increasingly used drying technology in the biopharmaceutical industry, with advantages in speed and cost-efficiency of the process and control over dried particle properties [4]. Spray-drying is potentially suitable for proteins but the process parameters must be carefully chosen to ensure preservation of protein activity. Furthermore, process parameters can affect the solid-state properties of the resulting powder and the physical stability of the formulation. For stable dry protein formulations, both the drying process and formulation must be optimized.

Trehalose and sucrose are commonly used stabilising excipients for solid protein formulations, but problems with crystallisation may arise during storage [5-7]. Alternative excipients should be evaluated to potentially broaden the current selection of formulation excipients. Melibiose and isomalt have shown potential in freeze-dried protein preparations but have not been tested with spray drying. Information on their spray-drying process behaviour, protein-stabilising efficacy and physical stability is needed.

As with large biomolecules, the structure of small molecule drugs (below 500 Daltons) determines the biological activity, but small molecules are generally more chemically stable. What can become more critical than degradation of the molecular structure, is the packing arrangement of the molecules in solids [8, 9]. The degree of order (crystalline or amorphous) as well as the characteristic lattice structure of different crystal forms (e.g. alternative polymorphs and solvates) result in different intermolecular interactions, which determine the physicochemical properties of the solid affecting e.g. the (apparent) solubility, stability and processability of the drug. Designing products with the active ingredient in an unstable solid-state form has become increasingly popular because a growing portion of new molecules in development have very limited solubility [10, 11]. These forms may have improved solubility, but they are inherently unstable, thermodynamically driven to convert into a more stable form. Production of different solid-state forms and their storage stability is controlled by manufacturing processes and formulation. Solid-state transformations, which could lead to unacceptable changes in product properties, can happen and need to be detected.

Given the importance of solid-state forms in different settings, there are numerous analytical tools for evaluating solid-state behaviour. Commonly used methods include thermal analysis, diffractometric and spectroscopic techniques [12]. Despite the availability of current techniques, there is a demand for advances in the field. Driving factors include the desire for reduced time and sample consumption of analyses, overcoming specific limitations of the techniques, as well as better in-line measurements for real-time process monitoring. Raman spectroscopy has become an established process monitoring tool in pharmaceutical industry because of its potential for fast, non-destructive measurements that can be performed from inside manufacturing vessels or product containers [13]. Limitations of conventional Raman spectroscopy include low sensitivity or signal deterioration caused by photoluminescence, such as fluorescence, of some materials.

Developments in instrumentation which allow measurement of a wider spectral range (access to the low-frequency or terahertz region [14, 15]) and separation of the Raman and photoluminescence signals (by time-resolved detection [16]), may result in even more wide-spread applicability of Raman spectroscopy. Unlike conventional mid-frequency Raman spectroscopy, low-frequency Raman spectroscopy probes low-energy lattice vibrations that are directly defined by the crystal structure, and therefore it can be particularly useful for solid-state analysis. Time-gated Raman spectroscopy may provide better analyses of fluorescent materials. The potential of these two more recently available Raman techniques should be further evaluated in the pharmaceutical setting. Multivariate data analysis methods have improved the potential for qualitative and quantitative interpretation of spectra [17]. Developments in chemometric methods may allow further advantages [18], and they should be actively investigated and implemented when appropriate also in the pharmaceutical research field.

2 Review of the literature

2.1 Pharmaceutical solids

Orally administered solid dosage forms, including tablets and capsules, are the most commonly used drug delivery systems [19]. They are convenient, acceptable and comparatively safe for the patient, can be cost-efficiently manufactured, are versatile with respect to design, and are relatively chemically and physically stable compared to e.g. liquid formulations [2]. In cases where oral administration does not allow adequate bioavailability, because of insufficient gastrointestinal wall permeation or degradation of the drug by the first-pass effect, other methods of administration are required. An example is protein drugs, for which the parenteral route by injection is the primary choice. The main component in parenteral formulations is usually water, which increases many degradation route rates. Thus, the preparation of solid dosage forms via water removal is also often essential with these products to obtain adequate stability during shipping and storage [20].

Solid dosage forms are thus extremely commonly encountered in the pharmaceutical industry and the manufacturing of practically all solid dosage forms involves working with powders. Powders may be used as the final product or they can be intermediates before e.g. compression to tablets. Pharmaceutical powders are composed of solid particles and air, and they often contain a mixture of materials: active pharmaceutical ingredient(s) (API) and excipient(s). Several properties govern the process behaviour of powders as well as the final product performance. Internal solid-state structure is one such important property.

2.1.1 Different solid-state forms

Solid materials can exist in various solid-state forms (**FIG 1**); these are determined by the packing arrangement of the molecules [1, 2, 21]. A first level classification can be made by separating crystalline and amorphous forms. In crystalline materials, the molecules are arranged in a defined order with elements of symmetry and the arrangement forms a repeating pattern in three dimensions (the crystal lattice). Amorphous solids lack such long-range order, even if they may exhibit short range order including favoured intermolecular interactions. Small molecules often exist in crystalline form, with the amorphous form being thermodynamically unstable [22]. In contrast, materials composed of large molecules, such as polymers or proteins, are more often amorphous because the size and flexibility of these molecules makes alignment into perfect order difficult. Polymeric materials often, however, show ordered regions, surrounded by disorder, and such a structure is

described as semicrystalline. In reality all pharmaceutical solids usually have both crystalline and amorphous content.

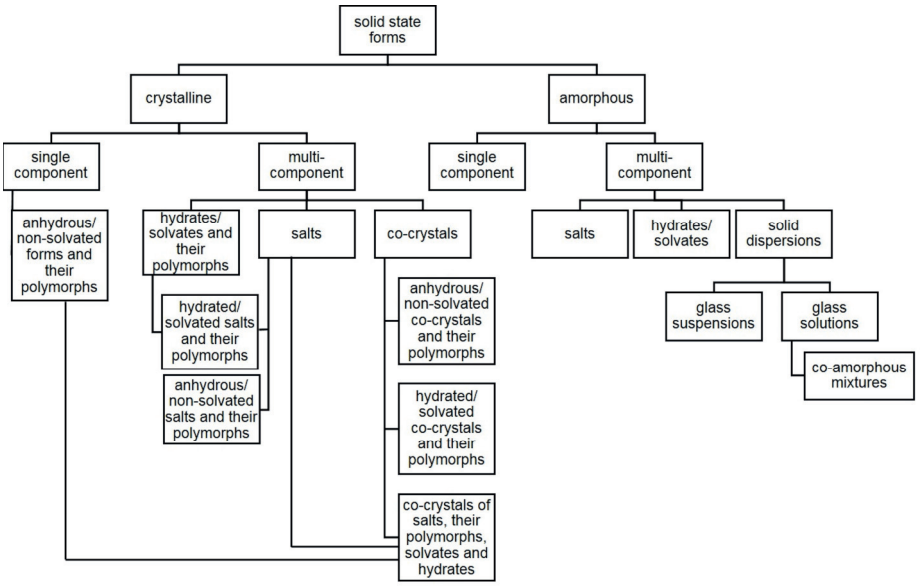

Figure 1 Different solid-state forms of pharmaceutical materials. Amorphous hydrates/solvates have variable quantities of water/solvent, they are not stoichiometric hydrates/solvates like the ordered crystalline ones. Modified from Healy et al., 2017 [1, 8, 21, 23].

Most organic crystalline compounds exhibit polymorphism [24]. Different polymorphic forms have the same chemical composition, but the orientational and positional order of the molecules that define the crystal structure varies. There is one thermodynamically stable polymorphic form at a given temperature and pressure, while all other crystal forms are metastable, and they will eventually convert to the stable form. At ambient pressure when the same solid state form is the stable form at all temperatures below its melting point, this is called monotropic polymorphism. In the alternative case of enantiotropic polymorphism, the stable form depends on temperature [2].

Both crystalline and amorphous solids can be composed of a single or multiple chemical components. Commonly encountered crystalline multicomponent solids include solvates and co-crystals. The term 'hydrate' is used when the secondary molecule is water [1]. Amorphous multi-component systems can be classified depending on e.g. the number of phases in the system (single-phase glass solutions and double-phase glass suspensions [21]), or the molecular weight of the co-former (low molecular weight for co-amorphous mixtures [23]).

An important difference between the solid-state forms (and a way to classify them) is the variation in the intermolecular interactions within the structures. The nature of the intermolecular bonds can be ionic or covalent

(e.g. hydrogen bonds, π-π-interactions) depending on the molecules involved, distinguishing salts from other multicomponent forms. The strength of the intermolecular forces varies between different polymorphs and the amorphous form of the same compound, because of differences in the functional groups involved and/or the distance separating the molecules. These interactions determine the thermodynamic parameters and many physicochemical properties of the compounds.

2.1.2 Significance in the pharmaceutical setting

Different solid state forms are a major concern in the pharmaceutical industry since they can significantly affect the drug product quality in terms of bioavailability, stability and processability, as well as having regulatory, legal and commercial (including intellectual property) implications [8, 9].

The difference in the intermolecular forces can result in significant variation of the physicochemical properties between different solid-state forms of a material. Collectively, the interactions are stronger in the thermodynamically stable crystalline form compared to metastable polymorphs or the amorphous form, which results in a higher melting point (for monotropic systems), but lower solubility and dissolution rate. Hydrates often show lower solubility compared to anhydrate forms [2]. The molecular order and packing can also affect the crystal habit and particle morphology, influencing mechanical properties such as powder flowability or compressibility [8, 25]. Amorphous materials are often more hygroscopic compared to crystalline forms. The powder characteristics and the performance of drug products can depend on the solid-state forms of both the APIs and excipients.

Considering the API, solid form selection has a crucial role in the development of a commercial pharmaceutical product [8, 9, 26]. Usually the thermodynamically most stable form is selected, in order to maximise the product stability. However, new drug candidates often present poor water solubility, and the dissolution rate may not be adequate to achieve good bioavailability. One strategy to improve the bioavailability with poorly soluble drugs is to select a metastable solid state form, or most commonly the unstable amorphous form [11]. The disadvantage with these forms is their inherently lower physical and chemical stability [8, 9]. Particularly hygroscopic amorphous materials demonstrate poor stability, since the absorbed moisture acts as a plasticizer, increasing chemical reactivity and the propensity to crystallise. Improved stability for the drug in the amorphous form may be provided by solid dispersion formulations, where the drug is molecularly dispersed with polymers [10, 11] or with low molecular weight compounds in co-amorphous mixtures [23]. In these approaches physical stability is still often a concern, however, since crystallisation of the drug during storage would negatively impact the therapeutic efficacy of the product.

With solid protein formulations, it is the solid-state form of excipients that may be crucial for product stability and performance. Stabilisation of proteins in the dried state usually requires interactions with stabilising excipients, only possible when the excipient and protein molecules both are in the same amorphous phase [27, 28]. Crystallisation of the stabilising excipient may lead to protein aggregation and loss of therapeutic activity [6, 29].

Where the solid state forms of the drug or excipients are critical to product stability or efficacy, they must be maintained appropriately through the drug product processing steps. However, it is not uncommon for solid-state transformations to occur during pharmaceutical processing or storage, and they are relevant concerns for the industry [12, 26, 30, 31]. Pharmaceutical manufacturing may involve several unit operations (e.g. milling, wet granulation, drying, tablet compression), which involve mechanical and thermal stresses, as well as exposure to solvents, which may induce various types of solid state changes (**FIG 2**).

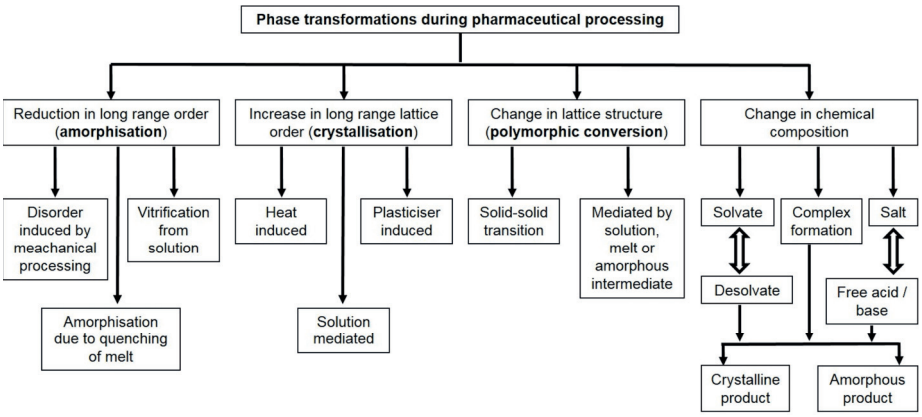

Figure 2 Process-induced solid-state transformations. Modified from Govindarajan and Suryanarayanan 2006 [32].

It is more common to obtain mixtures of solid forms rather than full conversions, with the occurrence of hydrate-anhydrate mixtures being one of the biggest challenges during routine processes [8, 26, 33, 34]. Furthermore, an issue concerning excipients in particular, is that the solid state form may vary between different suppliers [26]. The assessment of solid-state forms and their stability in solid dosage forms during manufacturing and storage, including early detection and quantification of transformations, is essential to ensure the quality of the final product. Process measurements that provide insight into events occurring during unit operations, as highlighted in the process analytical technology (PAT) concept [35], are valuable for understanding, controlling and optimising the processes, which are critical in ensuring product quality.

2.1.3 Solid-state characterisation techniques

Several solid-state analysis techniques are used to characterise pharmaceutical materials and monitor their behaviour in different processes and formulations. A combination of techniques is generally required, and the choices depend on the level of understanding needed. The most commonly used methods for solid state characterisation have been X-ray powder diffraction (XRPD), differential scanning calorimetry (DSC), mid-infrared spectroscopy (Fourier-transform infrared, FT-IR) and microscopy, which cover many physicochemical properties on both the molecular and particle levels [12]. Other routine techniques in pharmaceutical solid state analysis are Raman spectroscopy, near-infrared spectroscopy (NIR), solid-state nuclear magnetic resonance (ss-NMR) and thermogravimetric analysis (TGA) or dynamic vapour sorption (DVS). Spectroscopic methods are particularly useful as process monitoring and control (PAT) tools [36]. Analytical techniques important in pharmaceutical powder technology are listed in **Table 1**, categorised based on the properties investigated: molecular level (properties of individual molecules), particle level (individual particles) and bulk level (assembly of particles).

Distinguishing between amorphous and crystalline materials is one important goal. The difference (lack) in long range order of molecular packing can be observed with various methods, though sensitivity differs. Some general rules are that amorphous materials do not give peaks in XRPD diffractograms because of the lack of in-phase reflections from crystal planes. Crystalline materials have characteristic melting points (depending on the amount of energy required to break the attractive forces in the crystal lattice), but amorphous materials do not melt because there is no crystal lattice to break. Instead, amorphous materials show a glass transition (T_g) at the temperature where the material transforms from a glassy state (the solid-like form) to a supercooled liquid state (a viscous liquid-like form) on heating [22]. Amorphous materials can also be identified by other methods, including vibrational spectroscopy techniques, where the differences in intermolecular bonding between different solid state forms result e.g. in vibrational band broadening in the mid-frequency spectral region or in the absence of distinct features in the terahertz spectral region [37].

Table 1. *Characterisation techniques commonly used for solid-state analysis of pharmaceuticals. Modified from Chieng et al. 2011 and Heinz et al. 2009 [12, 30].*

Technique	Information provided	Advantage	Disadvantage
Molecular level			
Spectroscopic techniques			
Mid-IR (FTIR transmission, DRIFTS, ATR)	Intramolecular vibrations, H-bonding (dipole moment changes) **Polymorphic forms**: unique bands, peak shifting **Amorphous form**: band broadening	No sample preparation (ATR) Fast measurements Chemical identification Spatial information with imaging setups Complementary structural information to Raman spectroscopy	Solid-state transitions possible with sample preparation (transmission or DRIFTS modes) Interference from humidity and excipients
Raman	Intramolecular vibrations (polarizability changes) **Polymorphic forms**: unique bands, peak shifting **Amorphous form**: band broadening	No sample preparation Fast measurements Non-destructive Ability to penetrate through containers Insensitive to water Relatively insensitive to particle size Fibre optic probes available - PAT Chemical identification, and at low frequencies also lattice vibrations Spatial information with imaging setups Complementary structural information to IR spectroscopy	Local heating of sample Sample fluorescence Photodegradation
Near infrared (NIR)	Overtones and combinations of molecular vibrations (dipole moment changes) **Polymorphs and solvates**: band splitting, changes in molecular symmetry **Solvates**: loss of solvent bands during dehydration identification of different states of water **Amorphous forms**: band broadening, lack of low-frequency bands	No sample preparation Fast measurements Non-destructive Ability to penetrate through containers Fibre optic probes available – PAT Also particle size and, water content information Spatial chemical information with imaging setups	Low sensitivity and selectivity (low intensity) Subtle differences between solid state forms Affected by water and particle size
ss-NMR	Magnetic resonance Nuclei and chemical environment within a molecule Molecular dynamics Interactions: drug-drug or drug-excipient	Non-destructive Qualitative and quantitative without calibration	Long measurements Expensive
Particulate level			
Spectroscopy			
Terahertz pulsed spectroscopy (TPS) (transmission, ATR, specular reflectance)	Intramolecular and intermolecular, lattice vibrations (phonon modes) **Polymorphic forms and solvates**: unique peaks **Amorphous form**: no spectral features	Information about crystal structure Fast measurements No sample preparation (ATR)	Affected by water, particle size Spectra may be difficult to interpret Relatively expensive May require sample preparation

X-ray diffraction			
XRPD	Structural information **Polymorphic forms**: unique diffraction peaks **Amorphous form**: no peaks, broad halo	Standard method for crystal form identification Quantification of the degree of crystallinity Non-destructive	Affected by particle size and orientation (preferred orientation) No chemical information Probes not common
Single crystal XRD	Structural information	Traditionally used to solve crystal structures Non-destructive	Requires a single crystal of >0.1 mm size
Thermal and gravimetric analysis			
DSC	Thermal events: T_g, crystallisation, melting, heat capacity Interactions: drug-drug, drug-excipient (heat flow vs temperature)	Sensitive Qualitative and quantitative about relative stability	Destructive May be difficult to interpret Impurities can affect
Modulated-temperature DSC	As DSC, with separation into reversible and non-reversible thermal events	Allows better interpretation of small (T_g) and overlapping thermal events	More experimental variables Longer measurements Interpretation may not be straightforward
TGA/DVS	Transitions involving a change in mass (mass vs temperature or relative humidity)	Amount of solvates and hydrates in a sample Sensitive	Destructive Interference with water-containing excipients
Isothermal micro-calorimetry (IMC)	Heat change in a reaction: e.g. enthalpy relaxation of amorphous materials, heat of crystallization (heat flow vs time)	High sensitivity Qualitative and quantitative Stability studies	Low specificity Large sample amounts
Solution calorimetry (SC)	Heat change in a reaction: e.g. heat of solution, heat of wetting, heat capacity (heat flow during dissolution)	Qualitative and quantitative	Low specificity Large sample amounts Destructive Long measurements
Microscopy			
Polarized light microscopy (PLM)	Crystallinity (birefringence) Morphology, colour, crystal habit	Little sample preparation Easy	Not quantitative
With hot / cryo / freeze drying stage	Complementary information on phase transition/physical changes in frozen state	Temperature variability	Careful sample preparation required
Scanning electron microscopy (SEM)	Topographical properties	Higher spatial resolution than light microscopy	Sample preparation and condition setup (vacuum) required
Bulk level/other			
Karl Fischer titration	Water content	High sensitivity	Sample needs to dissolve in the medium Large sample sizes
Brunauer, Emmett and Teller (BET) method	Surface area	Simple analysis Non-destructive	Degassing step required Large sample sizes
Density (gas pycnometer)	True density of the sample (mass divided by measured volume)	Simple analysis Non-destructive	Degassing step required Large sample sizes

DRIFTS: diffuse reflectance Fourier transform infrared spectroscopy; ATR: attenuated total reflection

2.2 Protein pharmaceuticals

The pharmaceutical industry has shifted from a small molecule-centric focus to a portfolio with equal shares of small molecules and biologics, and most major pharmaceutical companies are now involved with development of biological drugs, particularly protein therapeutics [38]. Compared with small molecules, proteins are large, complex and unstable. The inherent instability poses challenges for manufacturing operations, handling and storage, since protein degradation can result not only into loss of therapeutic activity, but also increased potential of stimulating adverse immune responses, a unique safety concern for protein therapeutics [39, 40]. The rate of degradation can be controlled by choice of proper formulation excipients and conditions [41]. The formulation must maintain the safety and efficacy of the product throughout the commercial distribution system, with adequate shelf life [42].

2.2.1 Protein structure and stability

Proteins are very versatile biomolecules, composed of different amino acids joined covalently through peptide bonds to form long polymers with a molecular weight above 10 000 [43]. Smaller amino acid polymers are referred to as polypeptides. Proteins present several levels of structure: 1) the amino acid sequence (primary structure), 2) the regular arrangement of amino acid residues in a segment of the polypeptide chain (secondary structure), 3) the complete three-dimensional folding structure, and 4) the arrangement of subunits in case of multisubunit proteins (quaternary structure). The unique three-dimensional structure reflects the specific function of each protein.

The folding arrangement or conformation is stabilised by weak interactions, resulting in the inherent instability of proteins. The polymeric structure is flexible and different conformations are possible without breaking covalent bonds. With soluble, globular proteins (representing therapeutic proteins) the folded structure is typically characterised by hydrophobic amino acid residues buried in the core of the structure and their exposure to the solvent minimised, while the surface is dominated by hydrophilic groups. The major contributors to the thermodynamic stability of this so-called native structure are the hydrophobic interactions, while hydrogen bonds and ionic interactions may provide additional stability [43]. This structure has evolved to function in particular cellular or extracellular environments, and conditions different from those often result in structural changes. A change in structure sufficient to cause loss of function is called denaturation. Denaturation can be reversible, however the exposure and interaction of the hydrophobic patches often results in irreversible aggregation or precipitation. Aggregation is a major concern when handling proteins and in the development of stable protein therapeutics [42, 44].

All proteins are subject to various instabilities that can lead to aggregation or other structural damage (**FIG 3**). The degradation mechanisms can be

generally divided into two categories, physical and chemical instabilities, however they are usually interrelated [38, 45]. Physical instabilities refer to changes in structure not requiring covalent modifications, while chemical degradation involves bond formation or cleavage. The tendency for degradation depends on the individual sequence of a protein [46]. The susceptibility of different amino acids to chemical reactions and contribution to aggregation varies, and their position in the protein structure determines their availability for degradation processes. Degradation rates are also largely affected by external factors, such as temperature, pH, exposure to surfaces or mechanical stresses including agitation and high-shear environments (e.g. pumping, filtration, mixing, fill-finish processes), freezing and drying [42]. Furthermore, the protein concentration affects aggregation tendency.

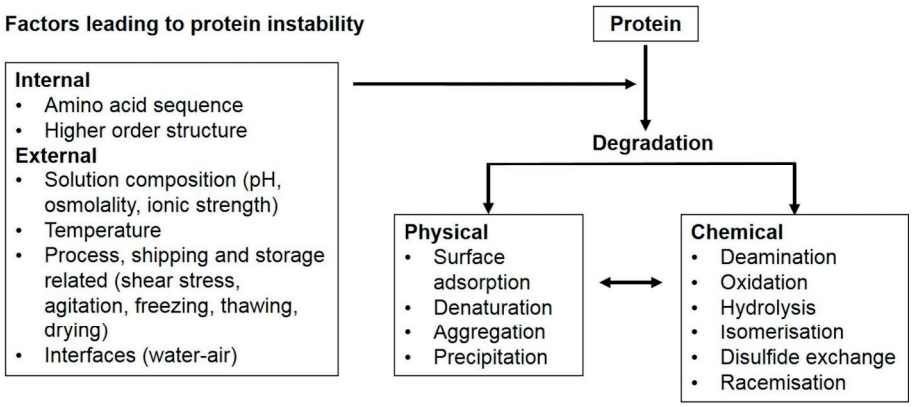

Figure 3 Common physical and chemical degradation mechanisms with pharmaceutical proteins. Modified from Ohtake and Wang 2014 [42].

2.2.2 Formulation strategies

The major aim for protein formulation development is to minimise the rate of all protein degradation processes and thereby optimise the stability of the native protein conformation during processing and storage, to meet the overall requirements for the target product profile [42, 46, 47]. Various excipients may be included in the formulation to protect the protein (**Table 2**). Liquids and freeze-dried solids present the two major product forms for commercial protein therapeutics. This is because most protein drugs are administered parenterally, and aqueous solutions are the standard formulation type in this context [48]. Approximately half of the commercial products are liquids and the other half are solid dosage forms prepared by lyophilisation [49]. Alternative manufacturing technologies, including spray drying, have been applied for the development of specific drug delivery options e.g., pulmonary or nasal delivery and parenteral depots [4, 46, 48].

Table 2. *Examples of formulation components in commercial pharmaceutical protein products, including cytokine, antibody (mAbs, fragment fusion proteins and conjugates), hormone and enzyme products [3, 46, 50].*

Category	Examples	Purpose
Buffers	acetate citrate succinate phosphate histidine glutamate Tris carbonate lactate	pH control
Salts	sodium chloride potassium chloride	Ionic strength and tonicity modifiers
Surfactants	polysorbate 80 polysorbate 20 poloxamer 188 SDS	Minimize aggregate formation at hydrophobic air-water interfacial surfaces. Poloxamer also increases viscosity, providing protein protection during agitation
Antioxidants	EDTA citric acid methionine tryptophan	Chelating agents (EDTA, citric acid) Oxygen scavengers (methionine, tryptophan)
Sugars, polyols	sucrose trehalose mannitol sorbitol maltose lactose	Protein stabilisers/lyoprotectants Lyophilisation bulking agents Tonicity modifiers
Amino acids	glycine histidine arginine lysine methionine	Protein stabilisers Buffer components Antioxidants Tonicity modifiers Bulking agent (glycine)
Polymers and proteins	polyethylene glycol human serum albumin	Protein stabiliser Lyophilisation bulking agents Increased viscosity, steric hindrance of protein-protein interactions, suppression of pH changes during freezing
Metal ions	zinc	Protein stabiliser (specific ligand)
Preservatives	benzyl alcohol m-cresol phenol	Prevent microbial growth in multi-dose products

EDTA: ethylenediaminetetraacetic acid, SDS: sodium dodecyl sulfate

Liquid formulations are typically preferred for products administered by injection due to simpler manufacturing and use, but they are generally less stable than solid dosage forms [42, 46]. Dried formulations are developed when the shelf life of the liquid dosage form is inadequate. Another reason for preparing dried products is when highly concentrated protein formulations are needed [48]. A general formulation strategy may proceed as outlined by Winter and Myschik 2012 [48]:

1) Buffer selection with adjustment to optimal pH and ionic strength, along with oxygen removal by nitrogen gassing may be sufficient to obtain a formulation with adequate stability. Multi-dose products require inclusion of a preservative.
2) If buffers and salts do not give sufficient stability (commonly presented as protein aggregation, oxidation or fragmentation), more active formulation measures are needed. Typically the next step is the addition of surfactants and antioxidants or chelating agents (methionine or EDTA).
3) If instability persists, additional stabilising excipients are required. Sugars, polyols, and amino acids (particularly glycine) are often used to stabilise proteins in aqueous solution. It is believed that these compounds (co-solutes) provide active stabilisation of the native conformation by the so-called preferential exclusion mechanism [51]. According to the theory, co-solutes inhibit protein unfolding by increasing the free energy difference between the native and unfolded states, thereby making the free energy of denaturation greater and thermodynamically unfavourable. In order to do this, there must be a high enough concentration of co-solutes and they must be preferentially excluded from the protein surface (i.e. not interact strongly), leaving the surface to be hydrated by water. As a result, the protein is surrounded by more structured water, leading to a decrease in system entropy. Unfolded states of the protein have larger surface areas exposed to the solvent compared to the native state. Denaturation would therefore lead to an even greater decrease in entropy, and thus the equilibrium between conformations shifts to more substantially favour the native state. Some stabilisers like arginine may also prevent aggregation and increase protein solubility through direct interactions [52, 53].
4) If long-term stability cannot be obtained in liquid formulation even with stabilisers, a dried (lyophilised) formulation may be developed. Similar formulations as with liquid products are used, however the freezing and drying as well as storage in the dried state may result in additional demands concerning the solid state properties of the formulation components. Crystallisation of buffer components causing pH shifts (particularly common with phosphate buffers) or other excipients can reduce product stability. With lyophilised formulations, a bulking agent is always required to confer an acceptable cake of high quality and production of a uniform powder that can easily be reconstituted [42, 49]. Mannitol and glycine are commonly used for this purpose. However, they might not provide sufficient stability to the protein in the dried state, since they crystallise during lyophilisation. Additional stabilising excipients (e.g. disaccharides or polymers) which remain amorphous are often required [49]. The relative amount of formulation components needs to be optimised, since they affect each other's solid state behaviour and stability (as well as tonicity) of the protein product.

2.2.3 Carbohydrates as stabilising excipients in dried formulations

Drying improves the shelf life stability of protein products because the removal of water decreases chemical degradation rates. Certain physical stresses, e.g. agitation and air-water interfacial stresses during shipping and storage, are also alleviated compared to liquid products, and dried products have better stability against temperature excursions [45]. However, drying and storage in the dried state causes other major stresses to proteins [41, 54, 55]. The main contributor affording thermodynamic stability to the native conformation (limiting solvent exposure of hydrophobic groups) is lost when the protein molecule is no longer in its natural aqueous environment. This increases the probability of unfolding. Since drying also results in a protein concentration increase, interactions between unfolded proteins become more probable than in dilute aqueous solutions, making aggregation a likely outcome. To stabilise proteins against these drying stresses, stabilisers called lyoprotectants are often needed. Carbohydrates generally perform well in this role [51, 54-56].

For optimal stabilisation efficacy, it is important for the stabilisers to be in the amorphous form and in the same phase with the proteins [27, 28, 57]. This allows kinetic immobilisation of the proteins in the glassy matrix, which inhibits molecular mobility, including unfolding, and protein-protein interactions that could lead to aggregation. Both polymeric and smaller carbohydrates can form such matrices.

However, disaccharides are the first choice for protection of solid protein formulations during storage [42, 49, 55]. This is because the glassy state is not sufficient for optimal stabilisation, but additionally direct coupling between the excipient and protein is important [57]. It is believed that the hydroxyl groups of carbohydrates hydrogen bond with the protein, and thus replace the interactions lost during removal of the hydration layer [54]. Protein stabilisation efficacy is dependent on excipient molecular weight, and larger molecules (with the same functional groups, e.g. dextran) commonly provide less efficient stabilisation [3, 58-63]. Smaller carbohydrates can get closer to the protein surfaces than polymers, and can thus better provide direct interactions. Additionally, there is less free space for protein mobility in the solid with disaccharides than with polymers.

The two requirements for stabilisation are interrelated. The amorphous structure allows more intimate contacts between the proteins and stabilisers and a higher possibility for the direct interactions, since the molecule positions are less constrained. There are also more hydroxyl groups available for interactions with the protein since they are not occupied in crystalline intermolecular interactions.

Among disaccharides, trehalose and sucrose are the common choices in commercial protein products [42, 44, 46, 49]. One reason for this is that they are non-reducing sugars, which is preferable for protein formulations, to reduce the risk of chemical degradation of proteins via the Maillard reaction route. However, the reducing sugars lactose and maltose have also occasionally been used in products (maltose with mAbs [46] and lactose with

an enzyme [3]) and they can provide equally good stabilising efficacy as trehalose [46].

Another reason for choosing trehalose and sucrose is that they both have a relatively high T_g for a sugar [64] and they do not crystallise easily during lyophilisation [46]. However, trehalose and sucrose crystallisation and resultant protein aggregation may happen during storage or further processing [5, 65]. Particularly with spray-dried formulations, ratios of sucrose or trehalose to protein that are too high can decrease protein stability during storage due to crystallisation [6, 29, 66].

2.2.4 Isomalt and melibiose

Isomalt is a polyol derived from sucrose, and produced by hydrogenating the disaccharide isomaltulose [67]. It is used in the food and pharmaceutical industries, e.g. in sugar-free products and as a tablet excipient [67-70]. Isomalt is a mixture of two diastereomers: 1-*O*-α-D-glucopyranosyl-D-mannitol (GPM) and 6-*O*-α-D-glucopyranosyl-D-sorbitol (GPS). The physicochemical properties are similar to those of sucrose and depend on the isomalt composition (ratio between GPM and GPS). Isomalt is not subject to the Maillard reaction, making it attractive for protein formulations. Studies investigating isomalt in dried protein formulations are limited, but it has shown some potential for protein stabilisation in freeze-dried formulations during storage [71].

Melibiose is a disaccharide, naturally present in e.g. honey and many plants, but industrially produced by enzymatic hydrolysis of raffinose, a trisaccharide found e.g. in agricultural by-products such as cottonseed and bean pulp [72, 73]. Melibiose is a reducing sugar and it is not commonly used with dried protein formulations. However, it can stabilise proteins in lyophilised protein formulations, and no evidence of Maillard reaction-based protein degradation was observed during a three-month study with monoclonal antibodies [74, 75]. The structures isomalt, melibiose, sucrose and trehalose are shown in **FIG 4** and some properties listed in **Table 3**.

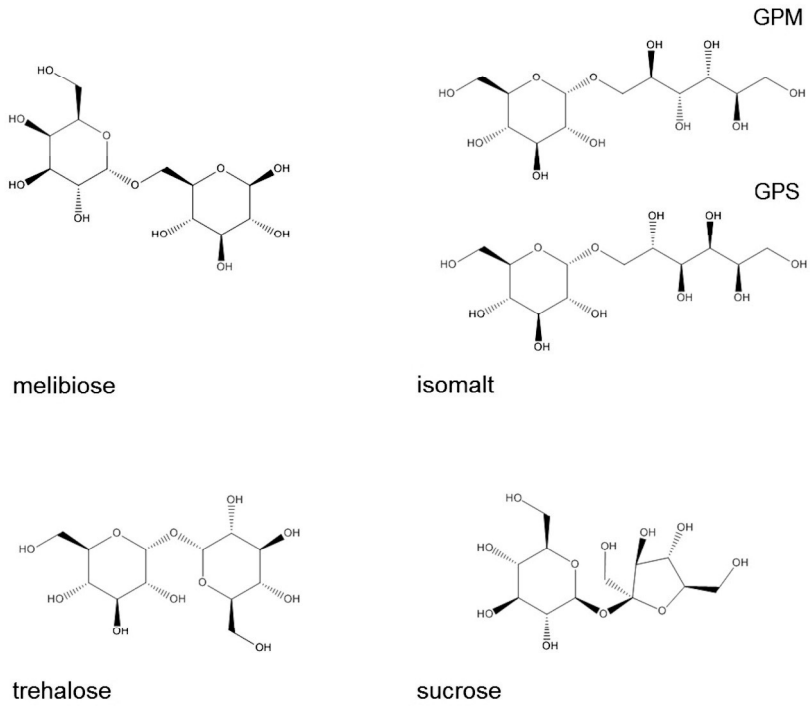

Figure 4 The molecular structures of melibiose, isomalt, trehalose and sucrose. Isomalt is a mixture of two diastereomers: gluco-mannitol (GPM) and gluco-sorbitol (GPS).

Table 3. *Properties of isomalt, melibiose, sucrose and trehalose. References: PubChem, CCDC, Handbook of Pharmaceutical excipients, and isomalt: [67, 76-78], melibiose: [72, 79-81], sucrose: [81, 82], trehalose: [64, 65, 83]*

	Isomalt	**Melibiose**	**Sucrose**	**Trehalose**
Description	Non-reducing mixture of disaccharide alcohols GPM and GPS	Reducing disaccharide of galactose and glucose with α-1,6-linkage	Non-reducing disaccharide of glucose and fructose with a α-1-2 -linkage	Non-reducing disaccharide of two glucose units with α, α-1,1-linkage
Chemical formula and molecular weight (anhydrous)	$C_{12}H_{24}O_{11}$ 344.3	$C_{12}H_{22}O_{11}$ 342.3	$C_{12}H_{22}O_{11}$ 342.3	$C_{12}H_{22}O_{11}$ 342.3
Solubility	soluble in water	soluble in water	soluble in water	soluble in water
T_g (°C) (anhydrous)	59 (isomalt 1:1) 55 (GPS) 66 (GPM)	100	60 [Ref. 82] 74 [Ref. 81]	120
Crystalline forms and their melting points (°C)	Isomalt (142) GPM dihydrate (166) GPS anhydrate (168)	α-melibiose monohydrate (179-186), stable form β-melibiose dihydrate (85-86)	anhydrate (160-186)	dihydrate (97-100; dehydration), stable hydrate form β–anhydrate (205-215), stable anhydrous form α–anhydrate (126) γ form[a] (120; transition to β anhydrate)

[a] Possibly a mixture of the dihydrate and β-anhydrate forms.

Neither isomalt nor melibiose are currently used in commercial pharmaceutical protein products. Their safety and toxicological aspects have not been fully characterised in terms of possible use as stabilising excipients for protein products, typically administered via the parenteral route.

Isomalt has regulatory approval as a food additive in all major regions of the world [67, 84]. It is also used as an excipient in pharmaceutical products approved in the US and in EU countries [85, 86], and it is included in the European and US pharmacopoeias [87, 88]. Isomalt has been found safe when administered orally, also considering chronic toxicity [89-92]. The safety of parenteral administration of isomalt is less studied, but regarding acute toxicity, the LD50 dose in rats has been reported to be over 2500 mg/kg when administered intraveneously or intraperitoneally [93].

The toxicological aspects of the use of melibiose are less studied. It does not have regulatory approval for use as an additive in food or drug products. However, melibiose occurs naturally in food products consumed by humans, including honey, cacao and soy beans [94-96]. It has also been described as a hydrophilic skin permeation enhancing agent in topical cosmetic formulations [97]. No hazard notifications are associated with melibiose in the European Chemicals Agency (ECHA) substance information database [98].

Melibiose is indigestible by humans, and the consumption of large doses can have laxative effects, similar to other indigestible sugars. For this reason melibiose has been used in intestinal permeability tests, where 5 g melibiose doses have been orally administered to paediatric patients [99]. In this test, the detection of melibiose in urine is a sign of decreased intestinal integrity (bowel disease), but the test itself was not reported to have toxic effects.

On the other hand, gut microbes can metabolise melibiose. Dietary melibiose has been proposed to act as a prebiotic and modulate the intestinal flora by supporting the growth of lactic bacteria (particularly bifidobacteria), thereby possibly acting towards inhibition or alleviation of allergic symptoms. Induction of immunological tolerance to orally administered antigens by dietary melibiose has been demonstrated in mice [100].

Data on the safety of parenteral administration of melibiose is limited. The pharmacokinetics of melibiose has been studied in rats, where melibiose was administered intraveneously as a single bolus dose (100 mg/kg), without reported side effects [101]. Melibiose has also been administered to mice as intraperitoneal injection for consecutive 7 days (24 mg/kg/day) [102]. In this study by Lee et al. 2015, melibiose was shown to have similar autophagy-inducing and polyQ aggregation inhibiting activities as trehalose, and was proposed to have potential pharmaceutical use in polyQ-mediated neurodegenerative disease treatment. No toxicological effects were reported.

Conclusive toxicological studies would be needed to prove that a new excipient is safe for human use in pharmaceutical products. Such studies would be very expensive. To ensure that the tests would be worth conducting, it would be useful to have strong proof that a new excipient provides advantages over the current selection of already approved excipients.

2.3 Spray drying

Spray drying is a process that converts solutions or suspensions to powders composed of microparticles. Development of the technology was driven by World War II, when huge amounts of food needed to be transported, which created requirements for better conservation and reduction of the weight and volume of the food products [103]. Today, spray drying is a widely used technology in various fields of industry, including the pharmaceutical industry [104, 105].

The main advantages compared to other drying techniques (including lyophilisation) are the short process cycle time, scalability, possible energy savings, and the ability to engineer particles with different physical properties by controlling the process variables [106-108]. Spray drying enables 1) the manufacturing of particles in the size range of 1-100 μm mean particle diameter with a narrow size distribution, 2) very fast solvent evaporation to produce amorphous solids, 3) control of the drying rate to adjust particle properties e.g. solid state form, particle size, morphology, density and 4) control of the surface composition.

As a result, there are several applications in pharmaceutical technology including production of amorphous excipients and active ingredients to improve their properties (e.g. lactose with better compressibility; improved solubility and bioavailability APIs), particles for pulmonary and nasal delivery, modified-release particles (via microencapsulation) as well as dried biopharmaceutical products and vaccines [4, 104, 106, 108-110].

2.3.1 The spray drying process

The underlying principle of spray drying is simple: a feed liquid is atomised into fine droplets, which are immediately exposed to a heated gas stream. The very large surface area of the atomised droplets allows efficient heat transfer from the drying gas to the liquid. The solvent evaporates rapidly and solid matter precipitates to form particles, which are then separated from the air stream and collected as the dried product [4, 103, 108]. Different designs are available for atomising the liquid stream (e.g. rotary atomisers and pneumatic [gas-assisted], hydraulic [high-pressure] or ultrasonic nozzles), powder collection (e.g. cyclones or bag filters), and mass flows in the drier (orientation of the atomiser in relation to the drying gas flow: co-current, counter-current, or mixed flow). A schematic of a co-current spray-drier with a two-fluid pneumatic nozzle atomiser and a cyclone is shown in **FIG 5**.

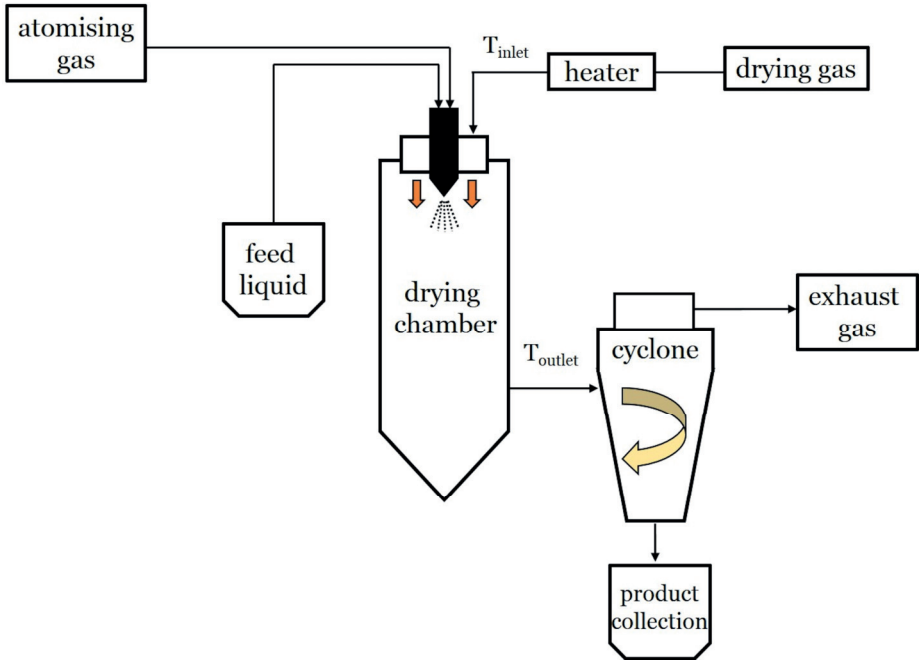

Figure 5 **Schematic diagram of a spray drying process**.

Despite the superficially simple principle, spray drying has also been described one of the most complicated types of drying [103]. There are several process variables, of which the operator can directly influence only some, including the inlet temperature of the drying gas (T_{inlet}), the drying gas flow rate, the liquid feed rate and the atomisation rate. The other process parameters that affect the process outcome, including the outlet temperature of the drying gas (T_{outlet}), the droplet size, the drying efficiency and the physical properties of the dried particles (e.g. particle size, moisture content, hygroscopicity), cannot be directly set but are dependent on the mutual relationships of the parameters adjusted by the operator, environmental conditions and material properties. The complex network of some factors affecting the spray drying process in shown in **FIG 6**.

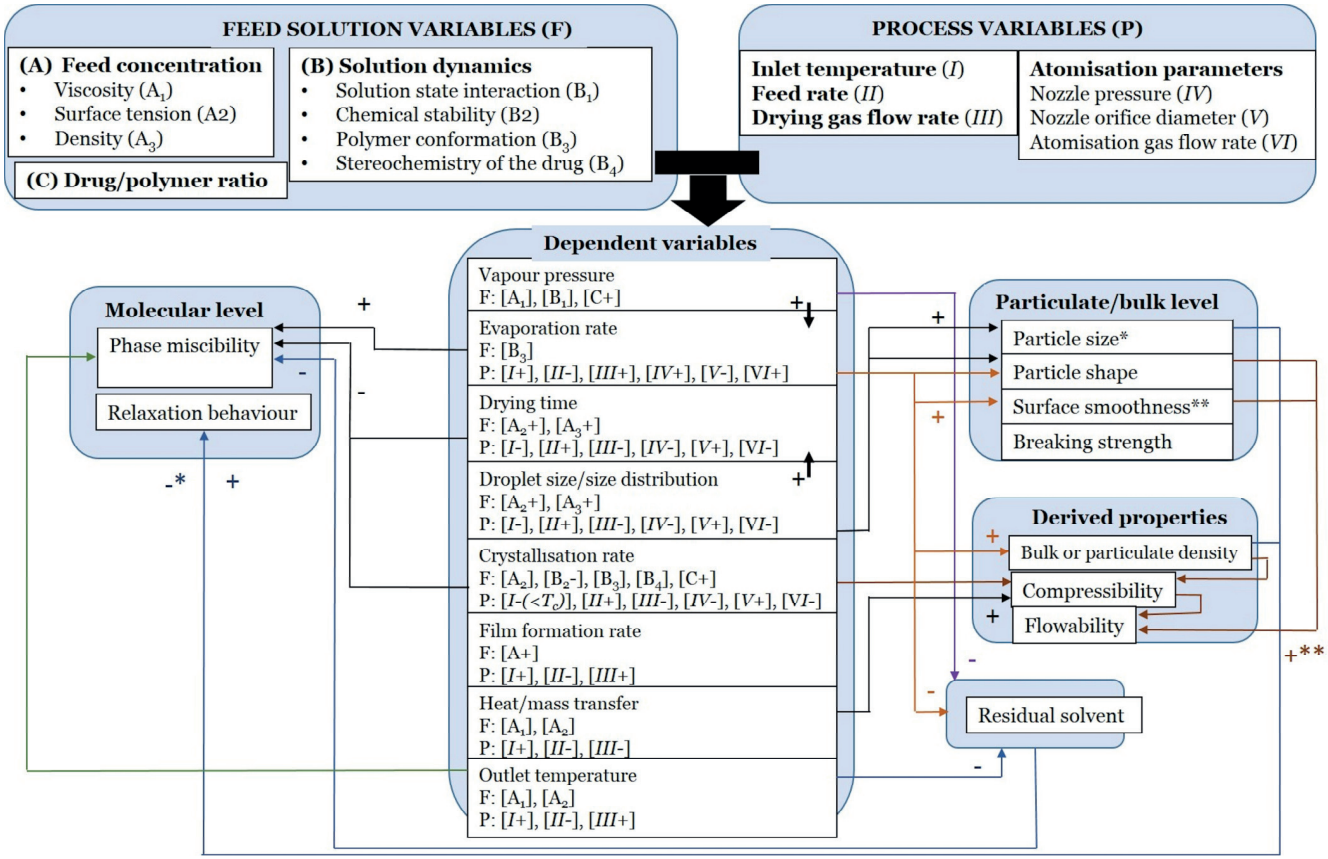

Figure 6 The influences of feed solution and process variables on the underlying processes during spray drying and on some properties of a spray dried dispersion product. (+): directly related, (-) inversely related, T_c crystallisation temperature. Modified from Paudel et al., 2013 [111].

The factors affect the final powder properties through influencing the drying of the droplets and particle formation [4, 112-115]. The drying stages of a droplet can be divided into initial, constant and falling rate periods, during which the droplet temperature changes (**FIG 7**). During the initial period, solvent evaporation is rapid and mainly controlled by the relative humidity, temperature and velocity of the drying gas surrounding the droplet. The droplet surface temperature increases to the lowest temperature that allows solvent evaporation, and the surface maintains 100% relative humidity (at the droplet surface and surrounding vapour cloud temperature which are equal).

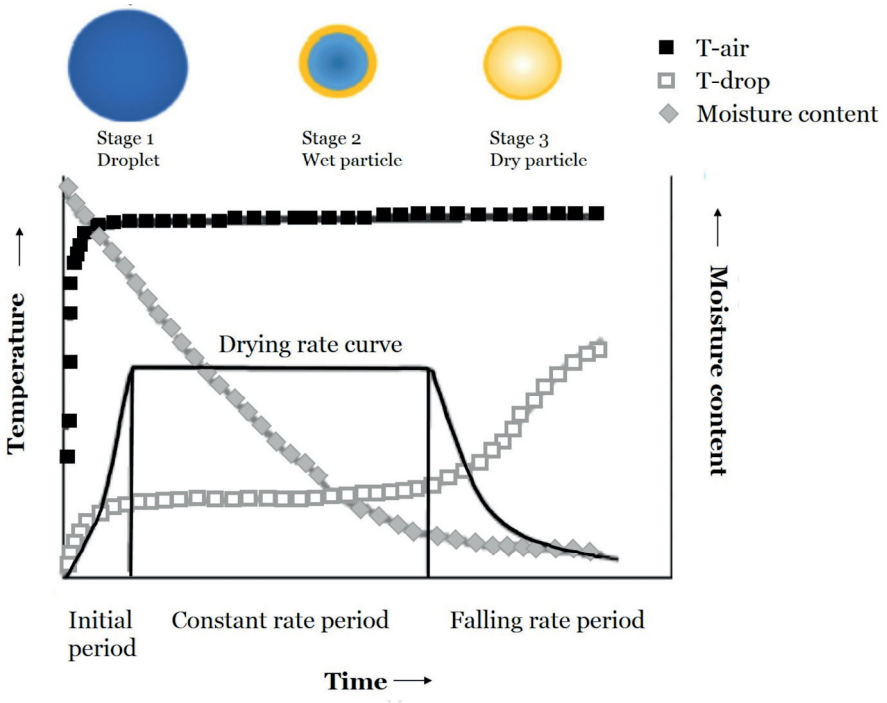

Figure 7 A typical drying curve, showing the different drying stages, the temperature of drying air, and the temperature and moisture content of the drying droplets. The drying curve is very much dependent on feed composition and process parameters. Modified from Haque and Adhikari 2015, and Singh and Van den Mooter 2016 [113, 116].

By the constant rate period, a concentration gradient has formed due to the solvent evaporation from the droplet surface. This initiates diffusion of the droplet components: the solutes migrate from the highly concentrated exterior towards the core of the droplet and the solvent moves outward. Simultaneously, evaporation occurs, which results in both evaporative cooling (keeping the droplet temperature constant) as well as shrinking of the droplet, as the surface recedes towards the centre. The solute usually diffuses slower than the solvent, resulting in increasing viscosity at the surface which further

restricts all diffusion, and ultimately the solute concentration reaches the solubility limit and solidification begins. By the end of this period, a solid shell or crust has formed around the still wet interior.

During the falling rate period, the evaporation rate falls because of the suppressed diffusion of water through the growing shell on the surface, and the droplet temperature begins to increase. However, even at the final drying stage, the product temperature never reaches the T_{inlet} but in practice remains below the T_{outlet} [4, 103].

The final particle shape and moisture content depend on the drying rate and the diffusion coefficient of the solutes, as well as the crust properties, such as permeability. When the diffusion of the solutes is faster than evaporation and surface recession, dense, solid particles with uniform composition may be formed. In contrast, when the diffusion of the solutes is slower than evaporation (i.e. with larger molecules and/or fast drying rates), surface enrichment occurs earlier, which can lead to the formation of either hollow spherical or irregular (e.g. folded, wrinkled) particles, depending on the rigidity and porosity of the formed shell. In case there are different solute molecules in the feed, separation of the components is possible, resulting in multi-layered particles. Relationships between process parameters and resulting particle properties are listed in **Table 4**.

Table 4. *The effect of spray drying process parameters on particle properties with solid dispersions. Modified from Vasconcelos et al. 2016 [11].*

Parameter (increase)	Particle size	Particle porosity	Particle moisture	Particle smoothness	Powder yield
T_{inlet}	Increase	Decrease	Decrease	Decrease	Increase
Drying flow rate	Decrease	Increase	Decrease	Increase	Increase
Feed rate	Decrease	Decrease	Increase	Increase	Decrease
Humidity	Increase	Increase	Increase	Decrease	Increase
Increase in droplet size	Increase	Increase	Increase	Decrease	Increase
Solid content in feed liquid	Increase	Decrease	Decrease	Decrease	Increase
Solution viscosity or surface tension	Increase	Decrease	Increase	Decrease	Increase

2.3.2 Spray-dried proteins

Lyophilisation is the standard drying technology with protein formulations, but spray drying is increasingly used in the biopharmaceutical industry [4, 108]. There are numerous examples of spray-dried proteins and polypeptides, e.g. insulin, haemoglobin, albumin, β-galactosidase, lactate dehydrogenase, trypsin, tissue-type plasminogen activator, monoclonal antibodies, growth hormone, calcitonin, parathyroid hormone, and rhDNase, excellently reviewed in Searles and Mohan 2010 [106]. There have been at least two commercial spray-dried insulin powders for inhalation (Exubera and Afrezza),

as well as a thrombin-fibrinogen powder (Raplixa) for controlling bleeding during surgery [117-120].

Spray drying is an attractive alternative to lyophilisation because of the general reasons mentioned above, including the process being faster and more scalable, as well as allowing control of particle properties and direct particle generation in a single unit operation. These advantages makes the technology much more suitable for production of products for pulmonary or nasal delivery. However, spray drying may also provide better stabilisation with some proteins, since the freezing step and the related risks of protein degradation (caused by ice surfaces, formulation component crystallisation and phase separation) is avoided. In addition to final dosage form production, spray drying is also an alternative for bulk intermediate production for storage, which is traditionally done by freezing, offering convenience for transportation and time savings since the thawing step following freezing is avoided [121]. Spray dried bulk intermediates would also allow admixing with other powders to obtain the final drug product, without the complexity of designing a liquid formulation for multi-dose products or the additional freeze drying step [106].

Spray drying poses several stresses to proteins, however. These include elevated temperatures, shear stresses, air-water surfaces and drying. Of these, heat stress can be negligible with many proteins since the drying temperature is adjustable, the time-scale of heat exposure can be short and the product temperature may remain relatively low because of the efficient evaporative cooling [4, 104]. The interfacial stresses can be significant because of the very large surface area of the atomised droplets. Drying is another major instability factor. Therefore, protein-stabilising excipients are usually required.

There are occasional examples where proteins have been successfully spray-dried without excipients, e.g. insulin [122] and crystallised trypsin [123], however, excipients are usually essential to protect the protein from the spray drying stresses. Both sucrose and trehalose are commonly used [6, 7, 124-130], and out of these trehalose has become the standard as the carbohydrate protein stabiliser with spray drying [121].

For efficient stabilisation, the protein and excipient must remain in the same amorphous phase. There is a risk of separation of the low-molecular-weight excipients from the high-molecular-weight proteins as a result of the particle formation process [107]. Proteins tend to accumulate on the drying particle surfaces since they have lower diffusion coefficients than the other components, and they may additionally be surface active, a quality shared by many proteins. It may happen that in the final product there is a large fraction of protein at the dry particle surface, not encapsulated in the sugar matrix [112]. Surface activity is very protein-dependent and the solute separation may be controlled by adjusting the drying rate (slower rates result in more even distributions).

2.4 Raman spectroscopy for solid-state analysis

2.4.1 Raman spectroscopy

Raman spectroscopy involves illuminating a sample with monochromatic laser light and detecting the inelastically scattered photons [131]. These Raman scattered photons have different energies compared to the single-frequency light source, because of energy exchange between the sample molecules and the incident photons, resulting in a series of Raman shifts which are dependent on the molecular vibrations (e.g. stretching or bending of chemical bonds) and rotations occurring in the sample. Therefore Raman spectroscopy is a vibrational spectroscopy technique and it gives information on the functional groups present and their chemical environments, dictated by the molecular conformation and interactions with neighbouring molecules. This allows both identifying the analytes, as well as distinguishing different solid-state forms of the same chemical entity [17].

When light interacts with matter, Raman scattering is a very unlikely event [131]. The great majority of the incident photons that scatter from the sample will not exchange energy with the molecules. This elastically scattered light is called Rayleigh scattering, and it needs to be efficiently removed in order to observe the intrinsically weak Raman signal. In Raman spectrometers this is achieved by laser rejection filters. The filters only allow light that has a different frequency than the laser to be detected, and enables the observation of the Raman spectrum, containing the informative Raman bands (**FIG 8**). Usually, Raman spectra represent the Stokes Raman scattered photons, which have transferred energy to the molecules. In most situations, there are symmetric but much less intense bands on the other side of the laser line, caused by opposite energy transfer which is a very rare event in normal conditions, called anti-Stokes Raman scattering.

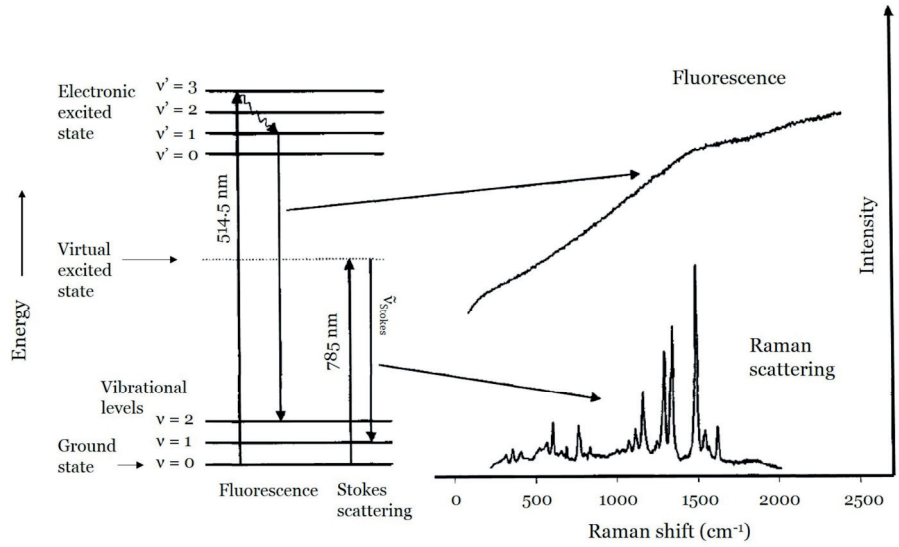

Figure 8 Energy levels associated with Stokes Raman scattering and fluorescence, and the corresponding signals. In the example a fluorescent sample is illuminated with either 514.5 nm or 785 nm light. The energy and intensity axes are not to scale, and the fluorescence intensity is several orders of magnitude greater than Raman scattering. Raman shifts appear at the same position irrespective of the incident light wavelength (always 0 cm^{-1}). ν is the vibrational quantum number. Modified from McCreery 2000 [131, 132].

Another phenomenon that can occur upon photon interaction with molecules, which can complicate the detection of the Raman signal, is fluorescence. Fluorescence involves photon absorption and transition of the molecule to an electronically excited state, and subsequent vibrational relaxation and emission. It may occur when the energy of the incident photon corresponds to the energy gap between the ground state and an excited electronic state of the molecule, and therefore it is dependent on the laser wavelength and the molecular structure of the analyte. When fluorescence appears, it can leave the Raman bands fully undetectable, since it is a stronger event (**FIG 8**).

Assuming negligible absorption and additional scattering interactions of the Raman scattered photons with the analyte, Raman scattering intensity is directly proportional to the number of molecules sampled, giving the basis for quantitative Raman analysis [17]. The intensity of a Raman band is also dependent on the change in the electronic polarisability of the molecule during the vibrational mode [131]. When the electron density distribution surrounding a molecule or a bond is easily distorted during a vibration, large polarisation changes occur and strong Raman bands may be observed. This selection rule for Raman activity results in Raman and infrared (IR) spectroscopy being complimentary techniques. Symmetric vibrations, non-polar bonds and molecules with extended π systems (delocalised electron systems, e.g. conjugated aromatic rings) can give strong Raman scattering (but

weak IR absorption, since IR requires a dipole moment change), while asymmetric vibrations and polar bonds (e.g. O-H) give weak Raman scattering (but strong IR signals). This is convenient for pharmaceutical analysis, since many active pharmaceutical ingredients (API) contain aromatic conjugated rings and give strong Raman signals, while water and many excipients are weak Raman scatterers [14]. Therefore, Raman signals of the API can often be collected without significant interference from excipients or aqueous environments. Some other advantages and disadvantages of Raman spectroscopy compared to other analytical techniques are listed in **Table 1.**

The versatility of Raman spectroscopy has resulted in its wide use in the pharmaceutical industry covering various analytical needs from the early drug discovery and development phases, through product manufacturing to quality control of finished products [13]. Some applications include solid form screening, API degradation analysis in different conditions, monitoring fermentation or crystallisation processes, raw material qualification, investigating the distribution of components e.g. in solid dispersions or lyophilisates, getting insight to drug dissolution behaviour or transportation to target tissues, content analysis of packaged products and counterfeit identification [13, 132].

A major application area is the detection and monitoring of solid-state transformations, which is routinely used in pharmaceutical manufacturing and quality control [30]. Polymorph conversions, transitions between solvated and non-solvated forms, amorphisation and recrystallisation of amorphous systems can all be evaluated [30].

The combination of the advantages of Raman spectroscopy (e.g. non-destructive, non-contact and fast measurements) makes the technique very suitable for monitoring the production of pharmaceutical solid dosage forms, and it is widely used as a PAT tool [36, 133]. Examples of in-process monitored events during unit operations include: blend homogeneity during blending, hydrate formation during granulation, phase transformations during drying, determining coat thickness and composition during tablet coating, solid state changes during pelletisation, and solid state conversions and process phase endpoint detection during freeze-drying [133]. Real-time monitoring and control of continuous pharmaceutical production processes are a major interest within the pharmaceutical industry [133]. Monitoring transitions requires reliable quantitative analysis of the collected spectral data. The inherent disadvantages of Raman spectroscopy, namely low sensitivity and fluorescence interference, may negatively impact the quality of such analyses.

2.4.2 Low-frequency Raman spectroscopy

The vibrations observable by Raman spectroscopy are not limited to intramolecular bond vibrations, intermolecular vibrations also occur. The latter are known as lattice vibrations or phonon modes in crystalline solids, and they are caused by many atoms or molecules in a crystal oscillating

coherently at the same frequency [15]. Lattice vibrations are directly related to the long range order and can be used to probe the solid-state structure of materials [134]. Different crystalline forms have distinct phonon spectra with sharp features corresponding to the lattice vibrations, while amorphous solids have no phonon peaks and only show an inhomogeneous broadening of features, sometimes called the Boson peak, similar to XRPD [134, 135]. The lattice vibrations have low energy, with small shifts from the laser frequency at the terahertz frequency region (below 100 cm^{-1}), in contrast with the intramolecular vibrations, which appear in the mid-frequency spectral region (usually between 500-2000 cm^{-1}) [14]. Raman scattering analysis of the low-frequency vibrations is therefore called low-frequency or terahertz Raman spectroscopy.

With conventional dispersive Raman instruments, the low-frequency shifts are normally blocked by the laser rejection filters together with the Rayleigh scattering. Spectrometers differ significantly in their ability to detect Raman shifts below 300 cm^{-1} [131]. The best notch filters today may allow spectral collection down to 50 cm^{-1} [13], but generally spectral data below 150 cm^{-1} is not observed with a standard Raman instrument [136]. Nevertheless, the detection of the full low frequency spectrum requires more sophisticated instrumentation compared to the established technology. Recent technological advancements, particularly related to volumetric holographic grating notch filters, stable diode lasers and amplified spontaneous emission suppression filters [137, 138], have made low-frequency Raman spectroscopy more practical and widely accessible than in previous decades.

Driven by these technical advancements, commercial and affordable low-frequency instruments have lately become available, which has made the technique attractive for pharmaceutical research applications [139]. Low-frequency Raman spectroscopy has been used for different solid-state analytical purposes, including identification of drug and excipient polymorphs and polymorph screening [15, 140-143], tablet composition analysis [144], evaluating crystallisation of amorphous systems [134, 136, 145, 146] and other solid-state changes [145, 147-150].

Despite such studies demonstrating the feasibility of low-frequency Raman spectroscopy for solid-state analysis, including quantitative applications [134, 136, 145, 147], low-frequency Raman spectroscopy is not yet a routine technique in pharmaceutical solid state analysis. Instead, the conventional instruments and mid-frequency region is normally used. Solid-state forms can often be distinguished and quantified using this spectral region dominated by intramolecular vibrations, because of the changes in local environments of the bonds within the molecules [17]. Still, this provides only an indirect measure of solid-state structure, and with some materials the mid-frequency spectral differences between solid-state forms are very subtle or even completely indistinguishable [141, 142, 145, 147, 149, 151]. Since low-frequency Raman spectroscopy measures the fundamental intermolecular modes, it is much more sensitive to intermolecular interactions [135]. However, studies directly

comparing the use of these two spectral regions for analytical purposes are limited, and it has not yet been thoroughly demonstrated that the additional spectral information obtainable by low-frequency Raman spectroscopy would provide additional value for routine solid-state quantification purposes.

2.4.3 Time-gated Raman spectroscopy

The elevated background signal induced by sample photoluminescence such as fluorescence (**FIG 8**) can inhibit or affect the reliability of analysis based on Raman bands, and restrict the use of Raman spectroscopy in applications involving fluorescent or otherwise photoluminescent materials. There are numerous methods that can be used to reduce the effect of fluorescence, including photobleaching, the use of longer excitation wavelengths (near-infrared 1064 or 785 nm lasers), frequency-domain methods (phase-modulation), shifted excitation Raman difference spectroscopy (SERDS), surface-enhanced Raman spectroscopy (SERS), nonlinear techniques e.g. coherent anti-Stokes Raman spectroscopy (CARS) or stimulated Raman spectroscopy (SRS), spatially offset Raman spectroscopy (SORS, [152]), computational methods (i.e. fluorescence removal by spectral processing), and time-resolved Raman spectroscopy [153].

Time-resolved methods rely on the different average lifetimes of Raman-scattered and fluorescence photons (**FIG 9)** [154]. Raman scattering occurs practically instantaneously during excitation, while the lifetimes of fluorescence signals are generally significantly longer [16]. This is because fluorescence involves a number of events: the absorption of one or more protons to excite the molecule to an electronic excited state, followed by internal conversions which can include various molecular changes at different time scales, before de-excitation and emission of the fluorescent photons [155]. The average time required for completion of all these events is considerably longer (typically in the nanosecond range from excitation) than for Raman scattering (in the picosecond range) [155]. With conventional Raman instruments, all these photons will contribute to the spectrum.

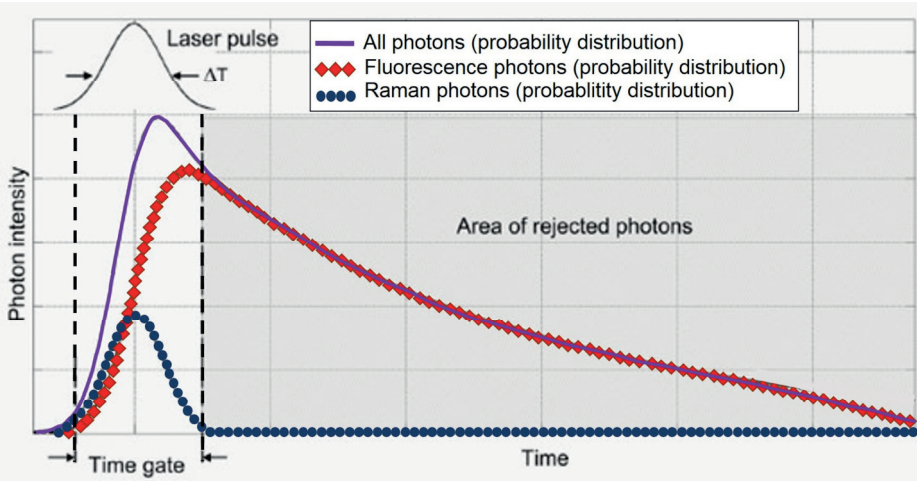

Figure 9 The principle of time-gated Raman spectroscopy. By synchronising the laser pulse and the time gate it is possible to reject a significant proportion of the fluorescence photons. The curves represent the probability distributions of the photons. Modified from Nissinen et al., 2017 [154].

In contrast, time-resolved measurements exploit this lifetime difference by using short laser pulses (instead of the continuous wave excitation used in conventional instruments) and synchronised temporally resolved detection. If the signal is only recorded during the laser pulses, it is possible to exclude the portion of the fluorescence photons emitted after the Raman scattered photons and collect Raman spectra with minimised fluorescence contribution (**FIG 9**) [16, 153, 156]. Different techniques can be used to achieve time-resolved measurements, e.g. based on optical Kerr gating or fast time-gated detectors, which may be photomultiplier tubes, intensified charge-coupled device cameras (iCCDs), streak cameras and complementary metal oxide semiconductor (CMOS) detectors [153].

Time-gated Raman spectrometers based on CMOS single photon avalanche diode (SPAD) detectors have recently become commercially available. The operational principle is based on the laser pulse simultaneously illuminating the sample and triggering a delay generator enabling the SPAD operation, thus allowing synchronisation, as well as controlled delays, between the laser pulse and photon detection, [156-158]. The use of these detectors allows more affordable and compact instruments compared to those relying on other detector technologies [154]. Since these instruments also allow measurements in ambient light and at elevated temperature because thermal interference is avoided, they are potentially suitable for in-line measurements in process settings. This makes the technology appealing also for pharmaceutical process monitoring purposes.

The feasibility of such time-gated Raman spectroscopy measurements using a picosecond pulsed laser and a CMOS SPAD detector for qualitative

solid state analysis of pharmaceuticals has been demonstrated [159]. However, the applicability of the technology for quantitative analysis of solid-state form mixtures, and thus potential for solid-state transition monitoring has not been evaluated previously.

2.5 Multivariate data analysis

The data collected by Raman spectroscopy may contain spectral variation which is important, but subtle and difficult to observe visually [30, 37]. Analyses are generally much more reliable when using spectral windows containing many Raman bands, compared to methods relying on a single band [17]. Furthermore, the amount of spectral data increases when the signals are composed of more dimensions, as is with time-gated Raman spectroscopy and the additional time domain. Very large datasets are also produced in process monitoring applications [13]. Similarly, the complex relationships between the multiple spray drying process parameters and their interdependencies with the various properties of spray dried powders (**FIG 6**) may be difficult to identify by evaluating individual parameters. The complex and large datasets require sophisticated data analysis approaches which can deal with large data matrices and reliably identify significant variation. Such analysis involving multiple variables is called multivariate data analysis.

There are various multivariate methods, out of which principal component analysis (PCA) and partial least squares (PLS) regression are some of the most often applied multivariate tools in the chemistry and technology fields, also in pharmaceutical research [17, 37, 160, 161]. They allow identification and quantification of systematic variation and correlations in data sets.

PCA is a qualitative method used to display the most significant and presumably meaningful data variation while rejecting noise, in order to better display and potentially classify the data [161]. In PCA, data is arranged in a data matrix (**X**), composed of *observations* (the rows) and *variables* (the columns) [162]. The *observations* can be e.g. analytical samples (different materials), process time points in a continuous process, batches from a batch process, or runs from an experimental design. The *variables* are measurements that characterise the properties of the observations, such as spectra or measurements from sensors in a process (e.g. temperature). PCA transforms the data matrix (**X**) into scores and loadings matrices, in which the most significant data variation is represented. The scores can be plotted to identify e.g. similarities between observations, trends or outliers. In combination with the loadings, it is possible to identify the specific variables (e.g. spectral regions or process temperature ranges) responsible for the similarities or differences between the observations.

PLS is a regression extension of PCA, particularly suitable for modelling multivariate relationships [160]. It is widely used for quantification of pharmaceutical solids in mixtures based on spectral data [17]. PLS is also used

for process modelling, where it can separate the simultaneous influences of several process variables on a number of product characteristics [163].

PLS relates the data in matrix **X** (descriptor or predictor variables) to the additional **Y** (response variables) matrix by a linear or polynomial multivariate model [160, 162]. In quantitative analysis, PLS is used for multivariate calibration. Here, **X** is composed of a set of spectra (rows) and the intensities at different wavelengths (columns), while **Y** contains the concentrations of the set of samples. PLS is used to create a model that can predict concentrations from the spectra of new samples. In process monitoring or optimisation, PLS finds relationships between the variables measured from the process (**X**), e.g. at different time points or from the different runs of an experimental design, and the corresponding values of responses (**Y**), such as different characteristics reflecting the quality of the product and yield.

PLS approximates the **X** and **Y** spaces by hyper-planes, i.e. high-dimensional spaces, and creates new variables (***t*** for the combinations of the original **X** variables using weights *w*, and ***u*** for the combinations of **Y** variables with weights *c*) independently for both **X** and **Y** matrices (**FIG 10**). Next, PLS analysis maximises the covariance between **X** and **Y** (***u*** and ***t***) by a linear or polynomial model.

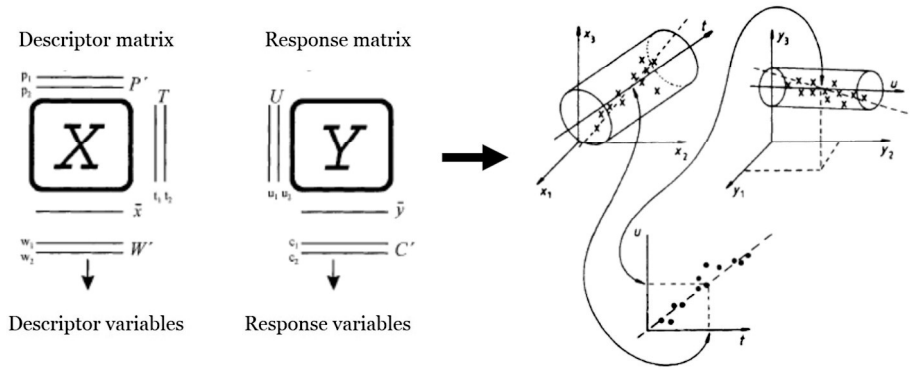

Figure 10 PLS principle. In PLS, PCA is first performed for both the X and the Y variables. The best correlation between X and Y is then calculated using the least squares technique. Modified from Gabrielsson et al., 2002 [161].

PLS can deal with numerous responses simultaneously, allowing fast analysis of massive datasets, and gives an overview of the relationship between the responses and all the variables that affect all the responses. Compared to traditional regression, PLS models the structures of the matrices, and is able to analyse data with many, noisy or collinear variables [160]. It can be used for very many data analysis problems, explaining its popularity.

However, there are also other multivariate analytical methods. Kernel based regularised least squares (RLS) is a well-established method in the machine learning literature [18, 164], but no so in the pharmaceutical field.

Similar to PLS and PCA, RLS methods can be used to solve regression and classification problems with complex data. Here, a least squares cost function is coupled with a kernel function as data similarity measure to solve the problem. Kernel functions are a powerful way to infer nonlinear predictors using linear algorithms such as RLS. Similar to PLS, the variables are spread into hyper-spaces [18]. Kernel-based RLS uses kernels, such as Gaussian radial basis functions, to find the best fitting surfaces in the high dimensional feature space [18]. There are a number of well-known similarity kernel functions, of which the Gaussian function is widely used, and the choice of the kernel is not limited to linear and polynomial functions like with PLS. RLS is however simultaneously designed to prevent overfitting, with a preference for less complicated models. The solutions of the kernel-based RLS are restricted by regularisation, which is applied to prevent overfitting and guarantee the model smoothness, with a preference for less complicated models by penalizing the solution to prevent increased complexity of the final model.

When using multivariate analysis with spectral data, for example for a quantification problem, some spectral preprocessing is normally needed. Normalisation methods, such as standard normal variate (SNV) transformation can correct for uninformative spectral differences, e.g. variation in sample focusing or laser power [165]. SNV and mean centering are established spectral pretreatment algorithms with quantitative analysis [166, 167]. Computational baseline correction methods are often used when the spectra contain elevated baselines, due to photoluminescence.

For quantitative analysis, measures are needed to evaluate the quality of the quantitative model. Commonly used are root-mean squared error of prediction (RMSEP) and root-mean squared error of cross validation (RMSECV). Both are calculated based on the differences between the values predicted by the model and the true values using **Equation (1**).

$$RMSEP = \sqrt{\frac{\sum_{i=1}^{n}(y-\hat{y})^2}{n}} \quad , \tag{1}$$

where y is the true value, $\hat{y}$ is the predicted value and n is the number of observations. The difference is that for RMSEP the predicted values are obtained from an independent test set, completely separate from the set used for model calibration. For RMSECV, cross validation is used, where one or more samples are removed from the calibration set. The model is built using the remaining samples and the removed sample(s) is/are used to calculate the error using **Equation 1**. Next the sample(s) is/are returned to the calibration set, and a new sample (group) is removed, and the process is repeated. At the end of this iterative process, all samples have been used for both model calibration and calculating the error.

3 Aims of the study

The overall aim of this thesis was to evaluate strategies for controlling stability and monitoring solid-state forms in pharmaceutical powders. The goals were to identify new stabilising excipients for spray-dried protein formulations and Raman spectroscopy-based methods for solid-state analysis in the pharmaceutical field.

The specific objectives were:

- to study the spray drying process behaviour and physical stability of amorphous isomalt and melibiose powders, in order to assess their potential as new protein-stabilising excipients for spray-dried formulations (**I**)
- to evaluate the stabilising efficacy and process behaviour of melibiose in spray-dried protein formulations in comparison to the standard excipient, trehalose (**II**)
- to investigate low-frequency Raman spectroscopy for quantitative analysis of solid-state form mixtures (**III**)
- to test time-gated Raman spectroscopy for quantitative solid-state analysis of fluorescent pharmaceutical powders (**IV**).

4 Experimental

4.1 Materials (I-IV)

The molecular structures of the two potential new excipients for spray-dried formulations, melibiose and isomalt, that were compared with trehalose and sucrose in (**I**), are presented in **FIG 4**. With the spray-dried protein formulations in (**II**), the protein-stabilising efficacies of formulations containing either melibiose or trehalose were additionally compared to reference formulations containing maltodextrin or erythritol, to evaluate the general stabilising effect of the disaccharides in regards with other types of molecules. Maltodextrin was an example of a higher-molecular weight compound, compared to the studied disaccharides, which produces amorphous powders with a high T_g (approx. 150 °C). Erythritol was an example of a carbohydrate compound, with a closer molecular weight to the studied disaccharides, but a low T_g (approx. -42 °C) and higher propensity to crystallise.

To investigate the Raman spectroscopy methods for quantitative analysis of solid-state form mixtures in (**III**) and (**IV**), the drug piroxicam was used (**FIG 11**). Piroxicam was selected as a model drug, because it has several solid-state forms that can commonly occur in industrial processing or storage situations. It also has low aqueous solubility and high permeability (belongs in the Biopharmaceutics Classification System class II), and therefore the solid-state form potentially matters therapeutically. Piroxicam also exhibits photoluminescence (fluorescence). The details of the studied materials are presented in **Table 5**.

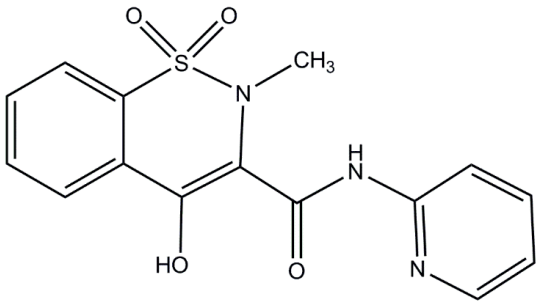

Figure 11 The molecular structure of piroxicam.

Table 5. *The materials used in the studies.*

Name	Purpose	Description	Mol. weight	Trade name or code / supplier	Publi-cation
Melibiose	A potential new stabilising excipient	Disaccharide	342.3	M5500 / Sigma-Aldrich	I-II
Isomalt	A potential new stabilising excipient	Disaccharide-based alcohol, GPM-GPS ratio 1:1	344.3	GalenIQ 720 / BENEO-Palatinit	I
Trehalose	Standard protein-stabilising excipient	Disaccharide	342.3	T9531 / Sigma-Aldrich	I-II
Sucrose	Standard protein-stabilising excipient	Disaccharide	342.3	84097 / Sigma-Aldrich	I
Maltodextrin	Excipient for a reference formulation (example of a high MW and T_g carbohydrate)	Glucose polymer (hydrolyzed starch), with dextrose equivalent 18	~1000 (average polymer size)	Maltrin M180 / Grain Processing Company	II
Erythritol	Excipient for a reference formulation (example of a crystalline, low MW carbohydrate)	Mono-saccharide-based sugar alcohol	112.1	E7500 / Sigma-Aldrich	II
β-galactosidase	Model protein	Lactase from *A. oryzae;* lactose-hydrolyzing enzyme	~105000	Lactase DS / Amano Enzyme	II
Piroxicam	Model polymorphic and fluorescent drug	Non-steroidal anti-inflammatory drug	331.3	USP grade / Hawkins	III-IV

4.2 Methods

4.2.1 Sample preparation (I-IV)

4.2.1.1 Solutions for spray drying (I-II)

The excipients were dissolved in purified water (at a 10-30% concentration), to prepare 100 ml solution for each spray drying experiment.

For the protein formulations, the received protein powder was rehydrated, filtered through a 0.2 μm filter (Acrodisc, Pall Corp, USA), and purified using desalting columns (PD-10, GE Healthcare, USA). The protein was then mixed with the 10% excipient solution. The protein concentration was measured using UV spectrophotometry (A280 nm, UV-1600PC, VWR, China). The final protein concentrations in the solutions were 0.39 ± 0.04 mg/ml, resulting in a protein:excipient weight ratio of approximately 1:250.

4.2.1.2 Solid-state form mixtures of piroxicam (III-IV)

Three solid-state forms of piroxicam were used: β anhydrate (Cambridge Structural Database [CSD]: BIYSEH13 [168], α2 anhydrate (CSD: BIYSEH06 [169]) and the monohydrate (CSD: CIDYAP02 [168]. The purchased piroxicam was characterised as form β, and used as received. The α2 form was

prepared by dissolving piroxicam in ethanol at 60 °C, and the monohydrate in water at 80 °C. The solutions were cooled to room temperature and vacuum filtered to harvest the crystals. Ternary powder mixtures (**FIG 12**) were prepared by gently mixing the components and analysed during the same day to avoid solid-state changes. **Fig 12A** shows mixtures optimized using special cubic model experimental design [163], which were used for quantitative model calibration (**III-IV**), as well as for model validation in **IV**. **Fig 12B** shows the independent set of mixtures used for model validation **III**.

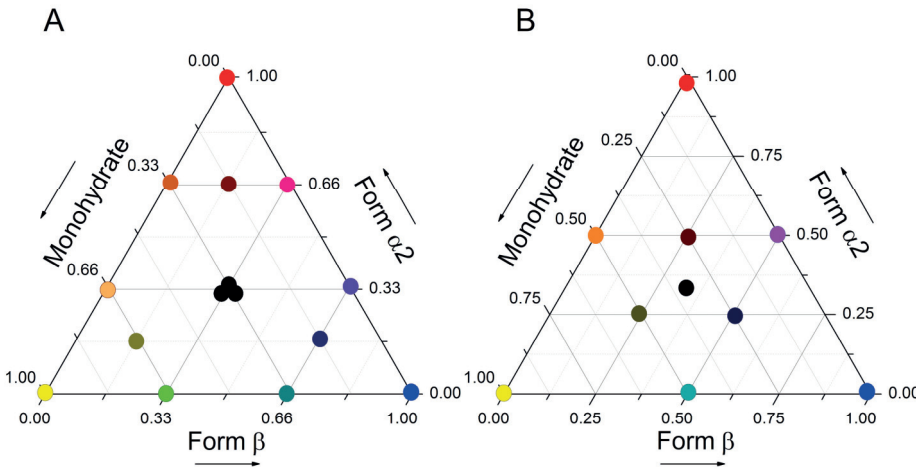

Figure 12 Mixture designs for the piroxicam solid-state form mixtures. A = mixtures for quantitative model calibration (III-IV), and validation (IV). B = mixtures for cross-validation (III).

4.2.2 Spray drying and storage of the spray-dried powders (I, II)

Spray drying was carried out using a Büchi Mini spray drier B-191 (Büchi Labortechnik AG, Switzerland), which operated in a co-current mode and was equipped with a two-fluid nozzle (0.7 mm). Dry nitrogen was used as the atomization gas and the nozzle was connected to a cooling water circulation.

Experimental designs were planned using MODDE (v. 10.1, Umetrics AB, Sweden). The process parameters that were adjusted included: inlet temperature (T_{inlet}), atomization gas flow rate, feed flow rate, feed concentration and aspirator rate. The aspirator setting (% motor output) controlled the drying air flow rate, and the volumetric drying air flow rates corresponding to the chosen aspirator settings were measured using an air flow meter (Testo 425, Humitec, Finland). The process parameters are presented in **Table 6** (study **I)** and **Table 7** (study **II)**. The reference protein formulations containing maltodextrin or erythritol (II), were processed using the mid-point parameters (T_{inlet} = 160 °C, Atom. = 650 L/h, Asp. = 90%).

Table 6. *Spray drying process parameters for the excipient solutions (**I**)*

	Inlet temperature (°C)	Atomizing gas flow rate (L/h)	Feed rate (mL/min)	Feed concentration (%)	Aspirator rate (%)
isomalt	40-100	500-800	1.4-5.5	10-30	50-100
sucrose	40-100	500-800	1.4-5.5	10-30	50-100
melibiose	50-180	500-800	2.7-4.9	10	100
trehalose	100-180	500-800	4.6	10	100

Table 7. *Process parameters for the protein formulations with melibiose or trehalose (**II**).*

	Inlet temperature (°C)	Atomizing gas flow rate (L/h)	Feed rate (mL/min)	Feed concentration (%)	Aspirator rate (%)
melibiose	140-180	500-800	4.8	10	80-100
trehalose	140-180	500-800	4.8	10	80-100

A standard Büchi cyclone separated the powders from the drying air stream, and the powder that could be recovered from the product collection vessel attached to the cyclone, and the metallic lid of the collection vessel, was considered the yield (as percentage of the initial solid mass used to prepare the feed solution).

The collected powders were transferred into glass vials and taken for analysis or placed into temperature- and humidity-controlled conditions for storage stability studies. The excipient powders (**I**) were stored for three weeks at two temperature conditions: 25 °C and 40 °C, at 20% relative humidity (RH). The protein formulations (**II**) were stored for 30 days at 20 °C and 40 °C, at 18 % RH. The powders were stored in open vials, where the material was directly exposed to the surrounding humidity.

4.2.3 Powder characterisation techniques (I-IV)

4.2.3.1 Solid-state determination (I-IV)

The solid-state form of the spray-dried samples (**I,II**) was investigated using X-ray powder diffractometry (XRPD, Bruker D8 Advance, Bruker Axs Inc, USA), with CuKα radiation (λ=1.54 Å). The samples were scanned over the 5-40° angular range (2θ) at a rate of 0.05°/s. Differential scanning calorimetry (DSC 823e, Mettler-Toledo GmbH, Switzerland) was also used, where the spray dried samples were equilibrated at 25 °C for 3 min and heated to 200 °C at a 10 °C/min rate with nitrogen as purge gas (50 ml/min). Glass transition temperatures (T_g) were determined as the midpoints of the transitions and

melting points as the onset temperatures of the endotherms, using STARe software (Mettler-Toledo GmbH, Switzerland).

The solid-state forms of the piroxicam samples were determined using XRPD, DSC and FTIR spectroscopy. The powders in publication **III** were measured using a PANalytical X'Pert PRO MPD system (PW3040/60, PANalytical B.V., The Netherlands), with CuKα radiation (λ=1.5 Å) and scanned from 5° to 35° (2θ) with a step size of 0.008° (2θ). The analysis in study **IV** was carried out using a Bruker D8 Advance diffractometer (Bruker, Germany) with a CuKα radiation source (λ = 1.54 Å) over the 5° - 40° (2θ) range with a step size of 0.01°. The solid state forms were confirmed by comparing the measured diffractograms with calculated diffractograms obtained from the CSD. With DSC (DSC Q2000, TA instruments in **III**, and DSC 823e, Mettler-Toledo in **IV**), the samples were scanned between 25 and 230 °C, at 10 °C/min, to detect the melting points (onset temperatures). Possible solid-state changes in the piroxicam powders were also investigated using FTIR. In **III**, a Vertex70 (Bruker Optics, Germany) fitted with a GladiATR diamond ATR accessory (Pike technologies, USA) was used to record 32 scans over 600-4500 cm^{-1} with a 2 cm^{-1} spectral resolution; these were averaged to obtain the sample spectrum. In **IV**, a Vertex70 (Bruker Optics, Germany) with a MIRacle diamond ATR accessory was used for the measurements, where each sample spectrum was the average of 64 scans over 650-4000 cm^{-1} with 4 cm^{-1} spectral resolution.

4.2.3.2 Moisture content analysis (I-II)

The residual moisture contents (total water % w/w) of the spray-dried powders were measured using volumetric Karl Fischer titration (V30, Mettler Toledo AG, Switzerland) in (**I**). In (**II**), the moisture contents of the powders were determined using the DSC results and water activity measurements (a_w). The a_w measurements were carried out using an AquaLab 3 water activity meter (Decagon Devices, USA), where the water activity was determined at 25 °C and in triplicate for each sample. The residual moisture content was calculated based on the measured a_w and T_g values, by using the correlation between each of these values and the sample water content. The average of these two determinations was recorded as the moisture content. The method was verified with Karl Fischer titration, and the error was ±0.3%.

4.2.3.3 Particle morphology (I, II, IV)

The particle morphology of the powders was imaged by scanning electron microscopy (SEM) using a FEI Quanta 250 FEG system (FEI Inc, OR, USA). The samples were fixed onto carbon tape and sputter-coated with platinum (Quorum Q150TS, Quorum Technologies, UK). With the spray-dried samples, the images were used to evaluate the visual appearance and approximate size

of the particles. With the piroxicam samples, the images were used to investigate solid-state conversion to the α2 form and the monohydrate after preparation, as well as mixing efficiency in the powder mixtures.

4.2.3.4 Protein activity assay (II)

Protein stability during spray drying and storage was evaluated based on remaining biological activity. The activities were determined by an enzymatic assay for β-galactosidase (according to Sigma quality control test procedure 11/01 based on [170] and [171]), which is a spectrophotometric o-nitrophenyl-β-D-galactopyranoside (substrate for β-galactosidase) cleavage rate test. The activity was measured for each sample after protein purification and mixing with the excipient solution: this was considered the initial activity and assigned as 100% relative activity for the corresponding experiment. To determine the remaining activity after spray drying and storage, the samples were rehydrated and diluted to the initial concentration. The relative activity (%) of the processed or stored sample compared to the initial activity was considered the remaining protein activity. The assay was performed with duplicate samples, and the measurements before and after spray drying were performed in parallel.

4.2.4 Raman spectroscopy for quantitative solid-state analysis (III-IV)

4.2.4.1 Low-frequency Raman spectroscopy and reference Raman measurements (III)

Three Raman spectroscopy instruments were used in (**III)**: two dispersive instruments with low-frequency capability (LF-785 and LF-830) and one Fourier-transform Raman spectrometer (FT-1064) as a reference.

The LF-785 was capable of simultaneously recording both low and mid-frequency spectra. This instrument was used for the direct comparison of low-frequency and mid-frequency spectral data. It was a home-built system with a 785 nm laser module (Ondax, USA) followed by BragGrate bandpass filters (OptiGrate, USA) to remove amplified spontaneous emission before irradiating the sample. Backscattered light from the sample was collected and filtered through a set of volume Bragg gratings (OptiGrate, USA) and focused into an LS 785 spectrograph (Princeton instruments, USA) via fibre-optic cable which dispersed the Raman scattered light onto a PIXIS 100 BR CCD detector (Princeton instruments, USA). The spectrometer was calibrated using sulfur and 1,4-bis(2-methylstyryl)benzene. Spectra were collected over -345-2055 cm^{-1} with 5-7 cm^{-1} resolution, and each spectrum was the average of 60 scans each with an integration time of 0.01 s. The focal spot diameter was ~500 μm.

The LF-830 system was a commercial 830 nm SureBlockTM XLF-CLM THz-Raman system (Ondax Inc., USA). This instrument was used to collect high-resolution low-frequency Raman spectra. The sample was arranged in a 180° backscattering geometry relative to a 10x microscope lens. The system was coupled via a fiber optic cable to an Acton Research SpectraPro 500i with a slit width of 50 µm. A 1200 grooves mm^{-1} grating was used to horizontally disperse the beam on a liquid-nitrogen cooled Spec-10:100B CCD, controlled by WinSpec/32 software (Roper Scientific, USA). The system was calibrated using sulfur. Spectra were acquired over the -60 to 430 cm^{-1} spectral window with 2 cm^{-1} resolution. Each sample spectrum was the average of 60 scans each with an integration time of 1 s. The setup had a focal spot diameter of ~5 µm.

The FT-1064 instrument consisted of a multiRam FT-Raman spectrometer (Bruker Optik, Germany), 1064 nm Nd:YAG laser and D 418 Ge detector. This instrument was used to collect high-resolution mid-frequency Raman spectra. Spectra were collected using OPUS 7.5 (Bruker Optik, Germany) using the defocusing lens, a laser power of 150 mW and 2 cm^{-1} resolution with each spectrum an average of 32 scans. The focal spot diameter was ~2 mm.

With all Raman instruments, three measurements per sample were recorded. The samples were rotated between replicate measurements to collect the signal from a new position each time and minimize error due to possible sample inhomogeneity.

4.2.4.2 Time-gated Raman spectroscopy and reference Raman measurements (IV)

The time-gated Raman spectroscopy measurements were carried out using a TG532 M1 Raman spectrometer (TimeGate Instruments, Finland), equipped with a picosecond pulsed laser (150 ps, 532 nm excitation), a time-gated single photon counting (CMOS-SPAD) array detector and a sampling probe (BWTek, USA) allowing measurements in ambient lighting. Sample spectra were collected over the 700-1700 cm^{-1} spectral window, and over a 0-5.5 ns delay time window (from the laser pulse) with a step size of 50 ps. The signal collection was performed with continuous sample rotation (to reduce the risk of subsampling), and three replicate spectra were collected for each sample, each from a new area. The laser spot diameter at the sample surface was ~85 µm, and with the rotation the sampled area was approximately 0.33 mm^2. The spectrometer was calibrated using cyclohexane.

As a reference method for the time-gated Raman analysis (performed with a pulsed laser operating at 532 nm excitation wavelength), a Raman instrument with the same excitation wavelength but with a conventional continuous-wave (CW) laser was used. Measurements of the pure piroxicam solid-state forms were taken to evaluate the fluorescence signal associated with the different solid-state forms. The reference instrument was a home-built Raman setup operating in a backscattering geometry and using 532 nm excitation produced with a CW single frequency laser (Alphalas, Monolas-532-

100-SM). A 100 x microscope objective (Olympus 100x with 0.70 N.A.) was used for signal collection, giving a spot size of approximately 0.9 µm (theoretical minimum spot diameter calculated by $d=1.22\lambda/N.A.$). The scattered light was dispersed in a 0.5 m imaging spectrograph (Acton, SpectraPro 2500i) using a 600 g/mm grating, and detected with a EMCCD camera (Andor Newton EM DU971N-BV) at a spectral resolution of 5 - 6 cm^{-1}. For each sample, a single spectrum was recorded that consisted of the average of 2 scans, each with an integration time of 5 s. The laser power was ~0.5 mW.

4.2.5 Data analysis and modelling

4.2.5.1 Evaluating spray drying process parameter effects (I-II)

The effect of spray drying process parameters on the powder yields and characteristics were evaluated with the modelling software MODDE (v. 10.1., Umetrics AB, Sweden). Partial least squares (PLS) fitting was used to identify relationships (covariance) between the process factors and the measured responses. The models were fitted using only the significant terms (coefficients), judged by their uncertainty levels (excluding those ranging across y=0), in order to maximise the predictability (by maximising Q^2) and reduce the risk of overfitting (by minimising the difference between the model fit R^2 and Q^2). The statistical significance was confirmed by analysis of variance (ANOVA), defined at $p<0.05$.

4.2.5.2 Comparison of low- and mid-frequency Raman spectroscopy for quantitative analysis (III)

The utility of the low-frequency and mid-frequency spectral regions for determining solid-state compositions in the mixtures was compared based on quantitative model performance. Standard spectral processing and multivariate methods were applied, all carried out with SIMCA software (v. 13.0.3, Umetrics AB, Sweden).

Quantitative PLS regression (PLSR) models were built using different spectral ranges, recorded with the calibration set samples (**FIG 12A**). All spectra were normalised by standard normal variate (SNV) transformation and mean centering. The performance of the models was determined based on the ability to predict the contents of the independent test set mixtures (**FIG 12B**), using the root-mean square error of prediction (RMSEP, **equation 1**) as a measure of quantitative capability.

4.2.5.3 Evaluating time-gated Raman spectroscopy for quantitative analysis (IV)

With time-gated Raman spectroscopy, quantitative solid-state analysis of the piroxicam mixtures was performed using two multivariate methods: (1) PLS regression and (2) kernel-based regularized least-squares (RLS) regression with greedy feature selection. For both, the used spectral range was 803-1609 cm^{-1}, the spectral data was baseline-corrected using an adaptive iteratively reweighted penalised least squares (airPLS) algorithm [172] (combined with local minima fitting for method (1)), and normalised using SNV transformation and mean centering.

For the PLSR models, the used delay time domain was selected manually, based on visual appearance. The PLSR models were built and evaluated using SIMCA software (v. 13.0.3, Umetrics AB, Sweden).

With the kernel-based RLS method, the time domain selection was performed by an algorithm (RLS algorithm with multi-target greedy feature selection), which used iterative optimisation to identify the optimal time domain. The algorithm also selected the most informative Raman shifts and model hyperparameters (controlling e.g. the risk of overfitting) by nested cross-validation. The RLS models were based on Gaussian kernel functions, and they were built and evaluated with the Python-based machine learning software library RLScore [164].

The performance of both the PLS and RLS-based models was evaluated based on leave-one-out cross-validation, and the used measure of quantitative capability was the root-mean square error of cross validation (RMSECV). Here, one piroxicam mixture (all replicate measurements of a mixture in the calibration set **FIG 12A**) at a time was not used for model calibration, but as an unknown sample, for which the prediction error value was calculated (RMSEP). This was repeated with all mixture samples (n=12), but not the pure piroxicam solid-state forms. The error values from all cross-validation rounds were averaged to get the RMSECV of the model.

5 Results and discussion

5.1 Spray-dried isomalt and melibiose in comparison to sucrose and trehalose (I)

The suitability of isomalt and melibiose as potential new excipients for spray-dried protein formulations was tested in comparison to the previously used excipients sucrose and trehalose. All studied excipients could be spray dried into amorphous powders, but there were significant differences in the process behaviour between the materials. Examples of spray drying processes are presented in **Table 8** where the experiments are classified into low, intermediate or high temperature processes. Production of melibiose powders was possible at all the temperature classes, while isomalt powders with acceptable yields could only be produced when low process temperatures were applied.

Table 8. *Spray drying processes with isomalt, sucrose, melibiose or trehalose. The results are divided into three groups representing process settings at low, intermediate or high process temperature. Atom. = atomising gas flow rate, Feed. = Liquid feed rate, Asp. = aspirator (drying air flow rate), M.C. = moisture content, n.d. = not determined due to lack of sample.*

	T_{inlet} (°C)	Atom. (L/h)	Feed. (mL/min)	Conc. (%)	Asp. (%)	T_{outlet} (°C)	Yield (%)	T_g (°C)	M.C. (%)
Low process temperature									
isomalt	50	800	1.4	20	100	37	44	42	2.7
sucrose	50	800	1.4	20	100	38	43	34	4.0
melibiose	50	800	4.9	10	100	39	52	47	5.1
Intermediate process temperature									
isomalt	100	800	1.4	20	100	73	2	50	n.d.
sucrose	100	800	1.4	20	100	66	26	51	1.9
melibiose	100	800	4.9	10	100	64	15	60	3.6
trehalose	100	800	4.9	10	100	65	36	45	5.5
High process temperature									
melibiose	180	800	4.9	10	100	110	27	77	2.0
trehalose	180	800	4.9	10	100	107	64	82	2.6

5.1.1 Powder yields

Yields above 50% could be obtained with all materials by adjusting the process settings. Trehalose was the only material that provided such yields at higher process temperatures. In fact, an increase in yield with increasing drying temperature was observed for trehalose (**Fig 13D**). For the other materials, the highest yields were observed when low process temperatures were used (**FIG 13**). The strongest correlation between process temperature and powder yield was observed with isomalt, where very low yields were obtained when the outlet temperature was above 50 °C (**FIG 13A**).

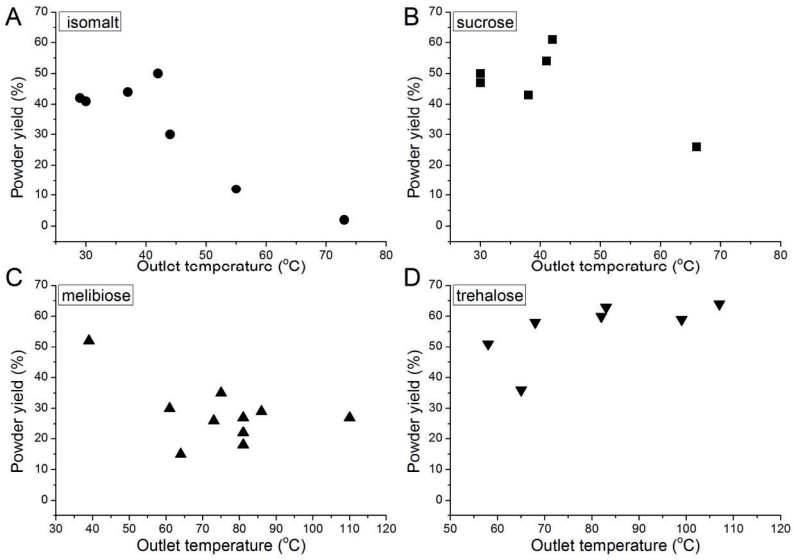

Figure 13 Effect of outlet temperature on powder yields with spray-dried isomalt (A), sucrose (B), melibiose (C) and trehalose (D).

In addition to temperature, the feed rate had a major impact on isomalt powder yields. The yields decreased rapidly when increasing the feed rate from the lowest setting (**FIG 14A**). The feed rate also influenced sucrose powder yields, but the effect was not as strong (**FIG 14B**). For melibiose (**FIG 14C**) and trehalose, the feed rate did not affect the yields. Isomalt was the most challenging material to spray dry, since not only the process temperature, but also the feed flow rate needed to be kept at a low setting in order to produce powders with acceptable yields. Sucrose is known to be a challenging material to spray dry [173, 174], and isomalt was found to be even more problematic.

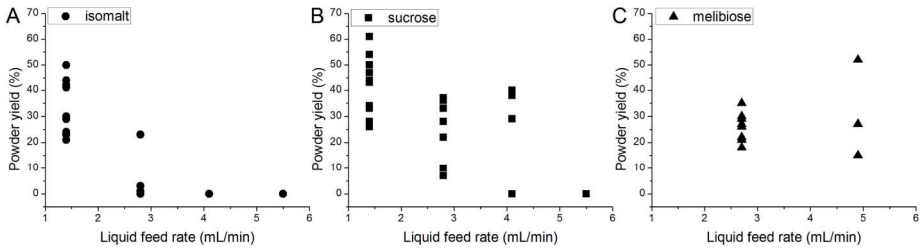

Figure 14 Effect of feed rate on powder yields with spray-dried isomalt (A), sucrose (B) and melibiose (C).

Both the atomisation gas flow rate and drying air flow rate (aspirator) also affected the yields. Decreased yields were obtained when the atomisation rate was ≤ 600 L/h or the aspirator setting ≤ 75%. With melibiose and trehalose the atomisation gas flow rate was the main factor affecting the powder yields. The feed liquid concentration did not affect the yields at the studied level (10-30%).

Trehalose is known for its good processability during spray drying for a sugar [124, 175]. Higher process temperatures and feed rates could be used with trehalose compared to the other studied excipients, and overall the yields were better. The process behaviour of melibiose was an intermediate between trehalose and the more challenging excipients sucrose and isomalt. Yields were lower compared to trehalose, unless the process temperature was low. The advantage over isomalt and sucrose was that the process parameters could be more freely adjusted without a significant yield decrease.

5.1.2 Powder characteristics

All produced powders were amorphous, and composed of smooth, spherical particles. The T_gs and moisture contents of the powders are presented in **Table 9**. Powders with the highest T_g values were obtained with trehalose, followed by melibiose. Isomalt and sucrose powders had the lowest T_g values. These T_g values reflect the material-specific properties and were also influenced by the moisture contents of the powders. The process temperature was the main factor determining the moisture content and T_g. Drying at higher temperature produced drier powders. When using the same process parameters, melibiose powders were drier than trehalose powders, and isomalt powders were drier than sucrose powders.

Table 9. *The T_g values and moisture contents of powders resulting from all spray drying processes which provided sufficient amounts of powders for analyses.*

	T_{outlet} (°C)	T_g (°C)	Moisture content (%)
isomalt	29-73	35-50	≤ 2.9
sucrose	30-67	34-63	1.9-4.0
melibiose	39-110	36-77	2.0-5.1
trehalose	58-107	42-82	2.6-5.5

The difference in the thermal behaviour of the materials partly explains the variation in the process yields. When the process temperature exceeds the T_g of the drying material, there is a risk of the material becoming sticky and being lost from the process stream on contact with the drier walls [175, 176]. Stickiness was a problem particularly with isomalt, which also presented the lowest T_g values.

5.1.3 Storage stability of the spray-dried powders

All of the powders remained amorphous during storage (three weeks at 40 °C/20% RH), as indicated by their XRPD diffractograms with amorphous halos and the presence of glass transitions in the DSC curves. However, the DSC results suggested possible partial crystallinity for isomalt. Furthermore, changes in particle morphology, with formation of aggregates, were observed with isomalt powders (**FIG 15**). No indication of crystallisation or other physical changes were detected with melibiose powders.

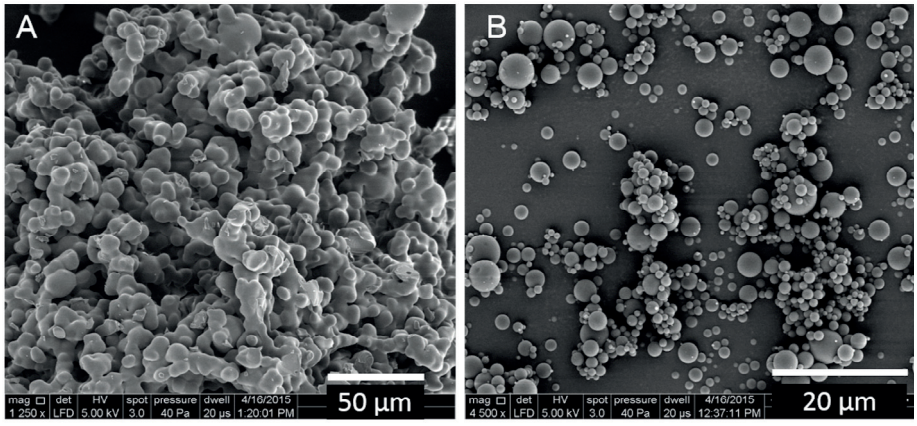

Figure 15 Spray-dried isomalt (A) and melibiose (B) after storage at 40 °C / 20% RH.

The storage conditions used were not according to the International Conference on Harmonization (ICH) quality guideline Q1A(R2): 25-30 °C/60% RH, or 40 °C/75% RH for accelerated stability studies [177]. However, according to the ICH protocol, the testing should be conducted with the material in a container closure system. It is expected that the material inside a packaging is exposed to a lower humidity than that mentioned in the guideline, but the exact conditions may remain unknown (dependent on the package sealing). In the current study, the amorphous powders were stored in open vials, where the material was directly exposed to the surrounding atmosphere and where it was possible to achieve well-defined humidity

conditions. The selected humidity condition was known to cause stress to such samples based on previous studies [77]. Regarding the intended use (dried amorphous biotechnology products), 20% RH can be considered relatively high in comparison to finished commercial formulations sealed inside protective packaging.

This was an early study investigating the potential of melibiose and isomalt for spray-dried formulations. Further studies to investigate the long term and stress condition stability of formulations containing these excipients are needed for a more complete understanding of their storage stability, e.g. using formal stability study protocols, and these should be conducted along with formulation optimization. It is expected that these types of spray dried amorphous materials are very sensitive to moisture uptake and a consequent higher risk of crystallisation. The moisture exposure of such products should therefore be limited by humidity-protecting containers.

To summarise, this study showed that both melibiose and isomalt could be spray-dried into amorphous powders by optimising the process parameters. However, the process behaviour of melibiose made it more suitable for spray drying processes than isomalt. Compared to trehalose, it was possible to produce drier powders with melibiose, but the powder yields were lower unless low process temperatures were used. The physical stability of amorphous melibiose powders was similar to trehalose and better compared to amorphous isomalt powders. In conclusion, out of the two potential new protein-stabilising excipients, isomalt and melibiose, melibiose was selected as the more promising one for spray-dried formulations.

5.2 Melibiose as a stabiliser in spray-dried protein formulations (II)

In this study, the applicability of melibiose as a new protein-stabilising excipient for spray-dried protein formulations was further evaluated. The protein-stabilising efficacy during processing and storage, as well as the spray drying process behaviour and physical stability were compared with trehalose, which is considered to perform well.

5.2.1 Protein activity stabilisation during spray drying

Both melibiose and trehalose provided protection against protein activity loss during spray drying. The remaining protein activity after spray drying was dependent on the process inlet temperature and aspirator (drying air flow) rate. In contrast, the atomising gas flow rate did not affect protein activity. The lack of atomising rate effect suggested that the model protein was not sensitive to mechanical stress. Thus, the observed protein degradation was mainly temperature-induced, since both the inlet temperature and the aspirator rate directly influenced the outlet temperature. The T_{outlet} can be considered the maximum process temperature that the product is exposed to [103].

The temperature-dependent activity reduction is shown in **FIG 16A**. There was a threshold temperature at 87 °C, below which the protein activities remained constant, and above which a decline in activities was observed. The group of experiments falling below this threshold temperature, called here the lower-temperature group, consisted of experiments with 140-160 °C for inlet temperature. The other, higher-temperature, group in turn had 180 °C for inlet temperature. The remaining activities from these two experiment groups are presented in **FIG 16B**. In both groups, melibiose was at least equally efficient in preventing protein activity loss during spray drying as the well-known stabiliser trehalose.

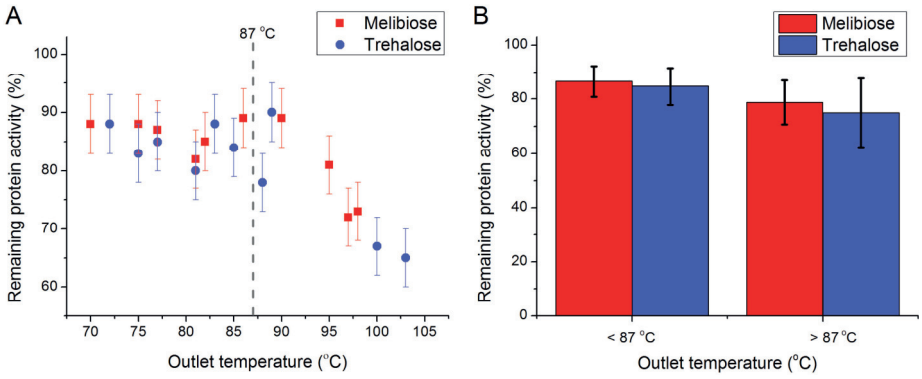

Figure 16 Remaining protein activities after spray drying as a function of outlet temperature (A) and the remaining protein activities, grouped based on process temperature. The lower temperature group (outlet temperature < 87 °C) had an inlet temperature of 140 or 160 °C and the higher temperature group (outlet temperature > 87 °C) had an inlet temperature of 180 °C.

Full activity preservation was not observed with either excipient, which is most likely due to the long process duration (20 min). The product was exposed to elevated temperature during the entire process time. However, when comparing to reference formulations, which had either maltodextrin or erythritol as excipient, the stabilising efficacy of both melibiose and trehalose was clear. The remaining activity was 40% with maltodextrin and only 3% with erythritol, while it was 82-89% with melibiose and trehalose dried at the same process settings. This result is in line with previous studies indicating the generally better protein-stabilising efficacy of amorphous disaccharides compared to higher molecular weight polymers (such as maltodextrin) and crystalline materials (such as erythritol). It can be expected that full protein activity preservation is possible with melibiose formulations by adjusting the process settings.

5.2.2 Protein activity stabilisation during storage

Melibiose was able to stabilise the protein activity during storage at least as well as trehalose (**FIG 17**). The spray-dried formulations could be stored at +40 °C / 18% RH for 30 days without further activity loss. The recorded remaining protein activity values trended higher for melibiose formulations compared to trehalose formulations. The difference was most pronounced with the samples that had been spray dried and stored at higher temperatures. This may suggest better stabilisation potential of melibiose, since high temperatures are stressful to the protein and solid-state stability. However, the overall difference between the stabilising efficacies of the two excipients was not statistically significant. These results show that melibiose was at least as good a protein-stabiliser during storage as trehalose.

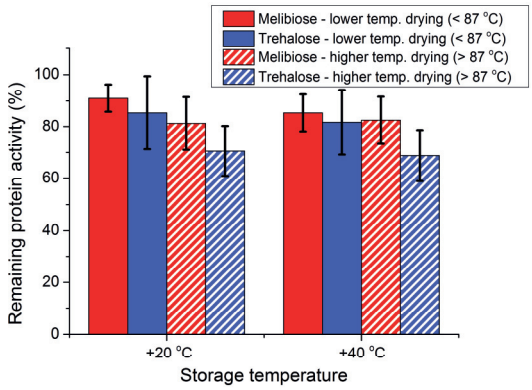

Figure 17 Remaining protein activities of the melibiose and trehalose formulations after 30 days of storage at +20 °C and +40 °C. The observations are divided according to the spray drying processes, into lower temperature processes (solid colour columns, inlet temperature 140-160 °C, outlet temperature <87 °C) and higher temperature processes (striped columns, inlet temperature 180 °C, outlet temperature >87 °C).

5.2.3 Process behaviour and powder properties

5.2.3.1 Powder yields

The powder yields were similar for melibiose and trehalose, and good yields were possible (≥70%). The yields of the formulations containing melibiose and protein were clearly better compared to melibiose spray dried alone (**I**). With trehalose, the addition of protein in the formulation did not have an effect on powder yields.

Trehalose yields were mainly determined by the atomizing gas flow rate (**FIG 18A**). Melibiose yields were influenced by both the atomizing rate (**FIG 18A**) and process temperature (**FIG 18B**). The best powder yields were obtained when using high atomizing rate and lower process temperatures.

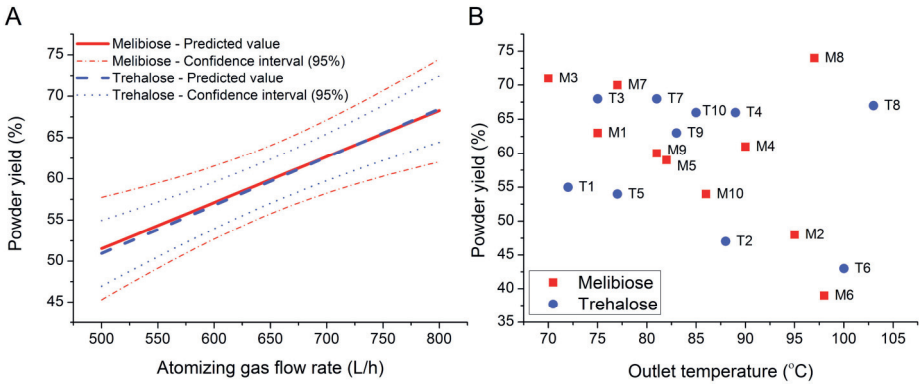

Figure 18 Effect of atomising gas flow rate (A) and outlet temperature (B) on powder yields. The predicted yields when the inlet temperature is constant at 160 °C and the aspirator at 90% (A) and the observed yields at different outlet temperatures (B).

The aspirator rate did not impact powder yields at the studied range 80-100%. It is known that drying air flow (aspirator) settings that are too low can reduce the separation efficiency of the cyclone, leading to lower yields [103]. In the previous study (**I**), it was shown that a reduction in yields occurred upon decreasing the aspirator setting to 75% or below. The result of this study (**II**) - that a decrease in the aspirator setting down to 80% was possible without affecting powder yields - is important because this setting should be minimized to reduce protein damage.

5.2.3.2 Powder properties

All of the spray-dried powders were amorphous, as determined by XRPD and DSC. The T_gs and moisture contents of the melibiose and trehalose formulations are presented in **Table 10**. During storage (20 or 40 °C / 18% RH), the water contents of the powders increased and the T_gs decreased, but all powders remained amorphous.

Table 10. *The T_g values and moisture contents of spray-dried protein formulations containing melibiose or trehalose. The measurements were performed immediately after spray drying, and after storage for 30 days at +20 °C or 40 °C, both at 18% RH.*

	T_g (°C)			Moisture content (%)		
	Before storage	Storage +20 °C	Storage +40 °C	Before storage	Storage +20 °C	Storage +40 °C
Melibiose	69-90	67-88	67-76	1.0-2.0	1.1-2.1	2.0-2.5
Trehalose	68-85	66-85	65-73	2.8-3.2	2.9-3.6	3.5-3.9

The T_g values were similar between the formulations containing either melibiose or trehalose (**Table 10**). Pure anhydrous trehalose has a higher T_g (~120 °C) than melibiose (~100 °C). The lack of such difference in the T_gs of the spray-dried formulations is caused by the higher water contents of trehalose formulations compared to melibiose formulations (**Table 10**).

Melibiose formulations were generally two-fold and at best three-fold drier than trehalose formulations when dried at the same process settings. The atomising gas flow rate affected the moisture contents of trehalose formulations (a higher rate resulted in drier powder). In contrast, the melibiose formulations were consistently dry, irrespective of the process parameters in the studied ranges. This result suggests that more efficient drying processes are possible when using melibiose as an excipient instead of trehalose. Furthermore, high residual moisture contents have been mentioned as a disadvantage of spray drying compared to e.g. lyophilization as a production method for solid protein formulations [178] . This makes melibiose a very promising excipient for spray-dried protein formulations.

All of the powders consisted predominantly of smooth, spherical particles and no morphological changes were observed during storage. The appearance of the particles was similar between the two excipients, and resembled that of particles containing pure disaccharide (no protein). The particle morphology depended on the process settings (**FIG 19**).

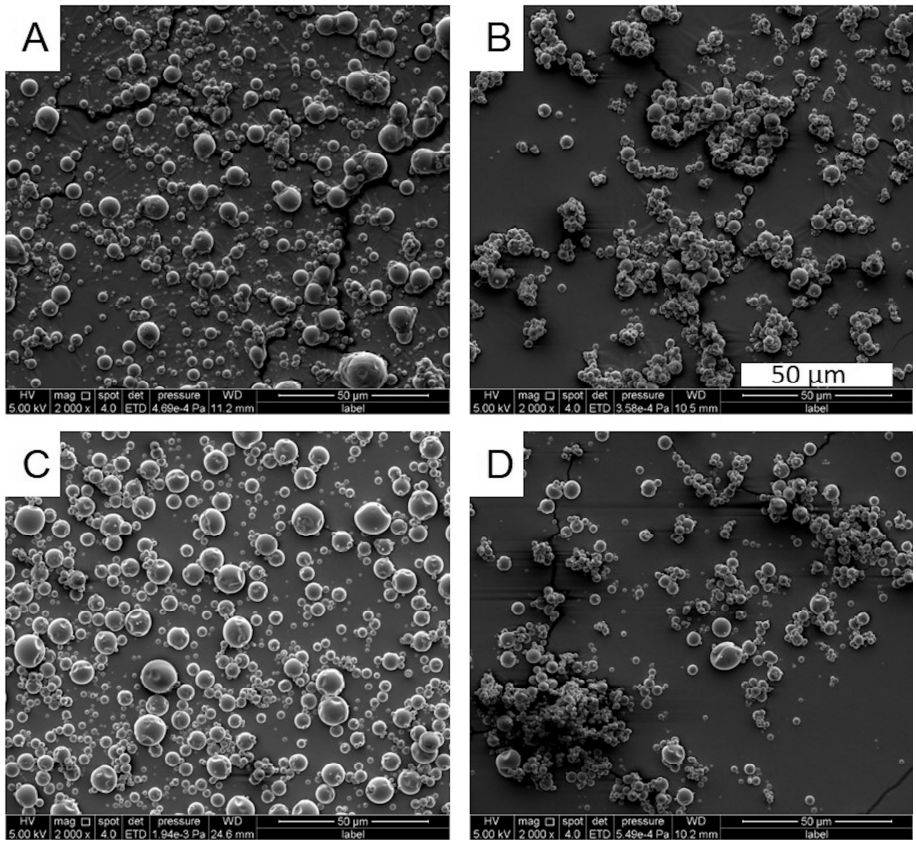

Figure 19 SEM images of powders spray dried using 140 °C T_{inlet} / 72-75 °C T_{outlet}, 500 L/h atomising gas flow rate, and 80% aspirator rate (low settings) containing β-galactosidase with melibiose (A) or trehalose (C), and powders spray dried at 180 °C T_{inlet} / 97-103 °C T_{outlet}, 800 L/h atomising gas flow rate, 100% aspirator rate (high settings) with melibiose (B) or trehalose (D). The scale bar (50 µm) is the same for all images.

As mentioned above, no crystallization was observed with any of the formulations during the 30-day stability study (at 20 or 40 °C / 18 % RH). However, during the DSC heat scans, trehalose always crystallised, while melibiose never did. This difference is related to the possible crystal forms of the two disaccharides. Trehalose can crystallise to both hydrate or anhydrate forms. In contrast, water plays a central part in the crystal structures of melibiose, and only hydrate forms (mono- and dihydrate) have been reported.

The DSC results indicated that in dry conditions melibiose can resist crystallisation better than trehalose. The highest water content of the melibiose powders in this work, (2.5% w/w, a_w = 0.139), was not sufficient to allow melibiose crystallisation even during heating. In contrast, trehalose can crystallise irrespective of the formulation water content, either to a hydrate or an anhydrate form. Earlier work has also shown that melibiose can be very stable in the amorphous form and has low molecular mobility compared to

other disaccharides [81]. It appears possible to produce physically very stable amorphous protein formulations with melibiose as excipient.

The conducted storage stability studies did not follow the ICH guideline protocols (12 months at 25-30 °C / 60 % RH and 6 months at 40 °C / 75 % RH) [177]. More stability studies are needed to investigate the long term and stressed stability of melibiose-containing formulations. However, the results from these early studies were promising.

In conclusion, the study showed that melibiose provided protein stabilisation during spray drying and storage at least equally well as the commonly used excipient trehalose. Melibiose was physically stable in the amorphous form, and it may resist crystallisation better than trehalose. The process behaviour with regard to powder yield was similar to trehalose. A possible advantage for processing and for formulation stability, was that the spray-dried protein powders with melibiose dried more efficiently to lower water contents than those with trehalose. Overall, melibiose showed several promising properties for spray-dried protein formulations.

5.3 Low-frequency Raman spectroscopy for quantitative solid-state form analysis (III)

In this study, the potential benefit of the additional spectral information provided by low-frequency (terahertz) Raman spectroscopy for standard solid-state analysis purposes was investigated. The performance of low-frequency Raman spectroscopy combined with established spectral processing and multivariate methods in quantifying crystal form mixtures was directly compared to conventional mid-frequency Raman analysis.

5.3.1 Raman spectra of piroxicam solid-state forms

The pure solid-state forms of piroxicam (β and α2 anhydrates, and the monohydrate) showed clear spectral differences in both the low-frequency (8-200 cm^{-1}) and mid-frequency frequency (700-1700 cm^{-1}) regions (marked by A and D in **FIG 20**). There were several unique peaks for each form in both spectral regions; the positions of several of these are indicated in **FIG 20**.

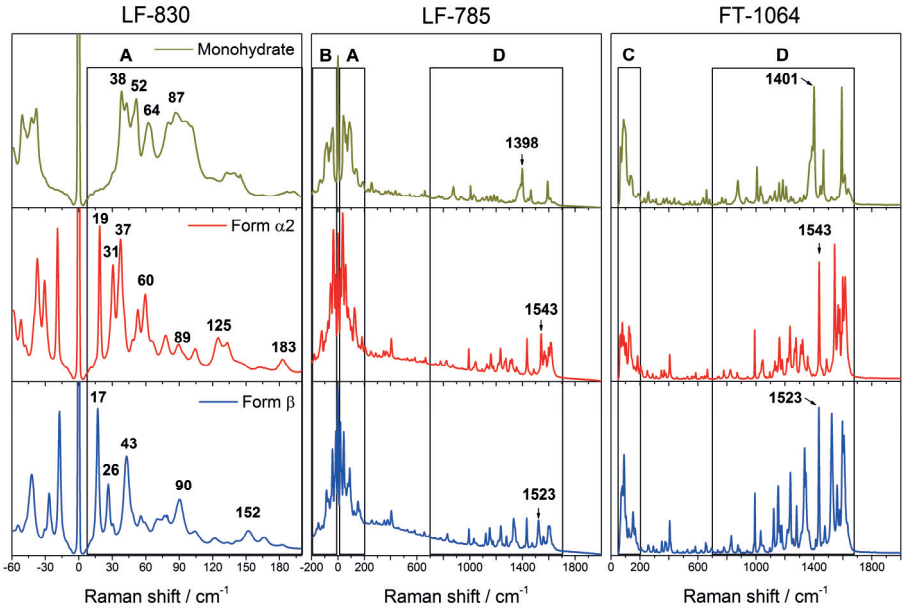

Figure 20 Raman spectra of piroxicam solid-state forms (the monohydrate, α2 anhydrate and β anhydrate), measured with three Raman instruments (LF-830, LF-785 and FT-1064) recording different spectral regions. The framed regions show the spectral ranges used for quantitative analysis: A: 8-200 cm^{-1}, B: -(200-12) cm^{-1}, C: 51-200 cm^{-1}, and D: 700-1700 cm^{-1}. The Raman peaks specified in the figure present some, but not all, characteristic peaks of each solid-state form.

The solid-state-specific Raman bands observed in the mid-frequency region (such as 1400, 1543 and 1523 cm^{-1} in **FIG 20**) are related to intramolecular vibrational modes. These vibrations differ mainly because of conformational differences and because the piroxicam functional groups are differently involved in intermolecular bonding in the different solid-state forms. Thus the peak positions give indirect information about the crystalline structures.

In contrast, in the low-frequency region there are spectral features that are directly caused by lattice vibrations in the crystalline arrangement. Piroxicam β and α2 anhydrates have a similar structure with respect to molecular configuration, conformation and intramolecular bonding, and they belong to the same monoclinic crystal system ($P2_1/c$). The observed spectral variation in the low-frequency region is related to the differences in intermolecular hydrogen bonding, π-π interactions and molecular packing arrangement between these forms.

The monohydrate structure differs substantially from the anhydrates, which is apparent also from the low-frequency spectrum. The monohydrate belongs to a lower symmetry crystal system (triclinic $P\bar{1}$) than the anhydrates. In addition, in the monohydrate form, piroxicam molecules are present in substantially different molecular conformations and there are water molecules in the structure. These molecules are connected to each other by a complex network of hydrogen bonds and π-π interactions [168, 179, 180]. The overlapping spectral features seen with the monohydrate reflect this complex network.

The most intense peaks with the piroxicam forms were observed below 50 cm^{-1}. This spectral region is dominated by lattice vibrations and it is also important for differentiating solid-state forms of other drugs (e.g. carbamazepine) [15].

The LF-785 measurements (the only instrument used in the study that was able to simultaneously record both spectral regions) showed that the signal intensities were higher in the low-frequency range than in the mid-frequency range (**FIG 20**). One reason for the strong signals at low Raman shift frequencies ($\tilde{\nu}_j$) is that the Raman cross section for a mode $j\left(\frac{\partial\sigma_j}{\partial\Omega}\right)$, **Equation 2** [181-183], which is related to the observed band intensity, is strongly dependent on the scattering frequency, $\left\{\tilde{\nu}_0 - \tilde{\nu}_j\right\}^4$, where $\tilde{\nu}_0$ is the laser frequency. This is particularly the case in π-bonded compounds, such as piroxicam, because the Raman amplitude, S_j[1], for such transitions is appreciable:

(2) $$\left(\frac{\partial\sigma_j}{\partial\Omega}\right) = \left(\frac{2^4\pi^4}{45}\right)\left(\frac{\left\{\tilde{\nu}_0-\tilde{\nu}_j\right\}^4}{1-exp\left[\frac{-hc\tilde{\nu}_j}{kT}\right]}\right)\left(\frac{h}{8\pi^2 c\tilde{\nu}_j}\right)S_j$$

In **Equation 2**, T denotes temperature in Kelvin, and the remainder are physical constants [184].

When the ternary mixtures of piroxicam solid-state forms β, α2 and monohydrate were measured, both the low- and mid-frequency spectral ranges could be used to differentiate the solid-state mixtures from each other using principal component analysis.

[1] The amplitude is related to the derivative terms for the mean (isotropic) polarizability for mode j ($\alpha_j'^2$) and the anisotropy ($\gamma_j'^2$) such that $S_j = 45\alpha_j'^2 + 7\gamma_j'^2$ [Horvath, Hertzberg].

5.3.2 Quantitative analysis of solid-state form mixtures: Comparison of using low- and mid-frequency spectral regions

Quantification of the piroxicam crystal forms in the ternary powder mixtures was possible using any of the studied spectral ranges, recorded by any of the instruments used in this study. However, there were differences in quantitative performance. The results obtained with partial least squares regression (PLSR) models using different spectral data are shown in **Table 11**. The predictive performance of the models are indicated by the RMSEP values.

Table 11. ***Summary of the PLSR models built using different spectral regions and data collected with the different instruments****. The letters indicating spectral ranges are the same as in* ***FIG 20****. The RMSEE and RMSEP values in the table refer to the averages of the three forms in the evaluated mixtures. The number of PLSR factors was two for all models. The abbreviations are explained below the table.*

Setup	Spectral range (cm^{-1})			Number of X variables	R^2X	R^2Y	Q^2	RMSEE (%)	RMSEP (%)
LF-785[a]	A	8-200	LF	108	0.974	0.993	0.991	2.6	3.0
	B	-(200-12)	LF (anti-Stokes)	106	0.981	0.995	0.994	2.1	3.3
	C	51-200	LF (partial)	84	0.983	0.976	0.974	4.6	5.0
	D	700-1700	MF	557	0.944	0.977	0.974	4.6	5.5
	A + B	8-200 + -(200-12)	LF (Stokes and anti-Stokes)	214	0.977	0.995	0.994	2.1	2.8
	A + D	8-200 + 700-1700	LF and MF	665	0.981	0.997	0.996	1.7	2.9
LF-830[b]	A	8-200	LF	528	0.970	0.974	0.964	4.8	5.1
	C	51-200	LF (partial)	413	0.977	0.962	0.959	5.8	5.8
FT-1064[c]	C	51-200	LF (partial)	156	0.983	0.971	0.968	5.0	5.5
	D	700-1700	MF	1038	0.963	0.979	0.976	4.3	4.6
	C + D	51-200 + 700-1700	LF (partial) and MF	1194	0.963	0.987	0.985	3.4	3.6

[a] LF-785 spot size ~500 µm, spectral resolution 5-7 cm^{-1}
[b] LF-830 spot size ~5 µm, spectral resolution 2 cm^{-1}
[c] FT-1064 spot size ~2 mm, spectral resolution 2 cm^{-1}

LF *= low-frequency;* ***MF*** *= mid-frequency;* ***X*** *variables refer to the spectral data points used in the analysis and they are dependent on the instrument spectral resolution; the coefficients* R^2X *and* R^2Y *describe the explained fraction of the variation of the variables X (spectral data) and Y (solid-state form composition);* Q^2 *is the predicted fraction of the variation of the Y variables;* ***RMSEE*** *describes the fit of the calibration set observations (model fit) and* ***RMSEP*** *measures the model performance with unknown samples, not used in building the model (predictive power).*

The low-frequency spectral region was better for quantitative analysis than the conventional mid-frequency region. This result was obtained with the LF-785, which was the only instrument applicable for direct comparison of the full low-frequency and mid-frequency spectral ranges without confounding sampling and instrumental variations. The average error in prediction was 3.0% when

using the low-frequency data (8-200 cm^{-1}) and 5.5% when using the mid-frequency data (700-1700 cm^{-1}). The specific error values for each solid-state form are shown in **FIG 21**. Combination of the anti-Stokes spectral data to the low-frequency Stokes Raman data resulted in a minor further improvement in quantitative performance.

The other Raman instruments (LF-830 and FT-1064) had different sampling volumes and spectral resolutions. Therefore, comparison should take such factors affecting quantitative performance into consideration. The FT-1064 had the largest spot size, and for this reason the least probability of error produced by sub-sampling, while for the LF-830 system this risk was highest due to the incorporated 10x objective for focusing. Accordingly, the FT-1064 performed better in quantification. Nevertheless, the quantification accuracy of the LF-830 and FT-1064 setups also improved when including low-frequency spectral data in the analysis.

The results also showed that the very lowest frequency spectral data below 50 cm^{-1} was highly important for accurate analyses. Developments in Raman instrumentation has allowed extension of the recorded spectral data down to relatively low frequency regions also with so-called conventional Raman instruments (such as the FT-1064 used in this study reaching 50 cm^{-1}). It appears however, that access below 50 cm^{-1} provides analytical benefits.

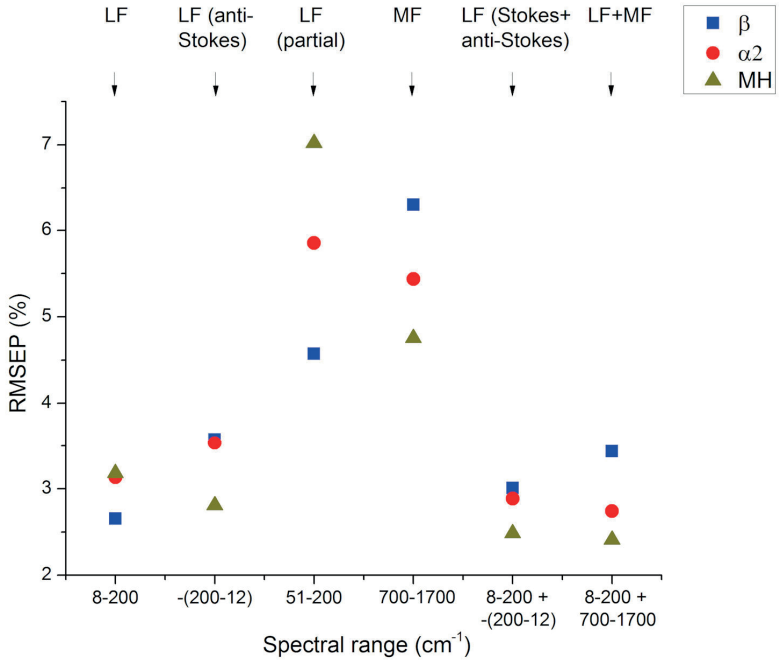

Figure 21 Performance of quantitative solid-state analysis of piroxicam crystal mixtures utilising different spectral ranges. The results refer to the LF-785 measurements, where the full low-frequency and mid-frequency spectral data was simultaneously recorded.

The reason low-frequency Raman spectroscopy enabled more accurate quantification of the solid-state form mixtures is likely to be due to the higher intensity scattering and signal-to-noise ratio. Furthermore, the differences between the solid-state forms in the low-frequency range are potentially larger since the vibrational modes are mainly intermolecular in nature and intrinsically linked to crystal structure. This should contribute to a higher sensitivity of low-frequency Raman for solid-state forms when compared to conventional mid-frequency Raman, giving the technique an advantage as a tool for solid-state analysis.

Piroxicam solid-state forms were readily differentiated using all of the studied regions of the Raman spectra. However, with other compounds, the changes in the mid-frequency fingerprint region can be too subtle to allow differentiation between solid-state forms, in contrast to distinctive solid-state specific low-frequency bands [141, 142, 145, 147, 149]. For example with sulfathiazole and phenobarbital, solid-state forms could not be differentiated by conventional Raman spectroscopy or even by XRPD, while they could be easily identified by distinct low-frequency Raman spectra [142, 151]. In such cases the use of low-frequency Raman spectroscopy is expected to have even more pronounced benefits than it did with the piroxicam mixtures in this study.

Low-frequency Raman spectroscopy is also a very useful technique with amorphous materials. Amorphous structures have no distinct lattice vibrations, therefore there are no peaks in the low-frequency spectral region originating from such vibrations, and the region is covered by inhomogeneous broadening instead [134]. This allows immediate differentiation between crystalline and amorphous materials similar to XRPD, and investigating crystallisation of amorphous samples. An additional benefit of using low-frequency Raman spectroscopy in pharmaceutical research is the possibility of solid-state analysis of active ingredients in the presence of excipients, since many drug compounds are strong Raman scatterers while many excipients only produce a weak Raman spectrum, including in the low-frequency range [14, 15, 150].

In summary, this study showed that the additional spectral data provided by low-frequency Raman spectroscopy was useful, and it enabled more accurate quantification of solid-state forms in mixtures than conventional mid-frequency Raman spectroscopy. This was attributed to the higher sensitivity for solid-state forms, due to the higher intensity scattering and signal-to-noise ratio, as well as larger differences between the solid-state forms in the low-frequency range. Overall, low-frequency Raman spectroscopy may be better for quantitative solid-state analysis, even in cases where the solid-state forms can be resolved using conventional mid-frequency Raman spectroscopy.

5.4 Time-gated Raman spectroscopy for quantitative analysis of fluorescent powder mixtures (IV)

In this work, time-gated Raman spectroscopy for quantitative solid-state analysis of fluorescent powder mixtures was evaluated. Chemometric analysis of the data consisting of both spectral and time dimensions was performed by two methods: (1) PLS regression, the most well established multivariate quantitative analysis method in pharmaceutics, and (2) kernel-based RLS with greedy feature selection, which optimised data use in both dimensions.

5.4.1 Fluorescence rejection by time-gated Raman spectroscopy

The three solid-state forms of piroxicam (the β and α2 anhydrates, and the monohydrate) fluoresced to varying degrees when excited by a 532 nm light source, as represented by the elevated baselines (**FIG 22**). The β form was more fluorescent than the α2 form and the monohydrate. In addition to fluorescence intensity, also the fluorescence signal lifetime profiles were solid-state specific. Differences in fluorescence profiles have previously been observed by time-gated Raman spectroscopy with different solid-state forms of another drug, the amorphous and γ-crystalline forms of indomethacin [159].

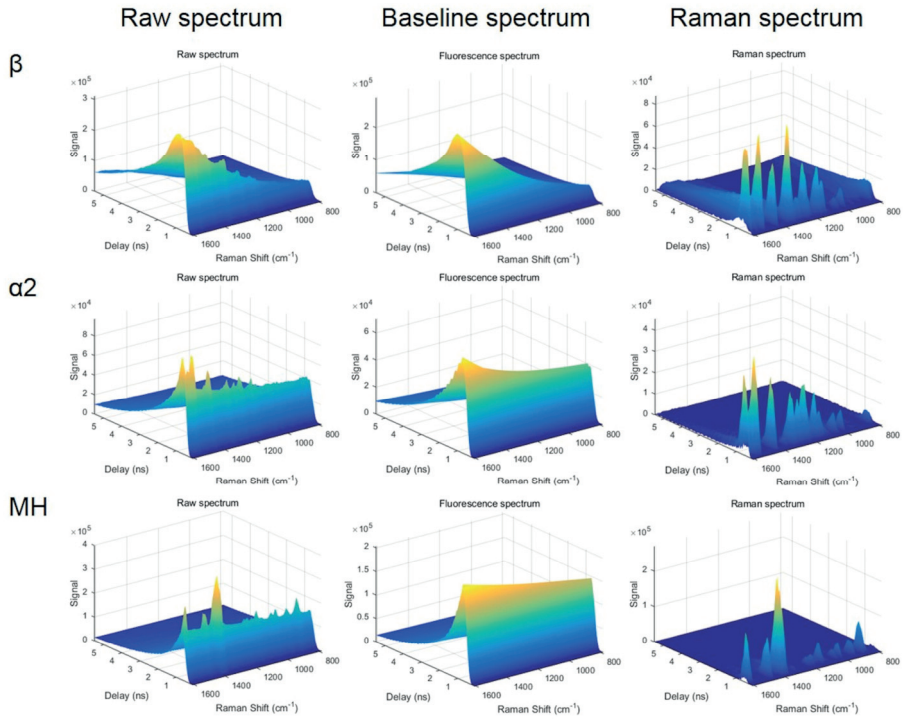

Figure 22 Time-resolved spectra of piroxicam solid-state forms (β and α2 anhydrates, and the monohydrate, MH), recorded with the time-gated Raman instrument. The spectra show the detected photon intensities in the Raman shift dimension (between 800-1600 cm^{-1}) and in the time dimension (delay from laser pulse between 0-5.5 ns). The raw spectra contain all detected photons, including Raman scattered and fluorescence photons. The baseline spectra represent the fluorescence signals. The Raman spectra are the spectra after fluorescence rejection, presenting mainly Raman scattered photons.

The observed fluorescence baselines were consistent between the time-gated Raman instrument, utilising a picosecond pulsed laser for excitation, and with the Raman system equipped with a conventional continuous-wave (CW) 532 nm laser (**FIG 23**). This confirmed that the observed fluorescence was not instrument setup-dependent.

The Raman scattering occurred immediately after the laser pulse (at approximately 0.4-0.8 ns delay based on visual evaluation), while the gradual decay of the fluorescence signal was detected over several nanoseconds (**FIG 22**). By utilising time-gating and selecting only the data recorded in the 0.4-0.8 ns time-domain, it was possible to reject the fluorescence tail. There was residual fluorescence which temporally overlapped with the Raman signal, which was removed by baseline correction. After time-domain selection and baseline correction, fluorescence-free time-resolved Raman spectra for the piroxicam crystal forms were obtained (the Raman spectra in **FIGs 22 and 23**). These spectra clearly showed the characteristic Raman peaks of the piroxicam solid-state forms [185].

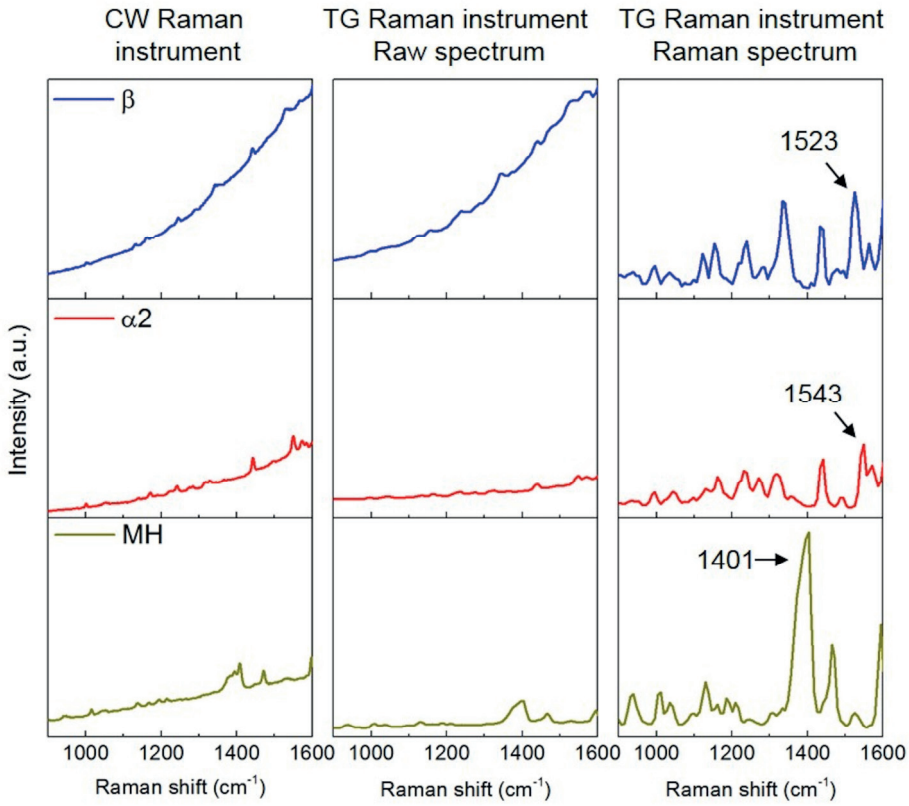

Figure 23 Spectra of piroxicam solid-state forms (β and α2 anhydrates, and the monohydrate), collected by the reference instrument equipped with a continuous-wave laser (CW Raman) and the time-gated Raman (TG Raman) instrument. The TG Raman instrument spectra are the 2D (summed) representations of the raw spectra and Raman spectra shown in **FIG 22.** The TG raw spectra contain the full temporal signals with fluorescence ('full time domain'). The TG Raman spectra are the signals after time-domain selection (0.4-0.8 ns) and fluorescence rejection ('selected time domain'). The specified Raman peaks are some, but not all, solid-state characteristic peaks.

The time-resolved (2D) spectra could be processed and evaluated by standard spectral processing and multivariate methods (such as PCA and PLS). When measuring the powders consisting of ternary mixtures of piroxicam solid-state forms, the mixtures could be differentiated from each other by performing PCA on the time-resolved Raman spectra.

5.4.2 Quantification of solid-state forms in mixtures

Quantitative analysis was performed using two chemometric methods: (1) PLS regression and (2) kernel-based RLS regression with greedy feature selection. For the PLS method, the used time-resolved data which utilised time-domain selection, was acquired using the 0.4-0.8 ns time-frame, as described above (**5.4.1**). This time-frame was chosen based on visual inspection of the raw data.

The kernel-based (RLS with greedy feature selection) analysis method was applied as an alternative approach that optimized the use of the recorded data in both the temporal and spectral dimensions. The kernel-based algorithm performed iterative optimisation of the time-domain and Raman shift selection.

Both methods were applied also with the equivalent of non-time-resolved spectral data. This data contained the full time domain signal (0-5.5 ns time-frame) that was baseline-corrected by computational spectral processing. This situation allowed a direct comparison between time-gated and essentially non-time-gated Raman measurements, without the complication of experimental and instrumental differences.

Both chemometric methods showed that determination of the solid-state composition of the ternary mixtures was possible based on the Raman spectra. Further, the methods showed that the use of time-resolved spectral data (with time domain selection) resulted in more accurate quantification compared to the essentially non-time-resolved (full time domain) data (**FIG 24**). This demonstrated that baseline correction for fluorescence signal removal was not as effective as the instrument-based fluorescence rejection. Baseline-correction represents a standard spectral processing procedure with conventional Raman spectroscopy, often performed when spectra have elevated baselines due to photoluminescence.

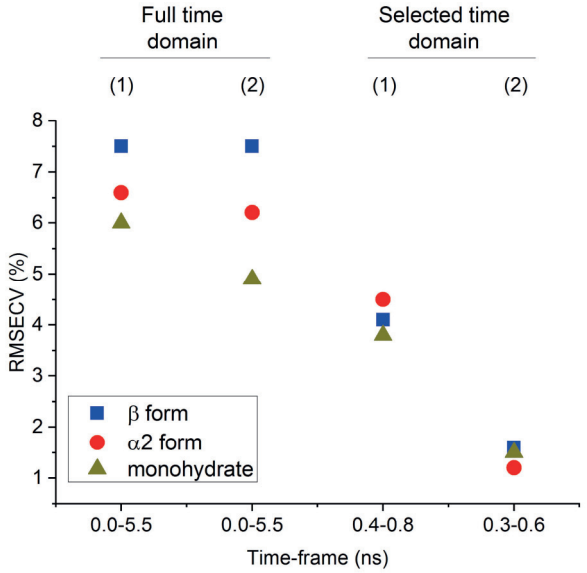

Figure 24 Errors in quantification for each piroxicam solid-state form, expressed as RMSECV (%), when using essentially non-time-resolved, baseline-corrected spectral data (full time domain) or time-resolved spectral data utilising time frame selection (selected time domain). (1) refers to the PLS method and (2) is the kernel-based method, with optimisation of data use. The time-frame refers to the selected signal in the time dimension, used for analysis.

Using time-resolved data (selected time-domain) with the PLS method resulted in an average quantification error of 4.1 % for the three solid-state forms, which was better than the essentially non-time-resolved (full time domain), baseline-corrected data (6.7 %). The quantitative performance could, however, be significantly improved by applying the kernel-based method for optimisation of data use. Three-fold better quantitative performance could be achieved compared to the PLS method, with an average error of 1.4 %. The iterative optimisation resulted in a different time-frame compared to the visually selected one, namely the optimisation resulted in a 0.3-0.6 ns time-frame instead of 0.4-0.8 ns.

The Raman signals of the piroxicam forms were detected over the fluorescence backgrounds. However, with other compounds the Raman scattering can be more completely masked by fluorescence. In such cases time-gated Raman spectroscopy for fluorescence rejection is expected to offer much more pronounced benefits than observed in this work. The technique may be widely applicable in pharmaceutical development and manufacturing, since not only some active ingredients including proteins, but also many excipients, such as cellulose-based polymers, fluoresce. Further practical advantages of Raman spectroscopy are the possibility to focus on the API properties over excipients in mixtures (in case of drug molecules with aromatic and π-bonded structures), as well as insensitivity to water, and for time-gated Raman spectroscopy in particular, the possibility to perform measurements in ambient lighting. These properties make time-gated Raman spectroscopy particularly suitable for process monitoring applications.

In conclusion, the study showed that time-gated Raman spectroscopy was applicable for solid-state form quantification and that it provided benefits for quantitative analysis of fluorescent powder mixtures. The instrument-based fluorescence rejection allowed better quantification performance compared to spectral-processing-based baseline-correction procedures. Quantification was possible with manual time-domain data selection and the standard PLS regression method, however substantially better results were achieved by data use optimisation with the kernel-based RLS method with greedy feature selection. This supports further exploring the possibilities of efficient data use optimisation and evaluating alternatives for the established data analysis methods in the pharmaceutical field. Overall, time-gated Raman spectroscopy was a suitable tool for analysing photoluminescent, including fluorescent, powders and quantification of solid-state forms in mixtures.

6 Conclusions

This work was carried out in order to identify possible new stabilising excipients for spray-dried protein formulations, and to evaluate quantitative solid-state analysis techniques based on Raman spectroscopy and multivariate data analysis methods, new in the pharmaceutical field.

By optimizing the process parameters both melibiose and isomalt could be spray dried into amorphous powders which remained relatively stable (i.e. did not crystallise). Melibiose showed better process behaviour and physical stability than isomalt, which made it a more favourable candidate for spray-dried protein formulations.

In the subsequent study melibiose showed protein-stabilising efficacy during spray drying and storage. The formulations were physically stable in the amorphous form. Compared to the current standard excipient trehalose, protein formulations with melibiose could be spray-dried more efficiently to drier powders, and protein activity was protected at least equally well. Overall, melibiose showed promising properties for spray-dried protein formulations.

In the application of Raman spectroscopy for solid state analysis, low-frequency Raman spectroscopy demonstrated higher sensitivity for solid-state forms and better quantitative performance compared to conventional mid-frequency Raman spectroscopy analysis. Pharmaceutical solids, during processes and storage, can be mixtures of solid-state forms, making reliable and accurate quantification important. Low-frequency Raman spectroscopy can be a valuable tool in pharmaceutical solid-state analysis, and provide improved analytical capabilities even in cases where solid-state forms can be resolved by mid-frequency Raman spectroscopy.

The other Raman technique, time-gated Raman spectroscopy, was useful for analysing fluorescent solids and provided a benefit for quantifying their mixtures. Standard multivariate analysis methods allowed quantitative analysis, while more recently adopted, kernel-based methods which optimised the use of the time-gated data, gave superior quantitative results.

In conclusion, melibiose was identified as a promising potential excipient for stabilising spray-dried protein formulations. Based on this work, melibiose is worth further investigations with other proteins - and also other materials requiring stabilisation in the amorphous form - along with longer term storage stability studies. Further studies regarding the toxicological aspects are also required before melibiose could be considered for commercial pharmaceutical products. Low-frequency and time-gated Raman spectroscopies, as well as kernel-based data analysis, were identified as advantageous methods for analysing solid-state form composition, also with fluorescent pharmaceuticals. These techniques can be adopted for various analysis applications and they could be particularly suitable with spray-dried biomaterial formulations where solid-state composition is critical for stability and where fluorescence can be an issue limiting the use of conventional Raman spectroscopy as a monitoring technique.

References

1. Healy, A.M., Z.A. Worku, D. Kumar, and A.M. Madi, *Pharmaceutical solvates, hydrates and amorphous forms: A special emphasis on cocrystals*. Adv Drug Deliv Rev, 2017. 117: p. 25-46
2. Buckton, G., *Solid-state properties*, in *Aulton's Pharmaceutics The Design and Manufacture of Medicines*, M.E. Aulton, Editor. 2007: Edinburgh. p. 110-120.
3. Mensink, M.A., H.W. Frijlink, K. van der Voort Maarschalk, and W.L. Hinrichs, *How sugars protect proteins in the solid state and during drying: Mechanisms of stabilization in relation to stress conditions*. Eur J Pharm Biopharm, 2017. 114: p. 288-295.
4. Abdul-Fattah, A.M. and V.L. Truong, *Drying Process Methods for Biopharmaceutical Products: An Overview*, in *Formulation and Process Development Strategies for Manufacturing Biopharmaceuticals*, F. Jameel and S. Hershenson, Editors. 2010, John Wiley & Sons, Inc.: Hoboken, New Jersey, USA.
5. Eriksson, H.J.C., W.L.J. Hinrichs, B. van Veen, G.W. Somsen, G.J. de Jong, and H.W. Frijlink, *Investigations into the stabilisation of drugs by sugar glasses: I. Tablets prepared from stabilised alkaline phosphatase.* Int J Pharm, 2002. 249(1): p. 59-70.
6. Vandenheuvel, D., J. Meeus, R. Lavigne, and G. Van den Mooter, *Instability of bacteriophages in spray-dried trehalose powders is caused by crystallization of the matrix.* Int J Pharm, 2014. 472(1): p. 202-205.
7. Tzannis, S.T. and S.J. Prestrelski, *Activity-stability considerations of trypsinogen during spray drying: effects of sucrose*. J Pharm Sci, 1999. 88(3): p. 351-9.
8. Elder, D.P., J.E. Patterson, and R. Holm, *The solid-state continuum: a perspective on the interrelationships between different solid-state forms in drug substance and drug product*. J Pharm Pharmacol, 2015. 67(6): p. 757-772.
9. Ticehurst, M.D. and I. Marziano, *Integration of active pharmaceutical ingredient solid form selection and particle engineering into drug product design*. J Pharm Pharmacol, 2015. **67**(6): p. 782-802.
10. Baghel, S., H. Cathcart, and N.J. O'Reilly, *Polymeric Amorphous Solid Dispersions: A Review of Amorphization, Crystallization, Stabilization, Solid-State Characterization, and Aqueous Solubilization of Biopharmaceutical Classification System Class II Drugs*. J Pharm Sci, 2016. 105(9): p. 2527-2544.
11. Vasconcelos, T., S. Marques, J. das Neves, and B. Sarmento, *Amorphous solid dispersions: Rational selection of a manufacturing process*. Adv Drug Deliv Rev, 2016. 100: p. 85-101.
12. Chieng, N., T. Rades, and J. Aaltonen, *An overview of recent studies on the analysis of pharmaceutical polymorphs*. J Pharm Biomed Anal, 2011. 55(4): p. 618-644.
13. Paudel, A., D. Raijada, and J. Rantanen, *Raman spectroscopy in pharmaceutical product design*. Adv Drug Deliv Rev, 2015. 89: p. 3-20.
14. Hédoux, A., *Recent developments in the Raman and infrared investigations of amorphous pharmaceuticals and protein formulations: A review*. Adv Drug Deliv Rev, 2016. 100: p. 133-146.

15. Larkin, P.J., M. Dabros, B. Sarsfield, E. Chan, J.T. Carriere, and B.C. Smith, *Polymorph characterization of active pharmaceutical ingredients (APIs) using low-frequency Raman spectroscopy*. Appl Spectrosc, 2014. 68(7): p. 758-76.
16. Kostamovaara, J., J. Tenhunen, M. Kogler, I. Nissinen, J. Nissinen, and P. Keranen, *Fluorescence suppression in Raman spectroscopy using a time-gated CMOS SPAD*. Opt Express, 2013. 21(25): p. 31632-45.
17. Strachan, C.J., T. Rades, K.C. Gordon, and J. Rantanen, *Raman spectroscopy for quantitative analysis of pharmaceutical solids*. J Pharm Pharmacol, 2007. 59(2): p. 179-192.
18. Hainmueller, J. and C. Hazlett, *Kernel Regularized Least Squares: Reducing Misspecification Bias with a Flexible and Interpretable Machine Learning Approach*. Political Anal., 2017. 22(2): p. 143-168.
19. Davies, P., *Oral solid dosage forms*, in *Pharmaceutical Preformulation and Formulation: A Practical Guide from Candidate Drug Selection to Commercial Dosage Form*, G. Mark, Editor. 2009, Informa Healthcare: New York. p. 367-430.
20. Broadhead, J. and M. Gibson, *Parenteral dosage forms*, in *Pharmaceutical Preformulation and Formulation: A Practical Guide from Candidate Drug Selection to Commercial Dosage Form*, M. Gibson, Editor. 2009, Informa Healthcare: New York. p. 325-347.
21. Laitinen, R., P.A. Priemel, S. Surwase, K. Graeser, C.J. Strachan, H. Grohganz, and T. Rades, *Theoretical Considerations in Developing Amorphous Solid Dispersions*, in *Amorphous Solid Dispersions: Theory and Practice*, N. Shah, et al., Editors. 2014, Springer New York: New York, NY. p. 35-90.
22. Hancock, B.C. and G. Zografi, *Characteristics and significance of the amorphous state in pharmaceutical systems*. J Pharm Sci, 1997. 86(1): p. 1-12.
23. Dengale, S.J., H. Grohganz, T. Rades, and K. Löbmann, *Recent advances in co-amorphous drug formulations*. Adv Drug Deliv Rev, 2016. 100: p. 116-125.
24. Bunaciu, A.A., H.Y. Aboul-Enein, and V.D. Hoang, *Vibrational spectroscopy used in polymorphic analysis*. TrAC Trends Anal Chem, 2015. 69: p. 14-22.
25. Yu, L., *Amorphous pharmaceutical solids: preparation, characterization and stabilization*. Adv Drug Deliv Rev 2001. 48(1): p. 27-42.
26. Steele, G., *Preformulation as an Aid to Product Design in Early Drug Development*, in *Pharmaceutical Preformulation and Formulation: A Practical Guide from Candidate Drug Selection to Commercial Dosage Form*, M. Gibson, Editor. 2009, Informa Healthcare, Inc: New York. p. 17-128.
27. Izutsu, K., S. Yoshioka, and T. Terao, *Decreased protein-stabilizing effects of cryoprotectants due to crystallization*. Pharm Res, 1993. 10(8): p. 1232-7.
28. Mensink, M.A., M.J. Nethercott, W.L. Hinrichs, K. van der Voort Maarschalk, H.W. Frijlink, E.J. Munson, and M.J. Pikal, *Influence of Miscibility of Protein-Sugar Lyophilizates on Their Storage Stability*. AAPS J, 2016. 18(5): p. 1225-32.
29. Tzannis, S.T. and S.J. Prestrelski, *Moisture effects on protein-excipient interactions in spray-dried powders. Nature of destabilizing effects of sucrose*. J Pharm Sci, 1999. 88(3): p. 360-70.

30. Heinz, A., C.J. Strachan, K.C. Gordon, and T. Rades, *Analysis of solid-state transformations of pharmaceutical compounds using vibrational spectroscopy*. J Pharm Pharmacol, 2009. 61(8): p. 971-988.
31. Alexandrino, G.L., M.R. Khorasani, J.M. Amigo, J. Rantanen, and R.J. Poppi, *Monitoring of multiple solid-state transformations at tablet surfaces using multi-series near-infrared hyperspectral imaging and multivariate curve resolution*. Eur J Pharm Biopharm, 2015. 93: p. 224-230.
32. Govindarajan, R. and R. Suryanarayanan, *Processing-induced Phase Transformations and Their Implications on Pharmaceutical Product Quality*, in *Polymorphism*. 2006, Wiley-VCH Verlag GmbH & Co. KGaA. p. 333-364.
33. Koradia, V., H.L. de Diego, M.R. Elema, and J. Rantanen, *Integrated Approach to Study the Dehydration Kinetics of Nitrofurantoin Monohydrate*. J Pharm Sci, 2010. 99(9): p. 3966-3976.
34. Zhu, H., J. Xu, P. Varlashkin, S. Long, and C. Kidd, *Dehydration, hydration behavior, and structural analysis of fenoprofen calcium*. J Pharm Sci, 2001. 90(7): p. 845-859.
35. FDA. *Guidance for Industry: PAT – A Framework for Innovative Pharmaceutical Development, Manufacture, and Quality Assurance. 2004. Available online at: http://www.fda.gov/downloads/Drugs/GuidanceComplianceRegulatoryInformation/Guidances/UCM070305.pdf*. [Accessed 29 April 2018].
36. Knop, K. and P. Kleinebudde, *PAT-tools for process control in pharmaceutical film coating applications*. Int J Pharm, 2013. 457(2): p. 527-36.
37. Aaltonen, J., K.C. Gordon, C.J. Strachan, and T. Rades, *Perspectives in the use of spectroscopy to characterise pharmaceutical solids*. Int J Pharm, 2008. 364(2): p. 159-169.
38. Shih, H.H., P. Miller, and D.C. Harnish, *An Overview of the Discovery and Development Process for Biologics*, in *Pharmaceutical Sciences Encyclopedia*. 2010, John Wiley & Sons, Inc.
39. Schellekens, H., *Immunogenicity of therapeutic proteins: Clinical implications and future prospects*. Clin Ther, 2002. 24(11): p. 1720-1740.
40. Jiskoot, W., T.W. Randolph, D.B. Volkin, C.R. Middaugh, C. Schoneich, G. Winter, W. Friess, D.J. Crommelin, and J.F. Carpenter, *Protein instability and immunogenicity: roadblocks to clinical application of injectable protein delivery systems for sustained release*. J Pharm Sci, 2012. 101(3): p. 946-54.
41. Wang, W., S. Nema, and D. Teagarden, *Protein aggregation--pathways and influencing factors*. Int J Pharm, 2010. 390(2): p. 89-99.
42. Ohtake, S. and W. Wang, *Protein and Peptide Formulation Development*, in *Pharmaceutical Sciences Encyclopedia*. 2014, John Wiley & Sons, Inc.
43. Nelson, D.L. and M.M. Cox, *Lehninger Principles of Biochemistry*. 4th ed., M.M. Cox, Editor. 2005, New York: W. H. Freeman and Company.
44. Schiffter, H.A., *Pharmaceutical Proteins – Structure, Stability, and Formulation*, in *Comprehensive Biotechnology 2nd ed.*, M. Moo-Young, Editor. 2011, Academic Press: Burlington. p. 521-541.
45. Manning, M.C., D.K. Chou, B.M. Murphy, R.W. Payne, and D.S. Katayama, *Stability of protein pharmaceuticals: an update*. Pharm Res, 2010. 27(4): p. 544-75.

46. Shire, S.J., *Formulation of proteins and monoclonal antibodies (mAbs)*, in *Monoclonal Antibodies*. 2015, Woodhead Publishing. p. 93-120.
47. Wang, W., *Protein aggregation and its inhibition in biopharmaceutics.* Int J Pharm, 2005. 289(1): p. 1-30.
48. Winter, G. and J. Myschik, *Formulation Strategies for Recombinant Protein and Related Biotech Drugs*, in *Pharmaceutical Biotechnology*. 2012, Wiley-VCH Verlag GmbH & Co. KGaA. p. 235-256.
49. Wang, W., S. Singh, D.L. Zeng, K. King, and S. Nema, *Antibody structure, instability, and formulation.* J Pharm Sci, 2007. 96(1): p. 1-26.
50. Lipiäinen, T., M. Peltoniemi, S. Sarkhel, T. Yrjönen, H. Vuorela, A. Urtti, and A. Juppo, *Formulation and Stability of Cytokine Therapeutics.* Journal of Pharmaceutical Sciences, 2015. 104(2): p. 307-326.
51. Arakawa, T., S.J. Prestrelski, W.C. Kenney, and J.F. Carpenter, *Factors affecting short-term and long-term stabilities of proteins.* Adv Drug Deliv Rev, 2001. 46(1-3): p. 307-26.
52. Ohtake, S., Y. Kita, and T. Arakawa, *Interactions of formulation excipients with proteins in solution and in the dried state.* Adv Drug Deliv Rev, 2011. 63(13): p. 1053-73.
53. Kamerzell, T.J., R. Esfandiary, S.B. Joshi, C.R. Middaugh, and D.B. Volkin, *Protein-excipient interactions: mechanisms and biophysical characterization applied to protein formulation development.* Adv Drug Deliv Rev, 2011. 63(13): p. 1118-59.
54. Prestrelski, S.J., N. Tedeschi, T. Arakawa, and J.F. Carpenter, *Dehydration-induced conformational transitions in proteins and their inhibition by stabilizers.* Biophys J, 1993. 65(2): p. 661-671.
55. Wang, W., *Lyophilization and development of solid protein pharmaceuticals.* Int J Pharm, 2000. 203(1-2): p. 1-60.
56. Crowe, J.H., L.M. Crowe, J.F. Carpenter, and C. Aurell Wistrom, *Stabilization of dry phospholipid bilayers and proteins by sugars.* Biochem J, 1987. 242(1): p. 1-10.
57. Cicerone, M.T., M.J. Pikal, and K.K. Qian, *Stabilization of proteins in solid form.* Adv Drug Deliv Rev, 2015. 93: p. 14-24.
58. Abdul-Fattah, A.M., D. Lechuga-Ballesteros, D.S. Kalonia, and M.J. Pikal, *The Impact of Drying Method and Formulation on the Physical Properties and Stability of Methionyl Human Growth Hormone in the Amorphous Solid State.* J Pharm Sci, 2008. 97(1): p. 163-184.
59. DePaz, R.A., D.A. Dale, C.C. Barnett, J.F. Carpenter, A.L. Gaertner, and T.W. Randolph, *Effects of drying methods and additives on the structure, function, and storage stability of subtilisin: role of protein conformation and molecular mobility.* Enzyme Microb Technol, 2002. 31(6): p. 765-774.
60. Rochelle, C. and G. Lee, *Dextran or Hydroxyethyl Starch in Sprayfreeze-Dried Trehalose/Mannitol Microparticles Intended as Ballistic Particulate Carriers for Proteins.* J Pharm Sci, 2007. 96(9): p. 2296-2309.
61. Tonnis, W.F., M.A. Mensink, A. de Jager, K. van der Voort Maarschalk, H.W. Frijlink, and W.L. Hinrichs, *Size and molecular flexibility of sugars determine the storage stability of freeze-dried proteins.* Mol Pharm, 2015. 12(3): p. 684-94.
62. Carpenter, J.F., S.J. Prestrelski, and T. Arakawa, *Separation of freezing- and drying-induced denaturation of lyophilized proteins using stress-*

specific stabilization. I. Enzyme activity and calorimetric studies. Arch Biochem Biophys, 1993. 303(2): p. 456-64.

63. Mensink, M.A., P.-J. Van Bockstal, S. Pieters, L. De Meyer, H.W. Frijlink, K. van der Voort Maarschalk, W.L.J. Hinrichs, and T. De Beer, *In-line near infrared spectroscopy during freeze-drying as a tool to measure efficiency of hydrogen bond formation between protein and sugar, predictive of protein storage stability*. Int J Pharm, 2015. 496(2): p. 792-800.
64. Cesàro, A., O. De Giacomo, and F. Sussich, *Water interplay in trehalose polymorphism*. Food Chem, 2008. 106(4): p. 1318-1328.
65. Ohtake, S. and Y.J. Wang, *Trehalose: Current Use and Future Applications*. J Pharm Sci, 2011. 100(6): p. 2020-2053.
66. Suihko, E.J., R.T. Forbes, and D.C. Apperley, *A solid-state NMR study of molecular mobility and phase separation in co-spray-dried protein–sugar particles*. Eur J Pharm Sci, 2005. 25(1): p. 105-112.
67. Sentko, A. and I. Willibald-Ettle, *Isomalt*, in *Sweeteners and Sugar Alternatives in Food Technology*. 2012, Wiley-Blackwell. p. 243-274.
68. Bolhuis, G.K., J.J.P. Engelhart, and A.C. Eissens, *Compaction properties of isomalt*. Eur J Pharm Biopharm, 2009. 72(3): p. 621-625.
69. Ndindayino, F., D. Henrist, F. Kiekens, G. Van den Mooter, C. Vervaet, and J.P. Remon, *Direct compression properties of melt-extruded isomalt*. Int J Pharm, 2002. 235(1): p. 149-157.
70. Quodbach, J., J. Mosig, and P. Kleinebudde, *Compaction behavior of isomalt after roll compaction*. Pharmaceutics, 2012. 4(4): p. 494-500.
71. Tuderman, A.-K., C.J. Strachan, and A.M. Juppo, *Isomalt and its diastereomer mixtures as stabilizing excipients with freeze-dried lactate dehydrogenase*. Int J Pharm, 2018. 538(1): p. 287-295.
72. Kanters, J.A., G. Roelofsen, H.M. Doesburg, and T. Koops, *The crystal structure of a disaccharide, [alpha]-melibiose monohydrate (O-[alpha]-d-galactopyranosyl-(1-->6)-[alpha]-d-glucopyranoside)*. Acta Crystallogr, Sect B, 1976. 32(10): p. 2830-2837.
73. Zhou, Y., Y. Zhu, Y. Men, C. Dong, Y. Sun, and J. Zhang, *Construction of engineered Saccharomyces cerevisiae strain to improve that whole-cell biocatalytic production of melibiose from raffinose*. J Ind Microbiol Biotechnol, 2017. 44(3): p. 489-501.
74. Heljo, V.P., K. Jouppila, T. Hatanpaa, and A.M. Juppo, *The use of disaccharides in inhibiting enzymatic activity loss and secondary structure changes in freeze-dried beta-galactosidase during storage*. Pharm Res, 2011. 28(3): p. 540-52.
75. Heljo, V.P., V. Filipe, S. Romeijn, W. Jiskoot, and A.M. Juppo, *Stability of rituximab in freeze-dried formulations containing trehalose or melibiose under different relative humidity atmospheres*. J Pharm Sci, 2013. 102(2): p. 401-14.
76. Borde, B. and A. Cesàro, *A DSC Study of Hydrated Sugar Alcohols. Isomalt*. J Therm Anal Calorim, 2001. 66(1): p. 179-195.
77. Koskinen, A.K., S.J. Fraser-Miller, J.P. Botker, V.P. Heljo, J.E. Barnsley, K.C. Gordon, C.J. Strachan, and A.M. Juppo, *Physical Stability of Freeze-Dried Isomalt Diastereomer Mixtures*. Pharm Res, 2016. 33(7): p. 1752-68
78. Cammenga, H.K. and B. Zielasko, *Thermal behaviour of isomalt*. Thermochim Acta, 1996. 271: p. 149-153.

79. Fletcher, H.G. and H.W. Diehl, *Improvements in the Preparation of Melibiose from Raffinose. A New Form of Melibiose.* J Am Chem Soc, 1952. 74(22): p. 5774-5776.
80. Lakio, S., J. Sainio, P. Heljo, T. Ervasti, N. Kivikero, and A. Juppo, *The tableting properties of melibiose monohydrate.* Int J Pharm, 2013. 456(2): p. 528-535.
81. Heljo, V.P., A. Nordberg, M. Tenho, T. Virtanen, K. Jouppila, J. Salonen, S.L. Maunu, and A.M. Juppo, *The effect of water plasticization on the molecular mobility and crystallization tendency of amorphous disaccharides.* Pharm Res, 2012. 29(10): p. 2684-97.
82. Simperler, A., A. Kornherr, R. Chopra, P.A. Bonnet, W. Jones, W.D. Motherwell, and G. Zifferer, *Glass transition temperature of glucose, sucrose, and trehalose: an experimental and in silico study.* J Phys Chem B, 2006. 110(39): p. 19678-84.
83. Sussich, F. and A. Cesàro, *Transitions and Phenomenology of α,α-trehalose Polymorphs Inter-conversion.* Journal of Thermal Analysis and Calorimetry, 2000. 62(3): p. 757-768.
84. *FAO/WHO Codex Alimentarius International Food Standards. Available online at: http://www.fao.org/gsfaonline/additives/details.html?id=180.* [Accessed 29 April 2018].
85. *FDA Drug Database, Inactive Ingredient Search, https://www.accessdata.fda.gov/scripts/cder/iig/index.cfm?event=BasicSearch.page.* [Accessed 29 April 2018].
86. *European Medicines Agency. http://www.ema.europa.eu/ema/.* [Accessed 29 April 2018].
87. *European Pharmacopoeia Online 9th Edition 2017 (9.2). http://online6.edqm.eu/ep902/.* [Accessed 29 April 2018].
88. *United States Pharmacopeial Convention, 2014. United States Pharmacopeia and National Formulary (USP 38-NF 33), Slp edition (May 2015). United States Pharmacopeial, Rockville, MD.*
89. Thiébaud, D., E. Jacot, H. Schmitz, M. Spengler, and J.P. Felber, *Comparative study of isomalt and sucrose by means of continuous indirect calorimetry.* Metabolism, 1984. 33(9): p. 808-813.
90. Waalkens-Berendsen, D.H., H.B.W.M. Koëter, and M.W. van Marwijk, *Embryotoxicity/teratogenicity of isomalt in rats and rabbits.* Food Chem Toxicol, 1990. 28(1): p. 1-9.
91. Smits-Van Prooije, A.E., A.P. De Groot, H.C. Dreef-Van Der Meulen, and E.J. Sinkeldam, *Chronic toxicity and carcinogenicity study of isomalt in rats and mice.* Food Chem Toxicol, 1990. 28(4): p. 243-251.
92. *World Health Organization, 1987. Isomalt in: Toxicological evaluation of certain food additives and contaminants. (WHO Food Additives Series No. 20). Available online at: http://www.inchem.org/documents /jecfa/jecmono/v20je14.htm.* [Accessed 29 April 2018].
93. Musch, K., G. Siebert, H. Schiweck, and G. Steinle, *Nutrition physiologic studies with isomaltite in the rat.* Zeitschrift fur Ernahrungswissenschaft, 1973. Sup.15: p. 3-16.
94. Fröschle, M., H. Horn, and O. Spring, *Characterization of Jatropha curcas honeys originating from the southern highlands of Madagascar.* LWT, 2018. 93: p. 525-533.
95. Cerbulis, J., *Sugars in caracas cacao beans.* Arch Biochem Biophys, 1954. 49(2): p. 442-450.

96. Valliyodan, B., H. Shi, and H.T. Nguyen, *A Simple Analytical Method for High-Throughput Screening of Major Sugars from Soybean by Normal-Phase HPLC with Evaporative Light Scattering Detection*. Chromatogr Res Int, 2015. 2015: p. 8.
97. Liu, J.-C., J. Miller, J. Kung, N. Susan, and N. Glenn, *Composition to enhance permeation of topical skin agents*. *EP1192938,* 2004.
98. *European Chemicals Agency ECHA*. *https://echa.europa.eu/substance-information/-/substanceinfo/100.008.700*. [Accessed 29 April 2018].
99. Taylor, R.M., I. Bjarnason, P. Cheeseman, M. Davenport, A.J. Baker, G. Mieli-Vergani, and A. Dhawan, *Intestinal Permeability and Absorptive Capacity in Children with Portal Hypertension*. Scand J Gastroenterol, 2002. 37(7): p. 807-811.
100. Tomita, K., T. Nagura, Y. Okuhara, H. Nakajima-Adachi, N. Shigematsu, T. Aritsuka, S. Kaminogawa, and S. Hachimura, *Dietary melibiose regulates Th cell response and enhances the induction of oral tolerance*. Biosci Biotechnol Biochem, 2007. 71(11): p. 2774-80.
101. Tomsik, P., L. Sispera, M. Rezacova, M. Niang, A. Stoklasova, J. Cerman, J. Knizek, E. Brcakova, J. Cermanova, and S. Micuda, *Increased melibiose/rhamnose ratio in bile of rats with acute cholestasis*. J Gastroenterol Hepatol, 2008. 23(12): p. 1934-40.
102. Lee, G.-C., C.-H. Lin, Y.-C. Tao, J.-M. Yang, K.-C. Hsu, Y.-J. Huang, S.-H. Huang, P.-J. Kung, W.-L. Chen, C.-M. Wang, Y.-R. Wu, C.-M. Chen, J.-Y. Lin, H.M. Hsieh-Li, and G.-J. Lee-Chen, *The potential of lactulose and melibiose, two novel trehalase-indigestible and autophagy-inducing disaccharides, for polyQ-mediated neurodegenerative disease treatment*. NeuroToxicology, 2015. 48: p. 120-130.
103. Cal, K. and K. Sollohub, *Spray drying technique. I: Hardware and process parameters*. J Pharm Sci, 2010. 99(2): p. 575-86.
104. Sollohub, K. and K. Cal, *Spray drying technique: II. Current applications in pharmaceutical technology*. J Pharm Sci, 2010. 99(2): p. 587-97.
105. Patel, B.B., J.K. Patel, and S. Chakraborty, *Review of patents and application of spray drying in pharmaceutical, food and flavor industry*. Recent Pat Drug Deliv Formul, 2014. 8(1): p. 63-78.
106. Searles, J. and G. Mohan, *Spray Drying of Biopharmaceuticals and Vaccines*, in *Formulation and Process Development Strategies for Manufacturing Biopharmaceuticals*. 2010, John Wiley & Sons, Inc. p. 739-761.
107. Vehring, R., *Pharmaceutical Particle Engineering via Spray Drying*. Pharm Res, 2008. 25(5): p. 999-1022.
108. Walters, R.H., B. Bhatnagar, S. Tchessalov, K.-I. Izutsu, K. Tsumoto, and S. Ohtake, *Next Generation Drying Technologies for Pharmaceutical Applications*. J Pharm Sci, 2014. 103(9): p. 2673-2695.
109. Sou, T., E.N. Meeusen, M. de Veer, D.A. Morton, L.M. Kaminskas, and M.P. McIntosh, *New developments in dry powder pulmonary vaccine delivery*. Trends Biotechnol, 2011. 29(4): p. 191-8.
110. Trows, S. and R. Scherließ, *Carrier-based dry powder formulation for nasal delivery of vaccines utilizing BSA as model drug*. Powder Technol, 2016. 292: p. 223-231.
111. Paudel, A., Z.A. Worku, J. Meeus, S. Guns, and G. Van den Mooter, *Manufacturing of solid dispersions of poorly water soluble drugs by*

spray drying: Formulation and process considerations. Int J Pharm, 2013. 453(1): p. 253-284.

112. Grasmeijer, N., H.W. Frijlink, and W.L.J. Hinrichs, *Model to predict inhomogeneous protein–sugar distribution in powders prepared by spray drying*. J Aerosol Sci, 2016. 101: p. 22-33.
113. Singh, A. and G. Van den Mooter, *Spray drying formulation of amorphous solid dispersions*. Adv Drug Deliv Rev, 2016. 100: p. 27-50.
114. Vehring, R., W.R. Foss, and D. Lechuga-Ballesteros, *Particle formation in spray drying*. J Aerosol Sci, 2007. 38(7): p. 728-746.
115. Vicente, J., J. Pinto, J. Menezes, and F. Gaspar, *Fundamental analysis of particle formation in spray drying*. Powder Technol, 2013. 247: p. 1-7.
116. Haque, M. and B. Adhikari, *Drying and denaturation of proteins in spray drying process*, in *Handbook of Industrial Drying*, A.S. Mujumbar, Editor. 2015, CRC Press: United States. p. 971-984.
117. FDA database, *Afrezza (insulin human) Inhalation Powder*. 2014. Mannkind, Corp.
118. EMA database, *Raplixa - Human fibrinogen/human thrombin*. 2015. Mallincroft Pharmaceuticals Ireland Ltd.
119. White, S., D.B. Bennett, S. Cheu, P.W. Conley, D.B. Guzek, S. Gray, J. Howard, R. Malcolmson, J.M. Parker, P. Roberts, N. Sadrzadeh, J.D. Schumacher, S. Seshadri, G.W. Sluggett, C.L. Stevenson, and N.J. Harper, *EXUBERA: pharmaceutical development of a novel product for pulmonary delivery of insulin*. Diabetes Technol Ther, 2005. 7(6): p. 896-906.
120. Harper, N.J., S. Gray, J. De Groot, J.M. Parker, N. Sadrzadeh, C. Schuler, J.D. Schumacher, S. Seshadri, A.E. Smith, G.S. Steeno, C.L. Stevenson, R. Taniere, M. Wang, and D.B. Bennett, *The design and performance of the exubera pulmonary insulin delivery system*. Diabetes Technol Ther, 2007. 9 Suppl 1: p. S16-27.
121. Bowen, M., R. Turok, and Y.-F. Maa, *Spray Drying of Monoclonal Antibodies: Investigating Powder-Based Biologic Drug Substance Bulk Storage*. Drying Technol, 2013. 31(13-14): p. 1441-1450.
122. Maltesen, M.J., S. Bjerregaard, L. Hovgaard, S. Havelund, and M. van de Weert, *Quality by design – Spray drying of insulin intended for inhalation*. Eur J Pharm Biopharm, 2008. 70(3): p. 828-838.
123. Forbes, R.T., B.W. Barry, and A.A. Elkordy, *Preparation and characterisation of spray-dried and crystallised trypsin: FT-Raman study to detect protein denaturation after thermal stress*. Eur J Pharml Sci, 2007. 30(3): p. 315-323.
124. Adler, M. and G. Lee, *Stability and surface activity of lactate dehydrogenase in spray-dried trehalose*. J Pharm Sci, 1999. 88(2): p. 199-208.
125. Maury, M., K. Murphy, S. Kumar, A. Mauerer, and G. Lee, *Spray-drying of proteins: effects of sorbitol and trehalose on aggregation and FT-IR amide I spectrum of an immunoglobulin G*. Eur J Pharm Biopharm, 2005. 59(2): p. 251-261.
126. Ógáin, O.N., J. Li, L. Tajber, O.I. Corrigan, and A.M. Healy, *Particle engineering of materials for oral inhalation by dry powder inhalers. I—Particles of sugar excipients (trehalose and raffinose) for protein delivery*. Int J Pharm, 2011. 405(1): p. 23-35.

127. Yoshii, H., F. Buche, N. Takeuchi, C. Terrol, M. Ohgawara, and T. Furuta, *Effects of protein on retention of ADH enzyme activity encapsulated in trehalose matrices by spray drying*. J Food Eng, 2008. 87(1): p. 34-39.
128. Bürki, K., I. Jeon, C. Arpagaus, and G. Betz, *New insights into respirable protein powder preparation using a nano spray dryer*. Int J Pharm, 2011. 408(1): p. 248-256.
129. Liao, Y.-H., M.B. Brown, T. Nazir, A. Quader, and G.P. Martin, *Effects of Sucrose and Trehalose on the Preservation of the Native Structure of Spray-Dried Lysozyme*. Pharm Res, 2002. 19(12): p. 1847-1853.
130. Maa, Y.-F., P.-A. Nguyen, T. Sweeney, S.J. Shire, and C.C. Hsu, *Protein Inhalation Powders: Spray Drying vs Spray Freeze Drying*. Pharm Res, 1999. 16(2): p. 249-254.
131. McCreery, R.L., *Raman Spectroscopy for Chemical Analysis*. Chemical Analysis, J.D. Winefordner, Editor. Vol. 157. 2000, New York: John Wiley & Sons, Inc.
132. Smith, G.P.S., C.M. McGoverin, S.J. Fraser, and K.C. Gordon, *Raman imaging of drug delivery systems*. Adv Drug Deliv Rev, 2015. 89: p. 21-41.
133. De Beer, T., A. Burggraeve, M. Fonteyne, L. Saerens, J.P. Remon, and C. Vervaet, *Near infrared and Raman spectroscopy for the in-process monitoring of pharmaceutical production processes*. Int J Pharm, 2011. 417(1): p. 32-47.
134. Hédoux, A., L. Paccou, Y. Guinet, J.-F. Willart, and M. Descamps, *Using the low-frequency Raman spectroscopy to analyze the crystallization of amorphous indomethacin*. Eur J Pharm Sci, 2009. 38(2): p. 156-164.
135. Parrott, E.P.J. and J.A. Zeitler, *Terahertz time-domain and low-frequency Raman spectroscopy of organic materials*. Appl Spectrosc, 2015. 69(1): p. 1-25.
136. Mah, P.T., S.J. Fraser, M.E. Reish, T. Rades, K.C. Gordon, and C.J. Strachan, *Use of low-frequency Raman spectroscopy and chemometrics for the quantification of crystallinity in amorphous griseofulvin tablets*. Vib Spectrosc, 2015. 77: p. 10-16.
137. Moser, C. and F. Havermeyer, *Ultra-narrow-band tunable laserline notch filter*. Appl Phys B, 2009. 95(3): p. 597-601.
138. Carriere, J.T. and F. Havermeyer. *Ultra-low frequency Stokes and anti-Stokes Raman spectroscopy at 785nm with volume holographic grating filters*. in *Progress in Biomedical Optics and Imaging - Proc SPIE*. 2012.
139. Smith, G.P.S., G.S. Huff, and K.C. Gordon, *Investigating Crystallinity Using Low-Frequency Raman Spectroscopy: Applications in Pharmaceutical Analysis*. Spectrosc, 2016. 31(2): p. 42-50.
140. Ayala, A.P., M.W.C. Caetano, S.B. Honorato, J. Mendes Filho, H.W. Siesler, S.N. Faudone, S.L. Cuffini, F.T. Martins, C.C.P. Da Silva, and J. Ellena, *Conformational polymorphism of the antidiabetic drug chlorpropamide*. J Raman Spectrosc, 2012. 43(2): p. 263-272.
141. Ayala, A.P., *Polymorphism in drugs investigated by low wavenumber Raman scattering*. Vib Spectrosc, 2007. 45(2): p. 112-116.
142. Roy, S., B. Chamberlin, and A.J. Matzger, *Polymorph discrimination using low wavenumber Raman spectroscopy*. Org Process Res Dev, 2013. 17(7): p. 976-980.
143. Wang, H., M.A. Boraey, L. Williams, D. Lechuga-Ballesteros, and R. Vehring, *Low-frequency shift dispersive Raman spectroscopy for the*

analysis of respirable dosage forms. Int J Pharm, 2014. 469(1): p. 197-205.

144. Hisada, H., M. Inoue, T. Koide, J. Carriere, R. Heyler, and T. Fukami, *Direct High-Resolution Imaging of Crystalline Components in Pharmaceutical Dosage Forms Using Low-Frequency Raman Spectroscopy*. Org Process Res Dev, 2015. 19(11): p. 1796-1798.
145. Hedoux, A., Y. Guinet, and M. Descamps, *The contribution of Raman spectroscopy to the analysis of phase transformations in pharmaceutical compounds*. Int J Pharm, 2011. 417(1-2): p. 17-31.
146. Guinet, Y., L. Paccou, F. Danède, J.F. Willart, P. Derollez, and A. Hédoux, *Comparison of amorphous states prepared by melt-quenching and cryomilling polymorphs of carbamazepine*. Int J Pharm, 2016. 509(1-2): p. 305-313.
147. Hubert, S., S. Briancon, A. Hedoux, Y. Guinet, L. Paccou, H. Fessi, and F. Puel, *Process induced transformations during tablet manufacturing: Phase transition analysis of caffeine using DSC and low frequency micro-Raman spectroscopy*. Int J Pharm, 2011. 420(1): p. 76-83.
148. Hédoux, A., L. Paccou, P. Derollez, and Y. Guinet, *Dehydration mechanism of caffeine hydrate and structural description of driven metastable anhydrates analyzed by micro Raman spectroscopy*. Int J Pharm, 2015. 486(1-2): p. 331-338.
149. Bezerra, B.P., J.C. Fonseca, Y.S. De Oliveira, M.S.A. De Santana, K.F. Silva, B.S. Araújo, and A.P. Ayala, *Phase transitions in secnidazole: Thermal stability and polymorphism studied by X-ray powder diffraction, thermal analysis and vibrational spectroscopy*. Vib Spectrosc, 2016. 86: p. 90-96.
150. Hennigan, M.C. and A.G. Ryder, *Quantitative polymorph contaminant analysis in tablets using Raman and near infra-red spectroscopies*. J Pharm Biomed Anal, 2013. 72: p. 163-171.
151. Zeitler, J.A., D.A. Newnham, P.F. Taday, T.L. Threlfall, R.W. Lancaster, R.W. Berg, C.J. Strachan, M. Pepper, K.C. Gordon, and T. Rades, *Characterization of temperature-induced phase transitions in five polymorphic forms of sulfathiazole by terahertz pulsed spectroscopy and differential scanning calorimetry*. J Pharm Sci, 2006. 95(11): p. 2486-2498.
152. Eliasson, C. and P. Matousek, *Noninvasive authentication of pharmaceutical products through packaging using spatially offset Raman spectroscopy*. Anal Chem, 2007. 79(4): p. 1696-701.
153. Wei, D., S. Chen, and Q. Liu, *Review of Fluorescence Suppression Techniques in Raman Spectroscopy*. Appl Spectrosc Rev, 2015. 50(5): p. 387-406.
154. Nissinen, I., J. Nissinen, P. Keränen, and J. Kostamovaara, *On the effects of the time gate position and width on the signal-to-noise ratio for detection of Raman spectrum in a time-gated CMOS single-photon avalanche diode based sensor*. Sens Actuators, B, 2017. 241: p. 1145-1152.
155. Valeur, B. and M.N. Berberan-Santos, *Introduction*, in *Molecular Fluorescence*. 2012, Wiley-VCH Verlag GmbH & Co. KGaA. p. 1-30.
156. Nissinen, I., J. Nissinen, A.K. Länsman, L. Hallman, A. Kilpelä, J. Kostamovaara, M. Kögler, M. Aikio, and J. Tenhunen. *A sub-ns time-gated CMOS single photon avalanche diode detector for Raman spectroscopy*. in *2011 Proceedings of the European Solid-State Device Research Conference*. 2011.

157. Mosconi, D., D. Stoppa, L. Pancheri, L. Gonzo, and A. Simoni. *CMOS Single-Photon Avalanche Diode Array for Time-Resolved Fluorescence Detection*. in *2006 Proceedings of the 32nd European Solid-State Circuits Conference*. 2006.
158. Rochas, A., M. Gani, B. Furrer, P.A. Besse, R.S. Popovic, G. Ribordy, and N. Gisin, *Single photon detector fabricated in a complementary metal–oxide–semiconductor high-voltage technology*. Rev Sci Instrum, 2003. 74(7): p. 3263-3270.
159. Rojalin, T., L. Kurki, T. Laaksonen, T. Viitala, J. Kostamovaara, K.C. Gordon, L. Galvis, S. Wachsmann-Hogiu, C.J. Strachan, and M. Yliperttula, *Fluorescence-suppressed time-resolved Raman spectroscopy of pharmaceuticals using complementary metal-oxide semiconductor (CMOS) single-photon avalanche diode (SPAD) detector*. Anal Bioanal Chem, 2016. 408(3): p. 761-74.
160. Wold, S., M. Sjöström, and L. Eriksson, *PLS-regression: a basic tool of chemometrics*. Chemom Intell Lab Sys, 2001. 58(2): p. 109-130.
161. Gabrielsson, J., N.-O. Lindberg, and T. Lundstedt, *Multivariate methods in pharmaceutical applications*. J Chemom, 2002. 16(3): p. 141-160.
162. Eriksson, L., Byrne, T., Johansson, E., Trygg, J., & Vikström, C., *Multi- and megavariate data analysis basic principles and applications*. 3rd ed. 2013: Umetrics Academy.
163. Eriksson, L., E. Johansson, and C. Wikström, *Mixture design—design generation, PLS analysis, and model usage*. Chemom Intell Lab Sys, 1998. 43(1–2): p. 1-24.
164. Pahikkala, T. and A. Airola, *RLScore: Regularized Least-Squares Learners*. J Mach Learn Res, 2016. 17: p. 221:1-221:5.
165. Barnes, R.J., M.S. Dhanoa, and S.J. Lister, *Standard Normal Variate Transformation and De-Trending of Near-Infrared Diffuse Reflectance Spectra*. Appl Spectrosc, 1989. 43(5): p. 772-777.
166. Heinz, A., M. Savolainen, T. Rades, and C.J. Strachan, *Quantifying ternary mixtures of different solid-state forms of indomethacin by Raman and near-infrared spectroscopy*. Eur J Pharm Sci, 2007. 32(3): p. 182-192.
167. Kogermann, K., J. Aaltonen, C.J. Strachan, K. Pöllänen, J. Heinämäki, J. Yliruusi, and J. Rantanen, *Establishing quantitative in-line analysis of multiple solid-state transformations during dehydration*. J Pharm Sci, 2008. 97(11): p. 4983-4999.
168. Shi, X., N. El Hassan, A. Ikni, W. Li, N. Guiblin, A. Spasojević De-Biré, and N.E. Ghermani, *Experimental electron densities of neutral and zwitterionic forms of the drug piroxicam*. CrystEngComm, 2016. 18(18): p. 3289-3299.
169. Vrečer, F., M. Vrbinc, and A. Meden, *Characterization of piroxicam crystal modifications*. Int J Pharm, 2003. 256(1–2): p. 3-15.
170. Bahl, O.P. and K.M. Agrawal, *Glycosidases of Aspergillus niger. I. Purification and characterization of alpha- and beta-galactosidases and beta-N-acetylglucosaminidase*. J Biol Chem, 1969. 244(11): p. 2970-8.
171. Borooah, J., D.H. Leaback, and P.G. Walker, *Studies on glucosaminidase. 2. Substrates for N-acetyl-β-glucosaminidase*. Biochem J, 1961. 78(1): p. 106-110.
172. Zhang, Z.M., S. Chen, and Y.Z. Liang, *Baseline correction using adaptive iteratively reweighted penalized least squares*. Analyst, 2010. 135(5): p. 1138-46.

173. Elversson, J. and A. Millqvist-Fureby, *Particle size and density in spray drying-effects of carbohydrate properties*. J Pharm Sci, 2005. 94(9): p. 2049-60.
174. Adhikari, B., T. Howes, B.R. Bhandari, and T.A.G. Langrish, *Effect of addition of proteins on the production of amorphous sucrose powder through spray drying*. J Food Eng, 2009. 94(2): p. 144-153.
175. Maury, M., K. Murphy, S. Kumar, L. Shi, and G. Lee, *Effects of process variables on the powder yield of spray-dried trehalose on a laboratory spray-dryer*. Eur J Pharm Biopharm, 2005. 59(3): p. 565-573.
176. Bhandari, B.R., N. Datta, and T. Howes, *Problems Associated With Spray Drying Of Sugar-Rich Foods*. Drying Technol, 1997. 15(2): p. 671-684.
177. ICH, *Stability Testing of New Drug Substances and Products, revision 2 (Q1A-R2). The International Conference on Harmonisation of Technical Requirements for Registration of Pharmaceuticals for Human Use*. 2003.
178. Maa, Y.F., P.A. Nguyen, J.D. Andya, N. Dasovich, T.D. Sweeney, S.J. Shire, and C.C. Hsu, *Effect of spray drying and subsequent processing conditions on residual moisture content and physical/biochemical stability of protein inhalation powders*. Pharm Res, 1998. 15(5): p. 768-75.
179. Vrečer, F., M. Vrbinc, and A. Meden, *Characterization of piroxicam crystal modifications*. Int J Pharm, 2003. 256(1-2): p. 3-15.
180. Sheth, A.R., S. Bates, F.X. Muller, and D.J.W. Grant, *Polymorphism in Piroxicam*. Cryst Growth Des, 2004. 4(6): p. 1091-1098.
181. Polavarapu, P.L., *Ab initio vibrational Raman and Raman optical activity spectra*. J Phys Chem, 1990. 94(21): p. 8106-8112.
182. Horvath, R. and K.C. Gordon, *Understanding excited-state structure in metal polypyridyl complexes using resonance Raman excitation profiles, time-resolved resonance Raman spectroscopy and density functional theory*. Coord Chem Rev, 2010. 254(21–22): p. 2505-2518.
183. Guirgis, G.A., P. Klaboe, S. Shen, D.L. Powell, A. Gruodis, V. Aleksa, C.J. Nielsen, J. Tao, C. Zheng, and J.R. Durig, *Spectra and structure of silicon-containing compounds. XXXVI—Raman and infrared spectra, conformational stability, ab initio calculations and vibrational assignment of ethyldibromosilane*. J Raman Spectrosc, 2003. 34(4): p. 322-336.
184. Herzberg, G., *Molecular Spectra and Molecular Structure Volume II Infrared and Raman spectra of Polyatomic Molecules*. 1991: Krieger Publishing Company, Malabar, FL USA.
185. Redenti, E., M. Zanol, P. Ventura, G. Fronza, A. Comotti, P. Taddei, and A. Bertoluzza, *Raman and solid state 13C-NMR investigation of the structure of the 1: 1 amorphous piroxicam: β-Cyclodextrin inclusion compound*. Biospectrosc, 1999. 5(4): p. 243-251.

Recent Publications in this Series

12/2018 Tiina Mattila
Airway Obstruction and Mortality
13/2018 Lauri Jouhi
Oropharyngael Cancer: Changing Management and the Role of Toll-like Receptors
14/2018 Jukka Saarinen
Non-linear Label-free Optical Imaging of Cells, Nanocrystal Cellular Uptake and Solid-State Analysis in Pharmaceutics
15/2018 Olena Santangeli
Sleep and Depression: Developmental and Molecular Mechanisms
16/2018 Shadia Rask
Diversity and Health in the Population: Findings on Russian, Somali and Kurdish Origin Populations in Finland
17/2018 Richa Gupta
Association and Interplay of Genetic and Epigenetic Variants in Smoking Behavior
18/2018 Patrick Vingadas Almeida
Multifunctional Porous Silicon Based Nanocomposites for Cancer Targeting and Drug Delivery
19/2018 Lena Sjöberg
Reproductive Health in Women with Childhood-onset Type 1 Diabetes in Finland
20/2018 Perttu Päiviö Salo
Studies on the Genetics of Heart Failure
21/2018 Andrew Erickson
In Search of Improved Outcome Prediction of Prostate Cancer – A Biological and Clinical Approach
22/2018 Imrul Faisal
Genetic Regulation of Mammalian Spermatogenesis - Studies of USF1 and MAD2
23/2018 Katja Wikström
Socioeconomic Differences in the Development and Prevention of Type 2 Diabetes: Focus on Education and Lifestyle
24/2018 Laura Ollila
Genotype-Phenotype Correlations in Dilated Cardiomyopathy
25/2018 Elina Engberg
Physical Activity, Pregnancy and Mental Well-Being: Focusing on Women at Risk for Gestational Diabetes
26/2018 Anni Niskakoski
Molecular Alterations of Endometrial and Ovarian Tumorigenesis in Lynch Syndrome Mutation Carriers and the General Population
27/2018 Katariina Maaninka
Atheroinflammatory Properties of LDL and HDL Particles Modified by Human Mast Cell Neutral Proteases
28/2018 Sonja Paetau
Neuronal ICAM-5 Regulates Synaptic Maturation and Microglia Functions
29/2018 Niina Kaartinen
Carbohydrates in the Diet of Finnish Adults: Focus on Intake Assessment and Associations with Other Dietary Components and Obesity
30/2018 Tuija Jääskeläinen
Public Health Importance of Vitamin D: Results from the Population-based Health 2000/2011 Survey

Helsinki 2018 ISSN 2342-3161 ISBN 978-951-51-4282-5